

Some parts of this thesis may have been removed for copyright restrictions.

If you have discovered material in AURA which is unlawful e.g. breaches copyright, (either yours or that of a third party) or any other law, including but not limited to those relating to patent, trademark, confidentiality, data protection, obscenity, defamation, libel, then please read our [Takedown Policy](#) and [contact the service](#) immediately

THE UNIVERSITY OF ASTON

IN BIRMINGHAM

PHYSICAL STRUCTURE AND MECHANICAL PROPERTIES
OF INJECTION MOULDED POLYPROPYLENE

Malcolm Graham Wilkinson

A THESIS SUBMITTED FOR THE DEGREE OF PhD

THESIS
678-7423
WIL

15 Oct 73 165979

Department of Chemistry

July, 1973.

Summary

Samples of polypropylene have been injection moulded under different processing conditions, their structures closely examined and their mechanical properties determined.

Following the construction of a suitable mould cavity and modification of an injection moulding machine, a procedure for measuring the prevailing cavity pressure and temperature was established. Test-pieces were then prepared under a variety of conditions, including conditions under which the polymer readily crystallises, and the processing variables, in particular injection pressure, mould temperature and time, monitored carefully. Specimens were then sectioned and examined microscopically, and relevant structures photographed. Density of the specimens was also determined and percentage crystallinities calculated. The dynamic modulus and loss factor were determined.

Results showed that the injection pressure had a significant effect on the resulting spherulitic structure since crystallisation could be induced at higher temperatures than normal by increasing the injection pressure. Little correlation could be found between the size or number of spherulites in a sample and mechanical properties, although it was found that samples with some crystalline structure present had higher modulus values than samples which had been rapidly chilled. As the density (crystallinity) increased the modulus increased. Attempts have been made to analyse the pressure traces obtained from the mould cavity in terms of crystallisation kinetics, and the relationship between the nucleation and growth of the spherulites and mould temperature, injection pressure and time is discussed.

LIST OF CONTENTS

	<u>Page No.</u>
Summary	2
Chapter 1 Introduction to the problem	8
Chapter 2 Literature survey	10
2.1. Injection moulding	10
2.1.1. General	10
2.1.2. Pressure	12
2.1.3. Heating cylinder	13
2.1.4. Mould temperature	14
2.1.5. Time	16
2.2. Crystallisation	17
2.2.1. General	17
2.2.2. Polymer morphology	20
2.2.3. Nucleation and growth	22
2.2.4. Measurement of growth rates	25
2.2.5. Crystallisation kinetics	28
2.2.6. Kinetics of spherulite growth in polypropylene	30
2.2.7. Crystallinity determination in polymers	35
2.3. Mechanical properties of polymers	37
2.3.1. General	37
2.3.2. Dynamic mechanical test methods	40
2.3.3. Dynamic mechanical properties of polymers	43
2.4. Effect of injection moulding process variables on crystalline structure	46
2.5. Structure and mechanical properties of semi-crystalline polymers	55

Chapter 3	Experimental details	61
	3.1. Plan of work	61
	3.2. Material used	62
	3.3. Injection moulding of samples	62
	3.3.1. Injection moulding machine	62
	3.3.2. Mould cavity	64
	3.3.3. Mould temperature control	67
	3.3.4. Calibration of pressure transducer and thermocouple	69
	3.3.5. Preliminary examination of moulding behaviour	70
	3.3.6. Moulding procedure	72
	3.3.7. Samples prepared	75
	3.4. Examination of structure	78
	3.4.1. Preparation of specimens for sectioning	78
	3.4.2. Sectioning of samples	78
	3.4.3. Microscopy and photography	80
	3.4.4. Density determinations	82
	3.5. Dynamic mechanical testing	83
	3.5.1. Sample preparation	83
	3.5.2. General principles of Rheovibron	84
	3.5.3. Equation of modulus	85
	3.5.4. Taking readings	86
	3.5.5. Correction of complex modulus calculation	87

Chapter 4	Results	88
	4.1. Effect of process variables on pressure traces	88
	4.1.1. General description of pressure traces	88
	4.1.2. Effect of variables on time taken for pressure to drop by half	90
	4.1.3. Effect of variables on packing time	92
	4.2. Crystalline structure of mouldings	93
	4.2.1. General appearance	93
	4.2.2. Effect of mould temperature on structure	95
	4.2.3. Effect of injection pressure on structure	98
	4.2.4. Effect of moulding time on structure	100
	4.2.5. Variables producing voided structures	106
	4.3. Percentage crystallinities	108
	4.3.1. Effect of mould temperature and injection pressure on percentage crystallinity	108
	4.3.2. Effect of moulding time on percentage crystallinity	111
	4.4. Mechanical properties	112
	4.4.1. General	112
	4.4.2. Effect of mould temperature on dynamic mechanical properties	114
	4.4.3. Effect of injection pressure on dynamic mechanical properties	114
	4.4.4. Effect of moulding time on dynamic mechanical properties	120

		<u>Page No.</u>
Chapter 5	Discussion	121
	5.1. Experimental techniques used for preparing samples	121
	5.2. Analysis of pressure traces obtained	122
	5.3. Effect of processing variables on crystalline structure	129
	5.3.1. General appearance	129
	5.3.2. Explanation of observed structures	130
	5.3.3. Effect of moulding time on crystalline structure	136
	5.3.4. Nucleation levels	138
	5.3.5. Type of nucleation	143
	5.3.6. Voiding	145
	5.4. Effect of processing variables on percentage crystallinity	147
	5.5. Effect of processing conditions on dynamic mechanical properties	150
	5.5.1. General	150
	5.5.2. Effect of processing conditions	151
	5.5.3. Stress-strain measurements	154
Chapter 6	Conclusions	155
	6.1. Effects of processing on structure and properties	155
	6.2. Practical implications	157
	6.3. Suggestions for further work	160

	<u>Page No.</u>
Appendix	161
Appendix 1. Steam pressure/mould temperature - approximate calibration	161
Appendix 2. Density gradient column calibration	162
Appendix 3. Rheovibron calculating equations	163
3.1. Calculation of oscillating displacement	163
3.2. Calculation of oscillating load	164
3.3. Calculation of dynamic elastic modulus	164
3.4. Correction of complex modulus calculation	166
3.5. Specification of cross-sectional area	167
Photographic plates	
Fig.A.1. General view of injection moulding machine	168
.A.2. Mould halves and Dynisco pressure transducer	169
A.3. Measuring equipment	170
A.4. Cambridge rocking microtome	171
A.5. General view of Rheovibron	172/3
A.6. Clear and voided samples	174
Scale drawing of mould	175
Acknowledgements	176
References	177

CHAPTER 1 - INTRODUCTION TO THE PROBLEM

Processing of polymers is not only a means of converting them into articles, but also makes it possible to modify their properties by regulating the structure of the polymer. This is particularly true with semi-crystalline polymers.

Despite the great number of studies dealing with the structural mechanics of polymers, aspects such as the formation of the structure of a thick section during industrial processing of the polymer, characteristics of the structure, and its evaluation and relation to mechanical properties have received less attention. Many workers have shown how processing variables can be altered to give improved properties but without saying why the variables have produced a particular structure to give these improved properties. At the other extreme, a great deal of work has become available on the detailed morphological structure of certain semi-crystalline polymers and its effect on properties but without saying how processing will effect these. A "tie-up" between processing and ultimate properties of semi-crystalline polymers via the crystalline structure is therefore of considerable practical interest.

The effect of processing on structure, and the effect of structure on mechanical properties was reviewed and from a combination of the two a plan of work was initiated.

Isotactic polypropylene was chosen for this study because it is a readily available semi-crystalline polymer, but at the same time has good mechanical properties; also on cooling from the melt spherulite structures are produced which are easily identifiable under the optical microscope.

The processing operation chosen was injection moulding since this operation exposes the polymer to almost all of the general fundamental experiences of processing. Under normal processing conditions where the production rate is important, the polymer is given little time to crystallise and therefore little structural variation can be gained from the samples. In this study, however, samples will be prepared under a wide range of closely controlled processing conditions, including conditions under which the polymer readily crystallises. It is hoped that easily indentifiable structural differences will be produced which can be attributed to the difference in processing conditions. If general principles can be found under these more artificial conditions it may be possible to apply them to more realistic production conditions.

It is hoped that this will give an insight into what the mechanism of structure formation is during processing, and how the structure affects the mechanical properties. It should then be possible to control conditions to give predicted structures with known mechanical properties, and also to say whether it is justifiable to use more artificial processing conditions, and hence possibly reduce the production rate, to gain improvement in properties.

CHAPTER 2 - LITERATURE SURVEY

2.1. Injection moulding

2.1.1. General

The process of injection moulding (1) consists of the transfer, by pressure, of softened polymeric material from a heated reservoir into two mould halves held together. After a suitable cooling period the mould halves are separated and the moulding thus formed removed. The opening and closing of the mould halves is co-ordinated with the injection of material to establish a sequence of operations which can be continuously repeated.

In its simplest form the machine comprises a heating cylinder with a plunger at one end and a nozzle at the other, which is connected by channels to a relatively cold mould. The plunger end of the heating chamber is maintained at a low temperature where the granules of material are fed from the hopper. The granular charge is pushed forward and compressed by the injection plunger which simultaneously displaces softened material from the hot nozzle end of the cylinder into the mould cavity. During this stage the mould halves are kept in the closed position by the locking mechanism of the machine. The locking of the moulds is effected by hydraulic pressure or by a toggle mechanism. Pressure is maintained upon the material which has filled the cavity to ensure a feed of additional material. This is necessary to compensate for shrinkage which accompanies the rapid cooling in the mould. After the retraction of the injection plunger a suitable interval of time elapses whilst the moulding is allowed to cool to a temperature which will permit satisfactory removal. The mould halves are then opened and the moulding ejected, after which the machine is ready to commence another sequence of operations which together make up the "moulding cycle".

In recent years "screw preplasticising" machines have become very popular. The most popular type has been the "reciprocating screw" machine, in which the screw is used for melting and transporting the material and also for injecting material into the mould. A rotating screw is an efficient method of heating and transporting thermoplastic material. The rotational movement of the screw creates a desirable turbulence in the material which assists in the transfer of heat through the material from the barrel wall. The relative movement which occurs between the material and the surfaces of the screw and barrel ensures that fresh particles of material are continually being exposed to the heated surfaces. This contributes to the even distribution of temperature through the melt. The screw also provides a further source of heat when it overcomes the resistance to rotation and exerts shearing forces upon the material. This mechanical energy is converted to heat.

The mould normally consists of two halves of a suitable mould material in which a cavity (or cavities) is machined or inserted. The molten polymer is introduced through a small orifice, the "gate". The polymer is transferred from nozzle to cavity by a system of machined channels, the "runners" and "sprue".

The production injection moulding machine is equipped to control all phases of the injection moulding cycle and to measure hydraulic pressure and machine temperatures. It is not equipped, however, to measure any pressure or temperature conditions within the polymer (2). Under actual production moulding conditions it is generally true that heating cylinder temperature and hydraulic injection pressures do not closely resemble conditions in the polymer either in the heating cylinder or in the mould. The primary reason for this difference can be attributed to the inherent properties of polymers. Most thermoplastics

have a thermal conductivity of about 1% that of steel. During the injection moulding process, the temperature of a polymer must be raised in order to reduce its viscosity to a level at which it will flow under pressure. When the material enters the cavity this same heat must be removed.

2.1.2. Pressure

The pressure applied to the material by the screw during the injection stroke is transmitted through the polymer. The pressure variation that takes place in the mould cavity has been described by Glanvill (3). As the screw commences the injection stroke, polymer passes from the nozzle into the runner system and commences to fill the mould. Owing to the resistance of the cavity, the pressure necessary to fill rises to a peak. As cooling commences further material is forced in to offset thermal contraction. This continues until the gate is sealed or until the screw is returned (in which case there is leakage until the gate is sealed). As cooling and thermal contraction continue, the cavity pressure steadily falls until ideally a point is reached where residual pressure has decayed to zero or atmospheric. The mould can be opened at this point except that further cooling is usually required to allow the material to gain sufficient rigidity to prevent distortion on ejection.

Many methods have been developed to measure the pressure loss in the injection mould. Successful methods have included strain gauges on ejector pins, strain gauge transducers, pressure buttons, piezoelectric transducers, and mechanical devices. Rarely, however, have these methods been adapted to production usage since they must be rugged enough to withstand the regular mechanical shocks occurring during mould opening and closing operations. Response must be rapid without sacrificing accuracy, and pressure indication must be made independent of the large and rapid temperature

changes encountered in the mould during the cycle. The "Dynisco" pressure transducer (4) meets these requirements except possibly the latter, although allowance can be made for temperature effects. Simple recording devices can be used in most cases and satisfactory results are obtained with pen recorders.

Paulson (2) also points out that the location and the number of pressure sensing points depends upon the results required. To obtain information relating to the "packing" and "cooling" phases of the cycle, pressure exerted on the material in the mould must be measured by placing a pressure transducer at some location in the cavity. This transducer will measure all pressures occurring in the cavity. Any changes in machine operation, mould design, mould variables, or polymer, which affect the pressure during packing or cooling, will be reflected by this pressure recording.

2.1.3. Heating cylinder

The function of the heating cylinder in an injection moulding machine is to convert the granules into a homogeneous melt.

Thermoplastics are generally poor heat conductors. Consequently heat input is always limited by the amount of heat which the polymer can absorb in a specified time. Therefore even heating to plasticising temperature depends mainly upon the time the material remains in contact with the cylinder, the temperature difference between cylinder and material and surface finish of the cylinder. Even plasticisation is usually achieved by using various zones of heating.

Glanvill (3) states that assuming the material and grade are to be determined by the performance requirements of the component, the melt temperature chosen will be as low as possible to reduce cooling time and hence

increase production. Injection temperature is limited, however, by quality or performance requirements such as gloss or impact strength which are dependent on processing temperature.

Electric resistance heaters are used almost exclusively on heating cylinders. Heating capacity must be variable to suit process requirements, and this is normally achieved using on/off controllers. As its description implies the instrument causes the heating load to be switched on and off in response to a difference between the set temperature and the measured temperature recorded by a thermocouple. Location of thermocouples is very important as regards the delay before the measuring point is restored to the control temperature. It is recognised generally that "shallow" thermocouples provide the best control.

2.1.4. Mould Temperature

As discussed earlier, when the molten polymer has been injected into the mould the heat that has been put in to melt the material must be removed before the component can be ejected. Since the total heat content of the polymer mass and the time available for cooling remain unchanged it follows that for consistent conditions the mould cooling system must be capable of removing heat from this material at the same rate for every cycle. This required consistency cannot be obtained without control of the mould temperature. With the trend towards the improvement of moulding quality, and the development of the newer "engineering" thermoplastics, which depend to a great extent on closely controlled processing conditions, mould temperature control has become essential. For example nylons, polycarbonates, polyacetal and polypropylene are best processed with relatively high mould temperatures.

Continuous mould cooling is catered for normally by the cooling water supply points provided on the machine. However, mould temperature control

equipment which can supply or remove heat is preferable. The medium used for heating and cooling moulds is usually water where temperatures between approximately 5°C and 95°C are to be used (oil can be used for temperatures in the range 95°C to 175°C). Steam heating can be used for temperatures in the range 100 to 200°C by increasing its pressure appropriately, but although this is an economic method it has the disadvantage that a very accurate pressure reducing valve is required, and the system depends on a central generating plant. Electrical resistance heating can also be used but it is difficult to achieve a smooth temperature gradient and avoid hot spots.

G.T.Byast (5) discusses the temperature control of moulds not only from the point of view of equipment available but also from the mould design aspect. He states that the design of the mould itself influences the efficiency of its temperature control. The rate of heat transfer and the control of the cavity temperature can be varied by design features. Large cooling channels should always be provided. It is more practical to provide over large channels which will ensure high flow rates at low pressure for the heating/cooling liquid, than small channels which require high pressures and will not provide sufficient surface area to allow adequate heat transfer. It is well known that the mould by virtue of mechanical consideration, is constructed over large, relative to the cavity size. Where the wall thickness of the cavity can be reduced and thus the overall dimensions of the mould, the problem of temperature control can be eased. A layer of insulating material placed between the connecting surfaces of the mould and platen will prove an effective barrier against heat loss. Finally Byast discusses mould materials that can be used. He says that it is general practice to construct moulds from steel, particularly where long production runs are involved.

However use is made from time to time of metals having better heat conductivity characteristics than steel at particular hot areas in moulds. Care must be taken, however, since high clamp pressures can crush tools of low strength.

2.1.5. Time

The time variable is important since the polymer that has been injected into the cavity goes through a number of phases before the moulding cycle is complete, and the time of each phase can be varied to give optimum processing conditions.

The important time variables are:-

(a) The "injection time" which can be defined as the time taken for the melt to fill the cavity and for the pressure at the point furthest from the central runner to increase to a maximum.

(b) The "screw forward time" which is the time from when the screw commences its injection stroke to the time when the screw is returned.

(c) The "cooling time" which is the time that the polymer is allowed to cool before ejection.

Under normal production conditions it is endeavoured to keep these times, and hence the total cycle time, as short as possible.

Another important variable which affects the moulding cycle is the injection plunger speed. Usually, the maximum injection speed is used since this allows the mould to be filled in the shortest time, but occasionally the mould, the material, or other considerations may demand that the speed be reduced.

2.2. Crystallisation

2 2.1. General

In molecular systems, crystallisation is the orderly packing of molecules caused by the lowering of the free energy due to the fact that if two molecules have an attraction (van der Waal) for each other, there is a distance at which the potential between them is minimum. The free energy, G , is given by $G = U + PV - TS$. Thus, as U (internal energy) is reduced so is G thus creating a more stable phase (6).

As the temperature of a molten polymer is lowered, a point is reached at which the crystalline form is slightly more stable than the amorphous phase. At this temperature the polymer begins to crystallise as the chains align and are held together by the van der Waal's forces. Since the chains are larger than simple molecules, they do not align fast enough for this process to be at constant temperature as with simple systems. As the temperature decreases, the free energy increases leading to an increased rate of crystal formation. However, as the temperature decreases still further, the chains become increasingly less mobile and eventually the free energy is insufficient to induce part of a chain to a crystalline surface. These opposing forces result in a temperature range where crystallisation rates pass through a maximum. Above and below this temperature the crystallisation rates go to zero. Thus in an amorphous phase there will be no crystallisation if the temperature is too high or too low.

If the structure of a polymer is such that crystallisation is possible, the extent to which it will crystallise is dependent on its thermal treatment. Even at temperatures that are ideal for crystallisation there is an induction period before nucleation sites become active. Conversely, if the cooling rate is high

there may be no crystallisation and the resulting amorphous phase will be kinetically stable.

Many factors affect the ability of a given polymeric material to crystallise, thereby limiting both the crystallisation rate and attainable degree of crystallinity (7). These factors include such considerations as chain and repeat unit symmetry, stereospecificity, size and flexibility of side groups, chain stiffness, and for materials meeting the necessary criterion in each of the above categories, processing conditions.

In the case of the simplest linear polymer, polyethylene $(\text{CH}_2 \cdot \text{CH}_2)_n$, the molecules in the crystalline state take up the extended conformation in which the carbon atoms in the backbone zig-zag (8). The hydrogen atoms take up the staggered conformation (fig.2.1.) so that they are as far apart as possible and are thus in a position of minimum energy. In the crystal, these chains pack so that the hydrogen atoms on alternate carbon atoms are stacked vertically above each other; this arrangement also helps lateral packing.



Fig.2.1. Packing of polyethylene chains in the crystal (Ref.8)

In the polypropylene molecule $(\text{CH}_2.\text{CH}.\text{CH}_3)_n$, every other carbon atom contains one hydrogen and one methyl group. In atactic polypropylene, because of the random arrangement of the CH_3 - side groups, the chains cannot pack together closely and so it is non-crystalline. In contrast, both the isotactic and the syndiotactic forms of the polymer are easily crystallised. The alternating CH_3 - groups in the syndiotactic polymer can be easily packed together in the planar zig-zag crystal form typical of polyethylene. In the case of the isotactic form, the polymer molecules in the crystal take the form of a helix, as shown in figure 2.2.



Fig 2.2 Helical packing of isotactic polypropylene chains in the crystal (Ref.8).

This staggers the CH_3 - side groups, and allows the chains to pack together without strain. It can be seen that there is one complete turn of the helix for every three monomer units.

2.2.2. Polymer morphology

Early concepts of the structure of a crystalline polymer were based upon a long chain molecule, part of whose length was in an ordered or crystalline region and part in a less ordered or amorphous region. The polymer was regarded as consisting of small crystallites embedded in an entangled mass of randomly organised chains. This concept, known as the "fringe micelle model", has over the years been the subject of intense development and refinement (9,10,11).

This model was evolved during the 1930's in order to explain how crystallites of dimensions in the order of 10^{-5} to 10^{-6} cm could contain component polymer molecules having chain-like structures of far greater dimensions. Although the picture which emerged is now known to be very much over simplified (Fig.2.3.) it enables several features of polymer structure to be simply illustrated. For example, the long range and to a large extent reversible deformation which polymers can undergo, and their high but limited swelling in the presence of suitable penetrants can be adequately explained by this model.



Aston University

Illustration removed for copyright restrictions

Fig.2 3. Fringed-micelle structure for semi-crystalline polymers showing chain molecules passing successively through crystalline and amorphous regions (Ref.10).

Severe weaknesses in this concept were highlighted however by the discoveries of Keller (12) and Till (13), that single crystals of a polymer could be grown. Keller carried out X-ray, electron diffraction and electron microscope measurements on crystals of polyethylene grown from a 0.1% solution of polyethylene in xylene by cooling to 70-90°C, and found that the polymer chain axes were perpendicular to the large flat faces of the crystal. The length of the polymer chain was known to be much greater than the thickness of the crystal and, to explain his data, Keller postulated that the chains must be folded.

Although the majority of the single-crystal studies were made using dilute polymer solutions several attempts have been made to determine the precise relation between these well-developed single crystals and the more complex structures found in melt-crystallised products.

When a semi-crystalline polymer is allowed to crystallise from the molten state a polycrystalline structure develops of which the structural units are usually spherical in shape. These units have been given the name "spherulites", and when seen in a polarising microscope between crossed polaroids appear as a dark Maltese cross in an illuminated field. Electron and optical microscopy have revealed that the spherulite consists of thin, flat, ribbon-like structures or "fibrils", radiating from a central nucleus. It was previously shown (14) that these fibrils were, in fact, composed of thickly plated lamellae. An important feature (10) of the fibrillar development is that it involves branching; this is the process by which space is filled as the spherulite expands. In the early stages of growth, a spherulite probably develops from a single crystal, and becomes polycrystalline as branching eventually sets in. Amorphous regions are thought to be inter-fibrillar material rejected from growing fibrils. Sharples concludes that although the exact relation of single crystals to melt-crystallised structures is not yet fully determined, there would seem to be no doubt that some of the features of single crystal growth, which can be studied in considerable detail, are also likely to be applicable to melt crystallisation.

2.2.3 Nucleation and growth.

The crystallisation process is a combination of two factors: the formation of nuclei, and their subsequent growth.

Two distinct types of nucleation have been postulated to account for spherulitic growth. In order for spherulitic growth to start, primary nucleation must

occur either by a self nucleating mechanism - homogeneous nucleation, or on the surface of foreign particles - heterogeneous nucleation.

Homogeneous nucleation (10) involves the spontaneous aggregation of polymer chains below the melting point, in a manner which is reversible up to the point where a critical size is reached; beyond this point, the subsequent addition of chains is irreversible, and growth may be considered to have commenced. The distribution of these regions is random throughout the bulk of the polymer, and their rate of appearance is usually considered to involve a first-order dependence on time.

Heterogeneous nucleation, on the other hand, arises from adventitious impurities, either randomly distributed throughout the bulk, or possibly localised on a surface. With this type of nucleation a limited number of growth centres becomes effective instantaneously (i.e. with zero-order dependence on time), once the temperature of crystallisation is reached.

It can be seen then that the final size and number of the growth units will depend on the type of nucleation. For heterogeneous nucleation the final average volume of the individual bodies is given simply by the total volume at the end of the process divided by the number of nuclei. In the case of homogeneous nucleation the situation is more complicated because nuclei are still appearing whilst existing ones are growing; hence the rate at which growth occurs relative to the nucleation rate will determine how many further nuclei can form in the melt before it is fully transformed by growth. A further point of difference is that in the homogeneous case there is a wider distribution of growth-unit sizes.

The relation between the nucleation rate and temperature of crystallisation has been determined in a limited number of cases, for the temperature range just below the melting point (15), and the data shows that the

nucleation rate increases very rapidly once the degree of super-cooling exceeds a certain value. This confirms the theoretical treatment developed by Turnbull and Fisher (16) in which, by considering the free energy of formation of the critical size nucleus and its relationship with the degree of super-cooling, they predict that the nucleation rate does increase as super-cooling is increased, but that it passes through a maximum, and subsequently decreases with temperature, until the glass point is reached.

Several cases have been reported where the nucleation process is instantaneous, indicating that a limited number of heterogeneous centres is present, and are responsible for the nucleation process. Price (17) was one of the first workers to observe this effect, using the polymer polychlorotrifluoroethylene, and here the density of nuclei increases with the degree of super-cooling. Other workers have subsequently shown that instantaneous nucleation occurs in a range of polymers including polypropylene (see later).

Temperature of crystallisation is thus one variable which may result in modifications in growth unit size. In the specific case of heterogeneous nucleation, however, the nucleation rate can sometimes be modified by trace amounts of deliberately-added nucleating agents, and this is a far more important method for bringing size under control.

The size of the growth unit then depends on the type and extent of nucleation and also the subsequent growth from these nuclei. The growth of the nuclei will take place in one, two, or three dimensions, to give rods, discs, or spheres (three dimensional growth is assumed to take place during spherulite growth). The linear dimensions of the growing bodies increase with time. Ultimately the growth units impinge, in which event growth ceases locally and eventually the entire mass is converted to a new phase. However, bulk

crystallisation does not always terminate when impingement occurs. This primary stage is often followed by a secondary process (10), which involves a continual increase in crystallinity over a period of time which is often too long to enable its termination to be observed experimentally. Two possibilities have been suggested to explain this phenomenon of "secondary crystallisation"-

(a) that there is an increase in the amount of crystallinity, resulting from the crystallisation of a less easily crystallised fraction, .

(b) that there is an increase in the perfection of the existing crystallites.

The first suggestion was most favoured when it was suggested that the secondary stage involved the crystallisation of impurities which were rejected from the growing fibrils during spherulite development. However, this association with spherulite growth does not always follow since some polymers show no evidence of secondary crystallisation. Also the extent of secondary crystallisation appears to have no relation to impurity content. The second possibility is thus more likely, although little experimental evidence is as yet available.

2.2.4. Measurement of crystallisation growth rates

Crystallisation involves nucleation and growth, and the most satisfactory approach to the problem of determining how structure develops is to study these two steps separately. However, as Sharples points out, in practice the number of polymers in which nucleation and growth can be resolved conveniently in the optical microscope, is limited. Consequently, the alternative approach has also been adopted, of observing some property which is a function of the overall amount of converted material. Techniques used include dilatometry, light microscopy, electron microscopy, differential thermal analysis. The most widely studied property in

this respect is density, for the reasons that it can be measured simply, and with great accuracy using a dilatometer. During the crystallisation process there is a density change, and hence a volume change, and in the dilatometer this change is converted to a change in height of a mercury meniscus in a capillary. A typical crystallisation experiment involves transferring the dilatometer from a bath at a temperature above the melting point to a bath at the crystallisation temperature and measuring the change in meniscus height. The weight fraction of unconverted liquid polymer, W_L/W_0 , can then be found at any stage of the crystallisation process from -

$$\frac{W_L}{W_0} = \frac{h_t - h_\infty}{h_0 - h_\infty} \quad \dots\dots\dots(2.1)$$

where h_t is the height of the meniscus at time t , h_0 and h_∞ are the heights at the beginning and end of the crystallisation process. A typical dilatometer plot is shown (Fig.2.4).

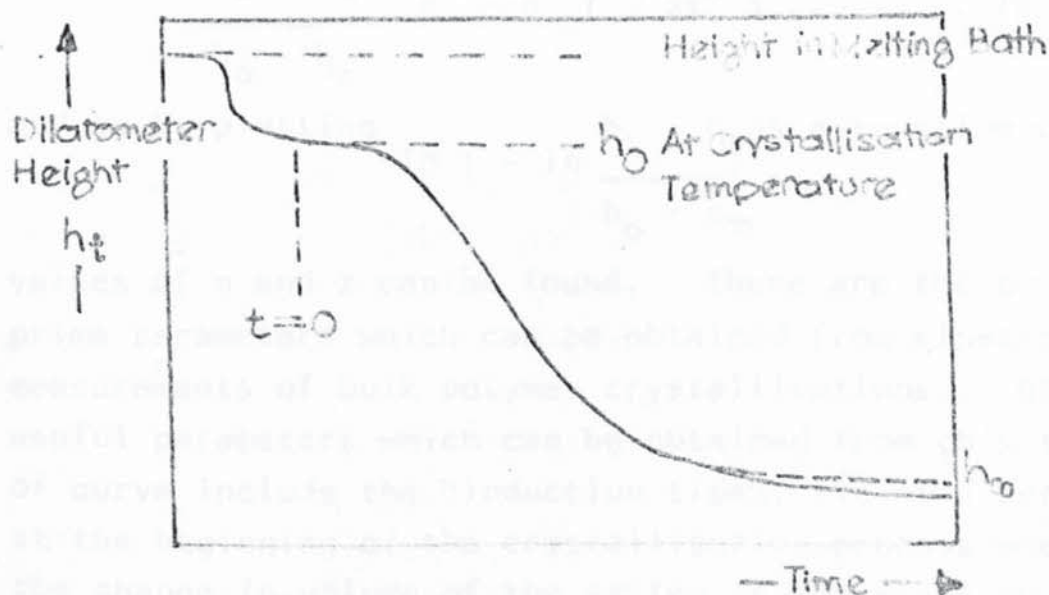


Fig.2.4. A typical dilatometer plot

A steady value of h_{∞} may never be attained if the polymer exhibits secondary crystallisation. Choosing the appropriate value of h_{∞} then becomes an arbitrary procedure which is liable to reduce the accuracy of the analysis.

This then is a simple method of following the rate of the crystallisation process under different conditions. The most important parameter that can be derived from such information is the Avrami exponent (18), which is a combined function of the number of dimensions in which growth takes place, and also of the order of the time dependence of the nucleation process. For example, where three-dimensional spherulitic growth units develop from nuclei whose numbers increase linearly with time, the Avrami exponent, "n", has a value of $3+1 = 4$. In addition, a rate constant "z", which is a combined function of nucleation and growth-rate constants, can be determined. A general form of the Avrami equation is thus:-

$$W_L/W_0 = \exp. (- zt^n) \dots\dots\dots(2.2)$$

or, if dilatometric heights are considered -

$$\frac{h_t - h_{\infty}}{h_0 - h_{\infty}} = \exp (- zt^n) \dots\dots\dots(2.3)$$

and so by plotting $\ln (- \ln \frac{h_t - h_{\infty}}{h_0 - h_{\infty}})$ as a function of $\ln t$,

values of n and z can be found. These are the two prime parameters which can be obtained from kinetic measurements of bulk polymer crystallisations. Other useful parameters which can be obtained from this type of curve include the "induction time", i.e. the period at the beginning of the crystallisation process when the change in volume of the system is too small to be detectable, and the "half-life" of the process given by:-

$$t_{1/2} = \left\{ \frac{\ln 2}{2} \right\}^{1/n} \dots\dots\dots (2.4)$$

Light microscopy is a useful technique for measuring the rate of crystallisation in terms of the radial growth rate of spherulites. The appearance and subsequent growth of spherulites can be followed using polarised light, together with a screw-micrometer eyepiece or facilities for photographic recording.

2.2 5. Crystallisation kinetics of polymers

The first kinetic studies of crystallisation in synthetic polymers were made by Morgan and co-workers in Britain (19) and by Flory and Mandelkern in the U.S.A. (20), and both were primarily concerned with the combined process of nucleation and growth, through measurements made on bulk crystallisation behaviour. The temperature dependence thus contained contributions from both steps, although it was to be expected that the growth step would predominate. Even earlier data obtained for the crystallisation of natural rubber (21) had established that the rate does not increase without limit as the degree of super-cooling is increased, but that in fact a maximum is reached. It is now known that it is a general feature for rate to increase to a maximum between the melting point and the glass-point, although in many cases the rate at the maximum is so high that the melt cannot be quenched to the glassy state, without some crystallisation having occurred. The temperature dependence of the growth rate for spherulites has also been determined for several systems, and in most cases a pronounced maximum is again observed.

The effect of pressure on the rate of crystallisation appears to have received very little attention. The most extensive quantitative work on the effect of pressure on crystallisation has been carried out on polyethylene by Matsuoka (22).

The most important consequence is that primary and secondary stages of crystallisation show a distinct break. It has been suggested that this may arise from the different dependence of the two processes on the degree of super-cooling, as the melting point is considerably affected by pressure.

Wunderlich (23) examined the crystallisation of low pressure polyethylene under pressure (up to 5400atm.) from the melt. Extended chain lamellae of increasing thickness became dominant. The morphology of linear polyethylene crystallised under pressure up to 5300 atm. has been investigated by Geil et al (24). Electron micrographs of fracture surfaces obtained from these samples show that the majority of the polymer, at the highest pressures, crystallises in the form of extended chain lamellae which can be as thick as $3\mu\text{m}$.

It was also stated that linear polyethylene crystallised under pressure may have a density approaching the theoretical perfect crystal density and a melting point close to the limiting value for large perfect crystals.

The effect of pressure on overall structure and properties has been discussed by Maxwell (25,26). He says that structural changes result from the application of hydrostatic pressure to the polymer while it is cooling. As the melt is cooled down to the melting point a discontinuity in the specific volume vs. temperature curve is found when the higher density crystalline phase is formed. The value of the melting point is pressure dependent. At higher pressures the lower energy crystalline state is reached at higher temperatures. That is, pressure can induce crystallisation.

He shows two photomicrographs of isotactic polypropylene exposed to two different pressure histories (Fig.2.5).

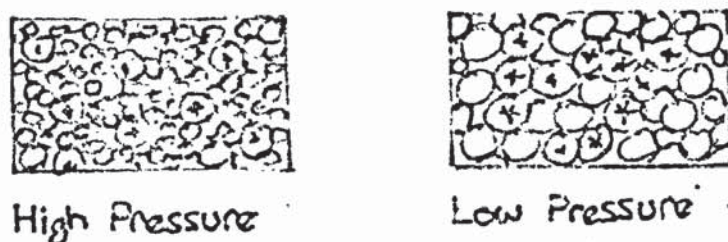


Fig.2.5.

For low pressure and a given thermal cycle large well-developed spherulites are produced. For high pressure and the same thermal cycle small, less well-formed spherulites are produced, together with some large ones which are apparently thermally nucleated. He concludes that one has the ability to control morphology in polymers by pressure-induced nucleation.

2.2.6. Kinetics of spherulite growth in polypropylene

Keller (12) used dilatometry to examine the crystallisation with time at various temperatures. He shows curves of crystalline volume fraction vs. time (Fig.2.6)

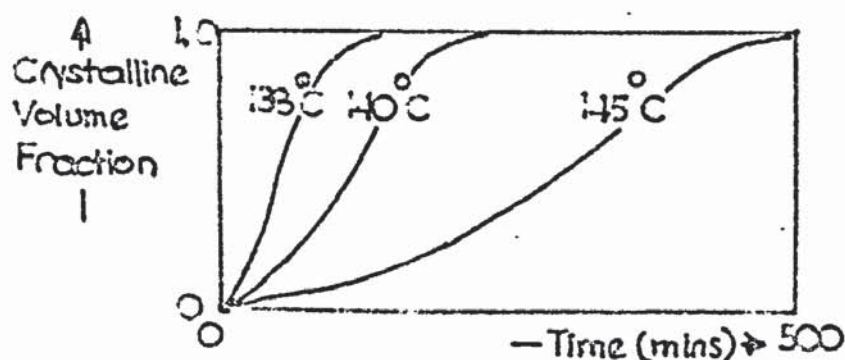


Fig.2.6.

and a table of half - time of crystallisation at various temperatures (Table 2.1.). One notes that the maximum measurable rate occurred at 130°C.

Cryst.Temp. °C	$t_{\frac{1}{2}}$ Mins.
125	Too fast to measure
130	13.5
135	40.2
140	115.0
145	264.0
Molten at 180°C for 15mins.	

Table 2.1..

Griffith and Ranby (27) also used dilatometry. They stated that when the crystallisation temperature of a polymer is lowered the crystallisation rate increases, passes through a maximum, then decreases as the glass transition temperature is approached. Polypropylene crystallises too rapidly at and below 133°C to permit meaningful dilatometric measurements to be made. The rate - temperature curve can therefore be defined neither in nor below the region of maximum rate using this method.

Measurements by Keith and Padden (28) indicate that the rate continues to rise as the temperature is lowered to 115°C., indicating that the rate maximum lies at or below 115°C.

Marker and Hay (29) used microscopy to study the kinetics of crystallisation of polypropylene. They followed the spherulite growth rate with time at various temperatures in the region 120 - 160°C by measuring the number of spherulites appearing with time. They found the expected relationship that the, lower the temperature of crystallisation, the faster the rate of growth, and also that the number of spherulites produced in a certain volume increased

initially with time but gradually reached a constant value as the spherulites began to touch each other. They managed to get down to a crystallisation temperature of 120.5°C at which the radial growth rate was $0.48 \mu\text{m s}^{-1}$ compared to the value at 145°C which was $0.0035 \mu\text{m s}^{-1}$.

Magill (30) followed the crystallisation of polypropylene using a polarising microscope technique. He shows curves of light depolarisation vs. time at various crystallisation temperatures (Fig.2.7).

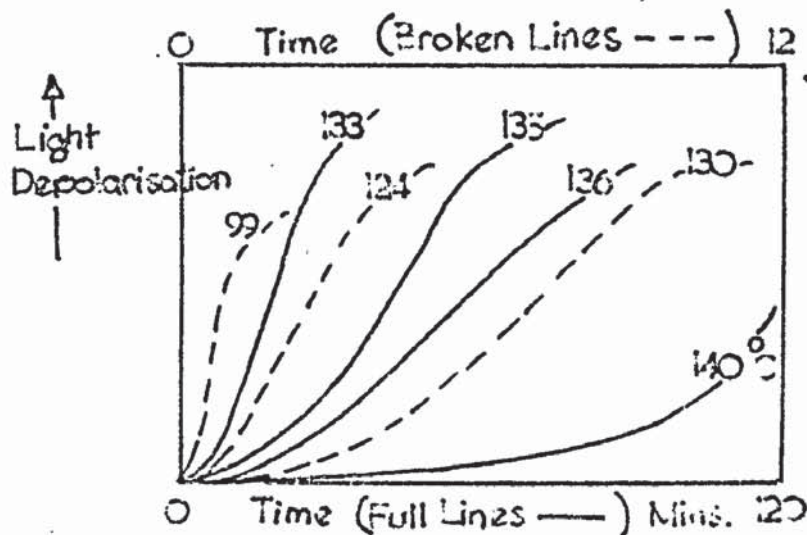


Fig.2.7.

From his results Magill predicted that a maximum in the crystallisation rate occurred in the region of $60 - 70^{\circ}\text{C}$ and that the generation of nuclei was simultaneous or predetermined and the morphology spherulitic above about 115°C . Below this temperature nuclei were sporadically formed (in time) and the geometry of the crystallised material ranged from spherulitic to unidentifiable shapes.

Binsbergen and De Lange (31) studied the kinetics of nucleated polypropylene and discovered that within a limited temperature region, a linear plot of $\log v$ vs. T was obtained where v is the linear growth rate of spherulites in cm s^{-1} and T is the temperature of crystallisation in $^{\circ}\text{C}$.

Kuhre et al (32) discuss the effects of crystallisation modified (nucleated) polypropylene. They state that without the additive the temperature of maximum crystallisation rate is about $114 - 121^{\circ}\text{C}$. With the nucleating agent present the temperature of maximum crystallisation can be raised as high as 142°C . This augmented nucleation produces much finer and far more numerous spherulites as the polymer solidifies from the molten state. Accompanying this change in polymer morphology are a marked increase in crystallisation rate and an upward shift in the crystallisation temperature.

Lane (33) also discusses the differences and advantages of nucleated and unnucleated polypropylene. In general the nucleated material has a more uniform crystalline structure and its higher crystallisation temperature results in larger crystallite dimensions and a higher degree of crystallinity. Nucleated specimens tend to give a large number of small spherulites and unnucleated ones a small number of large spherulites.

Beck and Ledbetter (34) studied the heterogeneous nucleation of crystallisation in polypropylene using differential thermal analysis. They state that a polymer's morphology and its degree of crystallinity are functions of the growth rate, i.e. the overall rate of nucleation and the spherulitic growth rate. At relatively low cooling rates i.e. at temperatures just below the melting point the

spherulitic growth rate predominates over the nucleation rate, and a few large spherulites and relatively high crystallinities are obtained. At more rapid cooling rates the large dependency of the nucleation rate predominates over the spherulitic growth rate, and many small spherulites with a resulting lower amount of crystallinity are obtained (Fig.2.8).

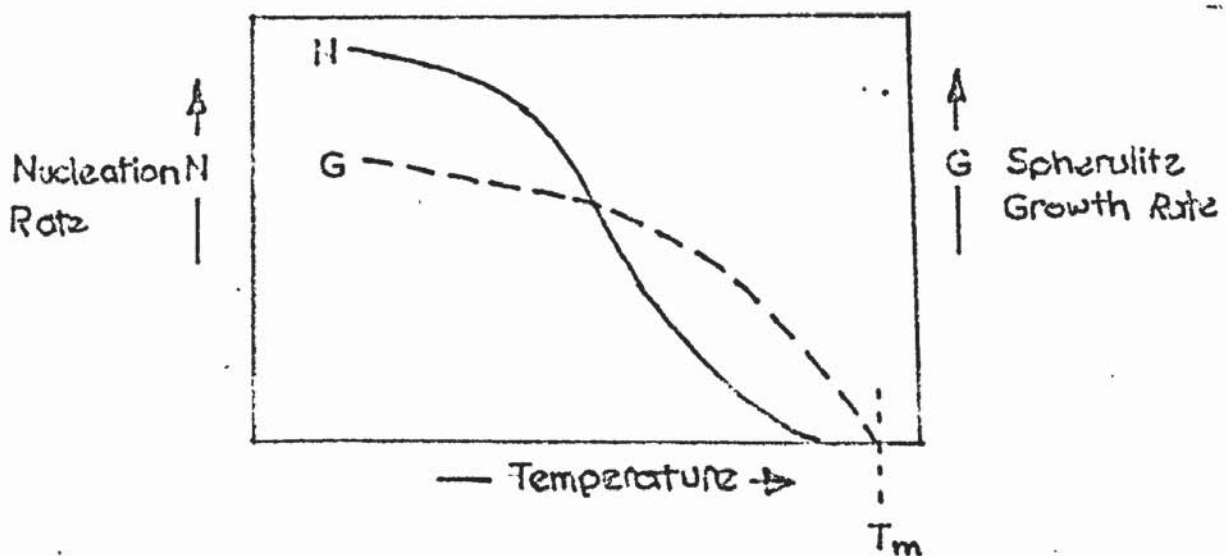


Fig.2.8.

There seems then to be some confusion as to the value of the temperature of maximum crystallisation, probably because no satisfactory method has been established for following the very fast rates at the lower temperatures of crystallisation. Values in the range $114 - 121^{\circ}\text{C}$. have been quoted. It is generally agreed that this temperature is markedly increased by the addition of nucleating agents.

Their addition also leads to an increase in the rate of crystallisation and a more uniform crystalline structure..

It appears that nearer the melting point spherulite growth predominates leading to a few large spherulites, and at the lower temperatures nucleation predominates and a lot of small spherulites are produced. The value of the melting point is pressure dependent and pressure can induce nucleation.

It also appears that heterogeneous nucleation is the process by which nuclei are produced, although Magill says that below 115°C. nuclei are sporadically formed.

2.2.7. Crystallinity determinations in polymers.

So far, techniques and theories have been discussed referring to the actual growth of spherulites on cooling from the melt to a suitable temperature. However, it is often desirable to have an indication of the extent of overall crystallisation that has taken place. To be able to do this a basic assumption has to be made, namely, that a semi-crystalline polymer is a simple two-phase structure of perfectly crystalline or amorphous regions. This is an oversimplification but if this is assumed then the concept of "degree of crystallinity" can be used. Richardson (35) says that this is probably justified if usage is restricted to unoriented polymers. He says that bulk polymer normally crystallises spherulitically; spherulites are highly ordered. Regions of disorder occur between growing fibrils, and a two phase model appears to be a good approximation. He adds that this does not favour any particular morphology but merely implies that interfacial effects are small. It has been shown by Segerman and Stern (36), using nylon fibres, that in

oriented polymers intermediate states of order exist.

Richardson also discusses the techniques available for measuring crystallinity, including specific volume, X-ray diffraction, infra-red absorption and enthalpy of fusion using differential calorimetry. A degree of crystallinity is in principle obtainable from any crystallinity dependent quantity although different techniques will give different values. Specific volume determination is the simplest and most convenient method. The weight fraction degree of crystallinity, X , is given by:

$$X = \frac{v_a - v}{v_a - v_c} \dots\dots\dots(2.5.)$$

where v , v_a and v_c are the specific volumes of the sample and completely amorphous and crystalline polymer respectively. The derivation of this equation assumes volume additivity of crystalline and amorphous phases. This, in turn, implies that interfacial effects are negligible and voids absent. Direct evidence for or against these assumptions is difficult to obtain on the basis of density measurements alone. A good test is the consistency, or otherwise, of crystallinities obtained using a variety of techniques and covering the widest range, and in fact results fully justify these assumptions. For the particular case of polypropylene, Danusso et al (37) have shown that the degree of crystallinity, X , is given by:

$$X = \frac{0.983 + 9 \times 10^{-4} (T + 180) - v}{4.8 \times 10^{-4} (T + 180)} \dots\dots\dots(2.6)$$

where T = temperature in $^{\circ}\text{C}$, v = specific volume

$(\text{cm}^3 \text{g}^{-1}) = 1/d$, where d = density g cm^{-3} .

Density can be determined by any of the common methods, although the "density gradient column" method is the most popular (38).

2.3. Mechanical Properties of Polymers.

2.3.1. General

The mechanical properties of polymers are of interest in any application where they are used as a structural material. Mechanical tests provide information as to the useful service life of polymers. They are also important, however, because they show how mechanical behaviour is related to different physical structures that may be produced under varying conditions.

Thermoplastics are visco-elastic materials whose properties are very dependent on temperature. Their behaviour depends on the relative values of the viscous and elastic components. On the application of stress there follows:

- (a) An instantaneous elastic deformation (owing to the bending and stretching of primary valence bonds).
- (b) A retarded, and recoverable, elastic deformation (owing to the molecular configuration moving to the new biased equilibrium associated with an elongated or orientated stressed state).
- (c) An irrecoverable deformation (owing to polymer chains or segments slipping past one another).

These effects can be shown diagrammatically by showing the variation of strain with time when a stress is applied and then removed. (Fig.2.9).

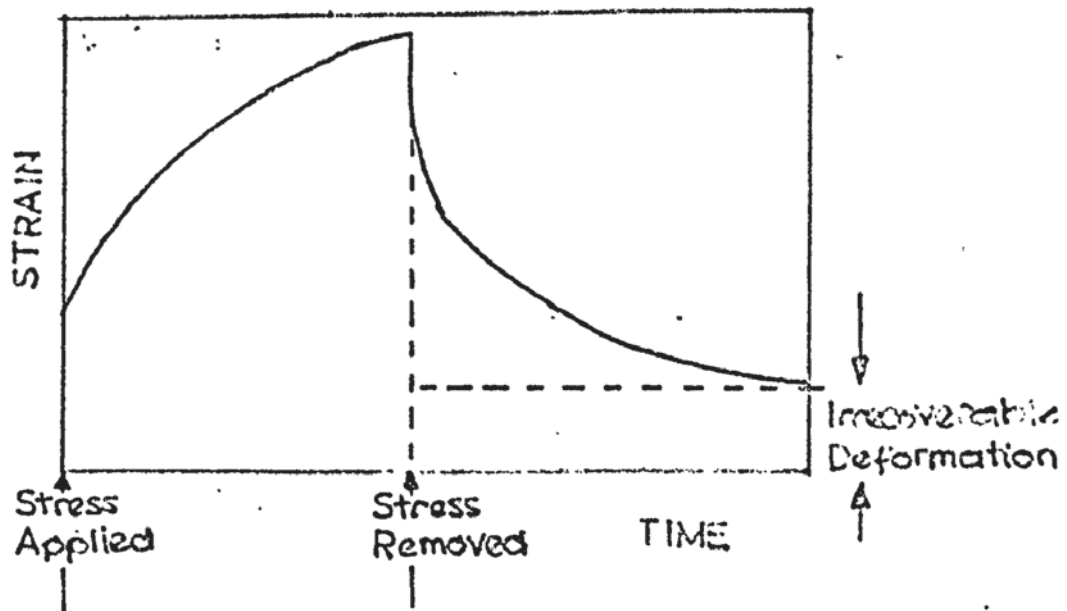


Fig.2.9. Variation of strain with time

A number of mechanical tests may be used to study visco-elastic materials (39). The most important tests include creep, stress-relaxation, stress-strain (tensile test), and dynamic mechanical behaviour.

For creep measurements a load is applied to a test specimen, and its length is measured as a function of time. In stress-relaxation measurements the test specimen is rapidly stretched to a given value, and the force required to hold the length constant is measured as a function of time.

Tensile tests, are made by stretching the sample at a constant rate of elongation until failure occurs. The stress gradually builds up until the specimen either breaks or yields. From the stress-strain curve one can calculate a modulus (ratio of

stress/strain over the initial part of the curve at low strains), the ultimate elongation, and the breaking or ultimate tensile strength of the material. The stress/strain curve also indicates whether a material is brittle or ductile in nature. If the rate of strain is very high, this type of test becomes similar to an impact test which measures toughness or energy required to break the test specimen. The area under a stress-strain curve is proportional to the energy absorbed in breaking the material.

The speed at which test pieces are stressed is important, since their mechanical properties are time - dependent by virtue of their long chain structure. At very slow speeds, molecules will tend to slip past each other and the magnitude of the tensile stress will depend on the magnitude of the forces between the molecules. At very high speeds however there will be no time for the molecules to move relative to one another and the specimen will break only when the individual molecular chains are broken. The tensile stress will generally be higher in the latter case.

In dynamic mechanical tests the test specimen is deformed by a stress which varies sinusoidally with time. The oscillating stress and strain are generally not in phase. Such tests enable the calculation of an elastic modulus and a mechanical damping or the dissipation of energy into heat. The measurements are generally made over a wide range of frequencies or at a number of temperatures. This type of test is especially useful in studies of the molecular structure of polymers and in the relation of structure to transitions in polymers.

2.3.2. Dynamic mechanical test methods.

In dynamic mechanical tests the oscillating stress and strain are generally not in phase; the strain lags behind the stress. The phase angle between the stress and strain is designated δ .

The stress can be split into two components, one which is in phase with the strain and another one 90° out of phase; this leads to the definition of two dynamic moduli:-

- (a) A 'storage modulus' (G' or E') which is the ratio of in-phase stress amplitude to strain amplitude.
- (b) A 'loss modulus' (G'' or E'') which is the ratio of 90° out-of-phase stress amplitude to strain amplitude.

In the case of shear, the dynamic moduli are defined by:-

$$G^* = G' + iG'' \quad \dots\dots\dots(2.7)$$

while the dynamic Young's moduli are defined by:-

$$E^* = E' + iE'' \quad \dots\dots\dots(2.8)$$

G^* and E^* are the complex moduli; G' and E' are the real parts of the shear and Young's moduli respectively. The quantity "i" is equal to $\sqrt{-1}$, so G'' and E'' are the imaginary parts of the moduli.

In general,

$$|G^*| = \sqrt{(G')^2 + (G'')^2} \quad \dots\dots\dots(2.9)$$

and

$$|E^*| = \sqrt{(E')^2 + (E'')^2} \quad \dots\dots\dots(2.10)$$

The imaginary parts of the moduli are damping terms which determine the dissipation of energy into heat when a material is deformed. The damping term is the "dissipation factor" or "loss tangent" and is defined as G''/G' or E''/E' . From a vector diagram relating the various moduli (Fig.2.10) it can be seen that the damping is equivalent to $\tan \delta$.

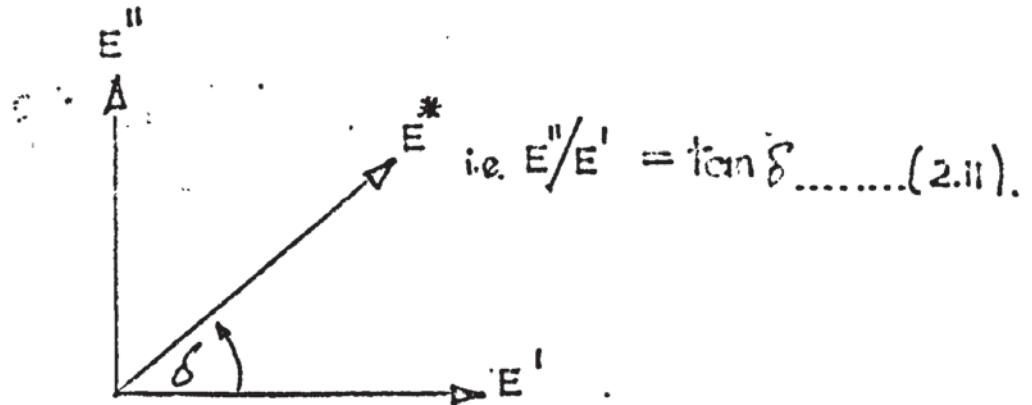


Fig.2.10 Vector diagram showing relationship between moduli.

Many types of instrument have been used to measure dynamic mechanical properties, and each type of instrument gives rise to terms which are defined differently for each test. The torsional pendulum (40) gives a measure of the shear modulus, and the damping is calculated from the logarithmic decrement, i.e. the ratio of the amplitudes of two successive oscillations. The vibrating reed (40), in which the specimen is clamped at one end and forced to vibrate transversely at the other, is widely used for measuring Young's modulus and damping. Forced vibrations are also used in which the applied load and the resulting deformation are measured separately; in this case the complex modulus can be calculated from the ratio of the magnitudes of amplitudes of load and deformation while the damping can be calculated from the phase shift between the load and deformation curves. Disadvantages of these techniques, include

- (a) difficulty of keeping the frequency constant as the temperature is changed,
- (b) careful preparation of large test specimens and complicated and time consuming calculations are often required, and
- (c) in some cases only a limited frequency range is available.

Recently, the "Rheovibron" a direct reading instrument (41) has become available for determining the dynamic tensile complex modulus and $\tan \delta$. An important feature is the furnace in which the sample is tested, since this enables the properties of a single specimen to be measured over a range of temperatures. The sample is clamped at both ends, one of which is driven at a definite frequency (a range of fixed frequencies are available) and a sinusoidal stress generated at the other. These are both measured electronically by means of dividers which subtract the values of the vectors allowing $\tan \delta$ to be read off directly. The dynamic modulus is simply calculated from a knowledge of the length and cross-sectional area of the specimen, and the amplitude of force on the sample. The apparatus makes it possible to measure at frequencies of 3.5, 11, 35 and 110 Hz. The measurement range of $\tan \delta$ is 0.001 up to approximately 1.7, and the dynamic modulus can be measured over the range of 1MNm^{-2} to 100GNm^{-2} by regulating the cross-sectional dimension of the sample. The size of sample generally used for measurement is 0.2 - 0.3mm in thickness, 2 - 3mm in width and from 2 to 6cm in length. An electric furnace is used

over a temperature range from ambient to 250°C (low temperatures can be achieved using air cooled in liquid nitrogen) and, since the instrument is direct reading and the measurement operation at one point is completed in a few seconds, dispersion curves of complex modulus of elasticity and $\tan \delta$ can be prepared over a wide range of temperatures in a very short time. A feature of the instrument is the relatively small sample size.

Dynamic data are especially important for structural applications of plastics as the variation of properties is easily determined as a function of temperature and frequency. Nielsen (39) states that dynamic mechanical tests have proved to be extremely useful in studying the structure of high polymers. These mechanical properties are very sensitive to glass transitions, crystallinity, crosslinking and many other features of the molecular structure of polymer chains and the morphology of the bulk materials. In order to exploit the full potentialities of dynamic mechanical tests, measurements should be made over a wide range of both temperature and frequency. However, much useful information may be obtained in a short time by measuring the modulus and damping over a wide temperature range while keeping the frequency constant.

2.3.3. Dynamic mechanical properties of polymers.

Nielsen (39) shows a typical graph of dynamic mechanical properties vs. temperature for an amorphous uncrosslinked polymer (Fig.2.11).

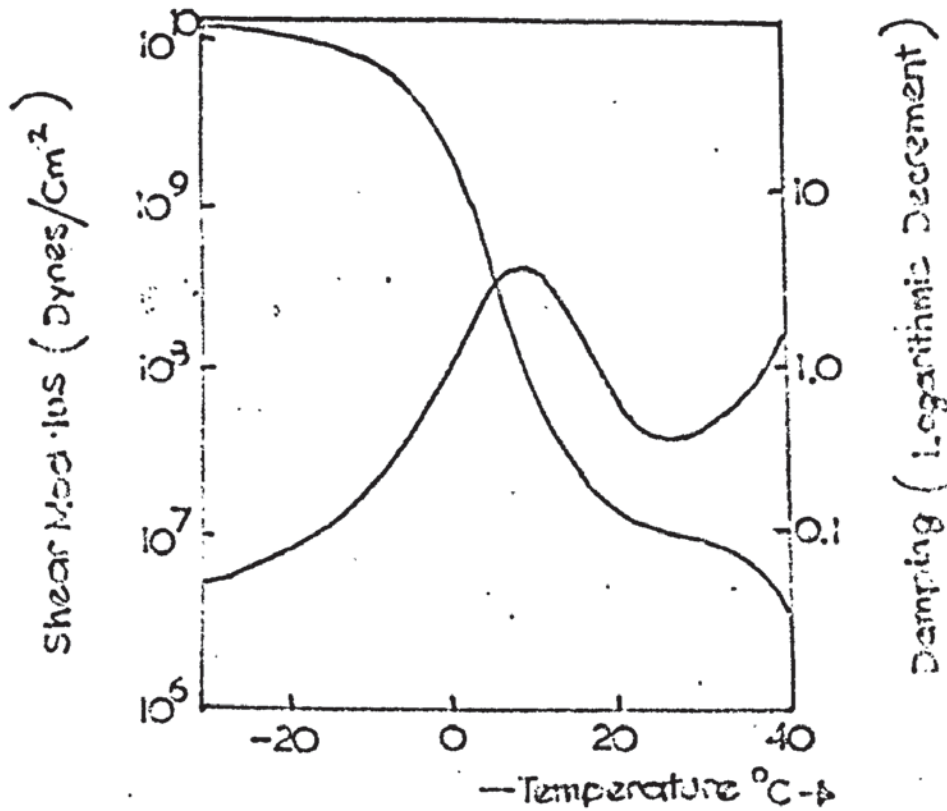


Fig.2.11 Typical dynamic mechanical behaviour vs. temperature

It can be seen that initially the modulus decreases very slowly as the temperature increases until in the region of the glass transition the modulus decreases by a factor of about a thousand in a short temperature interval. The modulus takes another drop at still higher temperatures due to the increasing role of viscous flow. The damping goes through a maximum and then a minimum as the temperature is raised. In the transition region the damping is high because some of the molecular chain segments are free to move while others are not. Below and above the glass transition the chain segments are frozen and free to move respectively and both states can store energy without dissipating it into heat.

Crystalline polymers generally show more complex dynamic mechanical behaviour than do amorphous polymers. Crystalline polymers always have a glass transition and generally at least one or two secondary transitions. There may also be transitions within the

crystalline phase. In addition according to Nielsen the mechanical properties are strongly dependent upon the degree of crystallinity, the size of the crystallites and the melting of the crystallites. The modulus decreases as the crystallinity decreases. Crystallites containing short chain sequences of polymer melt before crystallites which contain long chain sequences. Thus, small and imperfect crystallites melt at a lower temperature than large and more perfect crystallites. For this reason, the temperature dependence of the modulus above the glass transition temperature gives an estimate of the distribution of crystallite sizes. The difference between a highly crystalline isotactic polypropylene and a slightly crystalline, nearly atactic one, is illustrated (Fig.2.12). The high crystallinity of the isotactic polymer is reflected in its high modulus. The small size or imperfections of the crystallites in the nearly atactic material is partly responsible for its low melting point. Increasing crystallinity shifts the main damping peak to a higher temperature.



Fig 2.12 Dynamic mechanical properties of polypropylenes, (Ref.39).

In isotactic polypropylene three dispersion peaks have been distinguished (42), a weak peak between 30°C and 80°C , a very pronounced peak at approximately 0°C and a peak between -50 and -100°C . The agreement of T_g values from various experimental methods is not very good but ranges from about -30°C to 20°C . Dilatometric methods by Beck et al (43) have shown a transition between -20 and 0°C (depending on tacticity and thermal history), and a somewhat higher transition between 25 and 45°C . They attributed the low temperature transition to the presence of an amorphous atactic form of material and the higher transition to the presence of a non-crystalline isotactic form of polypropylene. They concluded that normal isotactic polypropylene was a three phase system made up of crystalline isotactic, amorphous isotactic, and amorphous atactic forms.

2.4. Effect of injection moulding process variables on crystalline structure.

So far, the crystallisation of polymers has been considered as occurring under quiescent conditions, but commercial processing involves some degree of stressing upon the crystallising polymer. As long ago as 1957 Keller (12) noted an effect of stress on crystallisation when he examined a piece of polyethylene that was crystallising while being stretched. He found that crystallisation was initiated from a continuous series of nuclei along the flow lines and produced a row of orientated lamellae which he called the "row structure".

In injection moulding the polymer melt is subject to the action of high shear stresses both as it leaves the nozzle, and during the filling of the mould cavity. This shearing of the polymer causes the entangled chains present in the melt to be "dragged out" and aligned along the direction of flow. This "orientation" is often confused with crystallisation since both processes

involve the aligning of polymer molecules.

However, orientation can effect the structure of moulded articles whether the polymer is semi-crystalline or non-crystalline. In the case of a semi-crystalline polymer, such as polypropylene, the crystallisation process will still have the predominant effect on the resultant structure, but orientation can induce crystallisation since the lining-up of the chains from the application of an external force favours the crystallisation process. A further complicating factor is that orientation is used to describe both the process (alignment, stretching) and the property present in the final product, and so it is quite usual to talk of certain crystalline regions as being "orientated".

In the injection moulding of semi-crystalline polymers the important factor is the process of crystallisation which occurs in the cooling of the polymer melt in the mould. After injection into the cavity rapid cooling of the melt takes place at the walls, while at the centre the polymer is still molten. The first portions of the molten polymer, as they come into contact with the walls of the mould, must be subject to shear stress in the direction of flow and crystallise rapidly at the walls of the mould. Growth of the crystals from the surface will continue unimpeded if new centres of crystallisation have not yet formed within the melt.

Whisson (44), who has reviewed the effects of processing conditions on the properties of injection moulded thermoplastics, states that on rapid cooling in the mould, crystalline growth in the outer zones of the moulding is inhibited and a more highly crystalline interior of higher density is formed. Ballman and Toor (45), who have proposed a mechanism of non-isothermal plastic flow during mould filling, have assumed that the incoming melt which contacts the mould walls first is unorientated because the flow pressure gradient will be zero there at the wave front. Subsequent layers cool

with increasing slowness and are subject to shearing forces, which results in an increase of orientation towards the centre, the maximum orientation occurring somewhere between the surface and the centre. The unorientated frozen skin concept is supported by Woebcken's work on birefringence measurements (46). However, other workers (e.g.47) suggest that the skin is highly orientated; but doubts have been cast as to the sensitivity of the shrinkage and reversion techniques used. Glanvill, (3) states that the surface of the moulding is only slightly orientated since this material is at a high temperature and has only been exposed to a low degree of shear. However, further material laid immediately beneath this skin will not solidify immediately, being thermally insulated from the mould by the first layer. As the material loses temperature, and becomes more viscous, under the influence of the injection pressure flow will continue, although more slowly than the hot central core. Shear under these conditions leads to a high degree of orientation (Fig.2.13).



Fig.2.13 Orientation profile across the thickness of the moulding (Ref.3).

E.S. Clarke (48 and later with Garber, 49) examined the structure of injection moulded tensile test bars of polyoxymethylene (polyacetal). This polymer crystallises very readily in the form of folded-chain lamellae. He proposed that three effects influence the orientation of lamellae during crystallisation; surface nucleation, temperature differentials, and induction time for crystallisation. The photomicrographs of cross sections that he obtained were consistent with the existence of three types of orientation of the lamellae. The relative amounts of these types of orientation in a bar were a function of the particular moulding conditions. The first type of orientation, found near the surface, was 0-125 μm deep. The lamellae were perpendicular to the surface of the moulding and perpendicular to the extrusion direction, and he attributed this first type of nucleation to the combined effects of thermal gradients and surface nucleation. The second type of orientation was found from a depth of 125-1,070 μm , and in this region the lamellae were perpendicular to the surface of the bar, but tended to lose their preferred orientation with respect to the injection direction. In this second region, some new nucleation occurred giving rise to spherulites. The third type of orientation began at a depth of 1,070 μm and extended to the centre of the bar 1,550 μm . Crystallisation in this core region was a consequence of spontaneous nucleation, which in the absence of strong temperature gradients, resulted in the formation of spherulites. No overall preferred orientation of lamellae was exhibited. Additional support for the proposed mechanism of crystallisation was gained by changing the temperature difference between the mould wall and the melting point of the polymer. It was expected that a higher temperature differential would result in a thicker surface of preferred orientation. As predicted the bar with the lower wall

temperature showed a deeper penetration of preferred orientation of lamellae. Temperature differential was also changed by changing the freezing point of the polymer. This was accomplished by changing the pressure on the melt. As the pressure on the melt was increased the freezing point of the polymer increased by about 1°C per 7 MNm^{-2} increase in pressure. And so the higher the injection pressure, the greater is the temperature difference between the freezing point and a constant mould wall temperature. As expected, the effects of high injection pressure were similar to the effects of low wall temperature.

Lapshin (50) discusses the effect of the degree of super-cooling of the polymer melt in the mould on the crystallisation rate. With a very small degree of super-cooling he predicts that the crystallisation process is similar to that of isothermal crystallisation. However these conditions are rarely used, since with short moulding cycles the articles are not sufficiently rigid to be ejected without deformation, while with too long cycles brittle articles are frequently produced. With a medium degree of super-cooling there is created in theory the most favourable relationships between the number of nuclei and their rate of growth. He predicts that under these conditions the crystallisation will take place inside an "envelope" formed by the rapid solidification of the melt at the walls. He assumes too that the orientation in this layer is far greater than that at any position in the centre. At the maximum degree of super-cooling the flow of the melt and its crystallisation take place simultaneously, and accordingly the crystallisation of the polymer in the stressed state takes place more rapidly than in relaxed specimens. However, the shear deformation at the boundaries between the growing supermolecular

formations may, he states, prevent the establishment of order at the boundaries and lead to the formation of layer structures with alternation of ordered and non-ordered layers. Thus, he concludes, the temperature of the mould is the most important parameter in the injection moulding of crystalline polymers since it determines the conditions of crystallisation of the polymer in the mould.

The fundamental thermal and mechanical treatments that a polymer undergoes during injection moulding, and their effects on polymer morphology have been analysed by Maxwell (26). From a simple analysis of the injection moulding process he decided that the effects of flow, shear deformation, thermal history and hydrostatic pressure on polymer morphology must each be considered. The effects of shear deformation and flow can be considered together. When the polymer is forced through the nozzle some of the mass will receive a high degree of orientation, whereas other parts will not. Maxwell states that shear deformation can change the kinetics of the crystallisation process. A photomicrograph is shown of polypropylene, to which a shear deformation was applied just at the time it was quenched to 120°C. By comparison with similar cycles the number of nuclei had greatly increased, leading to growth units of smaller size. To demonstrate the effect of thermal history a photomicrograph was prepared of a sample of polypropylene that had been allowed to grow spherulitically. The same sample was then remelted until all birefringence had disappeared, and then re-cooled. It was noted that the nucleation and growth of the spherulites on re-cooling had taken place in the periphery of the old spherulites. This illustrated that in the process of original growth of spherulites, impurities had been pushed from the centre of the spherulite out to the periphery.

Upon re-cooling, the foreign matter deposited in the periphery had acted as nucleation sites for new crystallisation. The literature contains other illustrations, however, where, upon briefly melting polymeric materials and then cooling, re-growth of exactly the same spherulites from the same nuclei and with the same size can be produced. Thermal history then has an important effect on resulting morphology, and, to ensure uniformity of structure, melting time must be long enough to destroy all previous nucleation history. It is possible, however, that for certain applications the thermal history effects, with brief melting, might be utilised to produce a grain structure. Finally, he discusses the effects of hydrostatic pressure on morphology. Pressure can induce crystallisation and to demonstrate this two photomicrographs were shown of polypropylene which was exposed to two different pressure histories (see section 2.2.5). Maxwell concludes that by controlling the above variables during processing, samples can be produced with desired morphology and properties.

Nikitin and Marusenko (51) have studied the effects of processing conditions on the structure of polypropylene. They describe results of the effects of melt temperature, mould temperature, injection pressure and screw forward time on the structure and density. In general they found that an increase in melt temperature and mould temperature led to an increase in spherulite size both at the centre and the edge of a moulded bar. An increase in injection pressure and screw forward time, however, led to a decrease in the spherulite size. Also as the variables are increased the density increases, although with an increase in melt temperature there is a slight reduction in the value of density.

Kvyatkovskaya and Lapshin (52) have shown that the use of higher mould temperatures in processing polyethylene produces the greatest increase in density. Only slight increases in density occur when either the melt temperature or the injection pressure is raised. They have suggested that these small increases are due to improved packing. The loss of pressure experienced on injection of the melt is minimised by using high melt temperatures and consequently the pressure developed in the mould under these conditions is greater than with lower melt temperatures. These effects are said to reduce the degree of crystallinity, and this has been noticed in polypropylene by Robb (53). The effect of melt temperature on density is, therefore, difficult to resolve.

It can be seen then that during the injection moulding process the polymer is not allowed to crystallise under quiescent conditions, but that it crystallises under conditions of high stress; the alignment of molecules or orientation affects the crystallisation process. The structure most commonly described is a structure consisting of a rapidly chilled 'skin' on the surface of the moulding with a central region consisting of larger structural units.

The mould temperature and the resulting temperature difference between polymer and wall has the dominant effect on crystallinity and density. An increase in mould temperature, reduces orientation, increases spherulite size and increases density. An increase in melt temperature reduces orientation, and since nucleation density is reduced leads to larger spherulites; density has been shown to both increase and decrease. An increase in injection pressure increases the shear stress and orientation.

It can also induce nucleation and smaller spherulites are thus produced; density, however, has been shown to increase, probably due to improved packing.

The skin has been said by different workers to be both highly orientated and un-orientated, but most orientation should occur at a point somewhere between the surface and the centre. The thickness of the skin has been shown to be approximately 100 μ m.

2.5. Structure and Mechanical Properties of Semi-Crystalline Polymers.

Mechanical behaviour of crystalline polymers can either be interpreted in terms of an imperfect single crystal or of a continuous amorphous phase reinforced with crystalline regions. The increase in modulus with increasing crystallinity, occurring without break from the point of zero crystallinity, as shown by Leitner (54) using raw rubber, would seem to favour the concept of a continuous amorphous phase.

The effect of crystallinity on the mechanical properties of polymers is complicated by the fact that as the degree of crystallinity changes, other factors such as spherulite size, fibril width, molecular tying between fibrils and orientation may change (10). A further difficulty in interpreting the data reported in the literature is that variations in mechanical properties may be correlated with changes in secondary variables, such as temperature of crystallisation. As these lead to changes in crystallinity it is probable that the true correlation is with crystallinity. Molecular weight is a further factor important in determining crystallinity and may therefore be considered as a secondary variable.

However it would appear that properties related to the initial part of the stress-strain curve, such as modulus, are determined mainly by crystallinity, whilst ultimate properties, such as load at break, involve more complex aspects of morphology such as spherulite size and composition. In general it may be said that hardness, stiffness, tensile modulus, heat distortion temperature and tensile yield increase, whilst elongation at break and impact strength both decrease with increasing crystallinity. Over and above this change, as spherulite size increases, it is found that impact strength, elongation at break and yield stress all decrease.

Results with polypropylene indicate that yield stress, Young's modulus, stiffness, hardness and softening point all increase, but impact strength decreases with increasing crystallinity.

A number of authors have reported the effect of spherulite size on the mechanical properties of semi-crystalline polymers. Starkweather and Brooks (55) showed that the yield point of polyethylene could be increased by decreasing the spherulite size at constant degree of crystallinity. However, concomitant changes in the lamellar microstructure were ignored in this study. Kargin (56) and Sogolova (57) found that the yield point and tensile strength of polypropylene were increased by additions of crystal-nucleating agents. The increasing strength was correlated with a decreasing spherulite size in these studies. Khure et al (32) noted a similar trend of increasing strength in polypropylene with additions of nucleating agents. The trend of reported results thus indicates that semi-crystalline polymers can be rendered somewhat stronger by decreasing the spherulite size.

Gumen et al (58) investigated the effect of spherulite size in the centre of a block of poly-formaldehyde on the mechanical properties. They discovered that the size of the spherulites in injection moulded blocks influenced mainly the elongation at break. For example, specimens which have central spherulites measuring $6\mu\text{m}$ break at 15% elongation, while those with central spherulites measuring $12\mu\text{m}$ break at 5% elongation. On the other hand, the size of the spherulites had practically no effect on the tensile strength or the linear region of the stress-strain curve and hence on the elastic modulus. They explain the increased deformability of the smaller spherulites by the fact that the structural reorganisation (orientation, recrystallisation) of small spherulites is more apt to occur than that of large spherulites.

Remaly and Schultz (59) examined the ageing of spherulites of polypropylene in an attempt to check whether the improved strength properties that can be obtained are associated with the strength increase which accrues with ageing in the polymer. Their results indicated that the spherulite size effect is not developed instantaneously upon formation of the spherulitic microstructure, but rather awaits additional structural rearrangements. These rearrangements will either be development of orientation in amorphous zones, the growth of new smaller spherulites in the original interspherulitic zones, or yet another microstructural variation.

The effect of degree of crystallinity on the dynamic visco-elastic properties of polymers, i.e. the dynamic modulus of elasticity, and the damping, has been studied by Perepechko et al (60). They found that an increase in the degree of crystallinity led to an increase in the dynamic modulus when the polymer was at temperatures higher than the glass transition temperature T_g . However during a study of the dynamic visco-elastic properties of polychlorotrifluoroethylene it was shown that the dynamic modulus was anomalously dependent on the degree of crystallinity at temperatures below 50°C . At temperatures above this the normal dependence was shown. They also observed this anomaly with polyethylene specimens below -50°C . These "inversion points" at which there is a change in the nature of the relationship between the dynamic modulus and the degree of crystallinity, correspond to the glass transition temperature region. They explained this anomalous dependence as the result of the coincidence of two phenomena. As the degree of crystallinity increases the total proportion of crystalline region in the polymer increases, and a certain amount of ordering occurs in the arrangement of the chains within the crystallites. This process, they said, should produce an increase in modulus. The other effect is, when the percentage

crystallinity increases, the density of the amorphous fraction decreases together with the efficiency of the molecular interaction, which should lead to a reduction in modulus. This, they say, should be particularly evident when the efficiency of the molecular interaction is fairly high, i.e. in the glassy state.

Neilsen (61) found an amazingly good correlation between the dynamic shear moduli of a series of polyethylenes and the specific volumes of the polymers at the same temperature over the temperature range between 20°C and the melting point. The relation was:-

$$\log_{10} G = 26.671 - 16.21 v \quad \dots\dots(2.12)$$

where v is the specific volume of the polyethylenes in ml g^{-1} , and G is the shear modulus in dynes cm^{-2} .

Sauer et al (62) and Van Schooten et al (63) have all found that the dynamic shear modulus increases while damping decreases as crystallinity is increased in polypropylene. Muus et al (64) have shown the effect of crystallinity on damping and shear modulus of polypropylene using the torsional pendulum. Figure 2.14 shows the results they obtained.

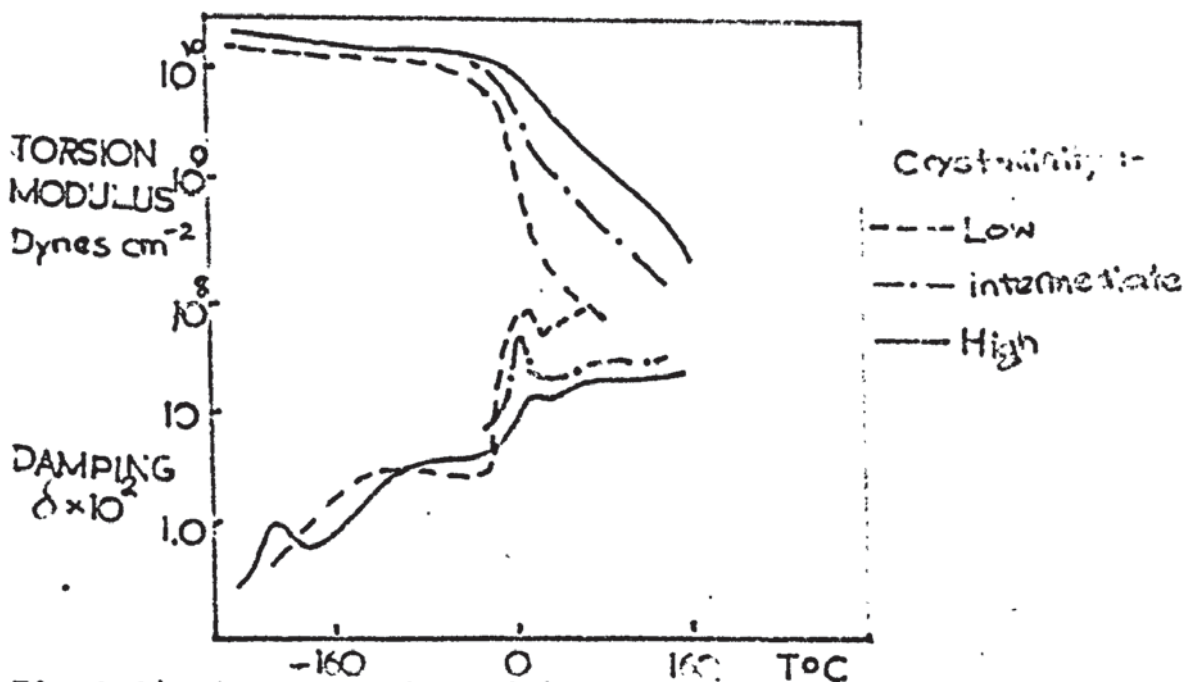


Fig.2.14 The variation with temperature of the torsion modulus and damping for three polypropylenes with different crystallinity.

The height of the transition is determined by the amorphous content. For instance between the temperatures of -160°C and -20°C the modulus of the highly crystalline polypropylene was 30% greater than that of the sample of low crystallinity. However, at 23°C , owing to the intervening transition at 0°C , the difference is more than 500%. Heijboer (65) examined the shear modulus and the damping at 10 - 0.5 Hz as a function of temperature for polypropylenes of different densities (Fig.2.15). The transition for the amorphous polymer was accompanied by a decrease in the shear modulus of more than 90%. Moreover this peak decreased with increasing crystallinity so its molecular origin must lie in the amorphous part.

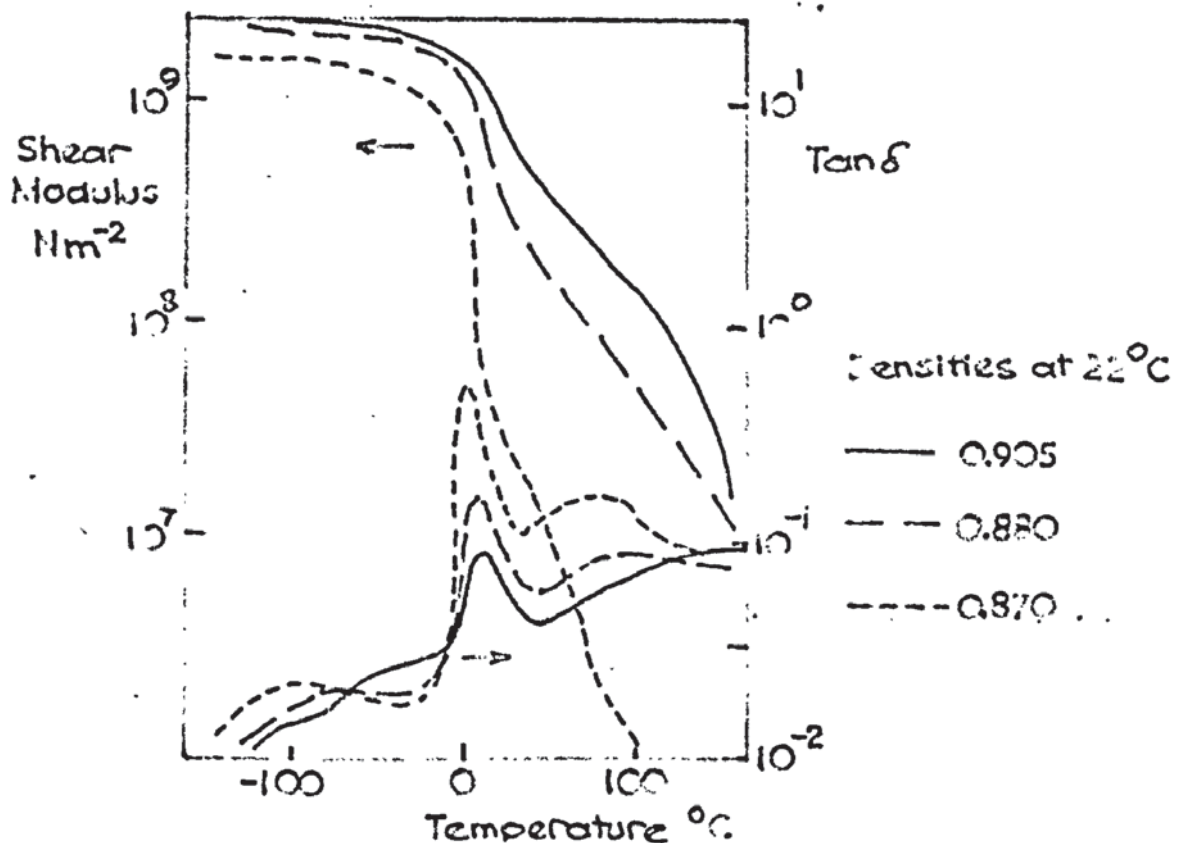


Fig.2.15 Variation of shear modulus and damping ($\tan \delta$) with temperature for polypropylenes of different densities.

The properties of a polymer are normally related to density or crystallinity since the two parameters can normally be interchanged. Sometimes properties are related to other variables although differences are still probably due to the resulting change in crystallinity. In general as crystallinity increases modulus or stiffness increases and damping decreases. Ultimate properties too, such as elongation to break, are lower. Variations in strength and toughness are in general more dependent on the spherulite size. Smaller spherulites increase strength and in particular elongation to break. An explanation as to why spherulite size is important as regards the ultimate properties can be found if the mode of deformation of spherulites is examined.

The size and number of spherulites present in a polymer influences the mode of deformation. Keith and Padden (66) have discussed the mode of deformation encountered in films of polyethylene 5 - 50 μm in thickness. A sample with large spherulites failed at a low stress with low elongation. The crack propagated around the boundaries and through spherulites, and there appeared to be no preferred fracture path. With smaller spherulites brittle fracture occurred at the spherulite boundaries. Very rapid quenching produced a film where drawing initially took place at the boundaries and then the spherulites began to yield in place of, or in conjunction with, boundary yielding. Yielding of the spherulites often produced a neck across the spherulite diameter. Keith and Padden suggested that the difference in deformation behaviour was due in some measure to the difference in the number of tie molecules holding the lamellae together. Other factors to be considered are that in thin films the spherulite boundaries are thinner than the rest of the film; any surface restraint will restrict contraction and so lead to voids at the spherulite boundaries.

CHAPTER 3 - EXPERIMENTAL DETAILS

3.1. Plan of work.

The important injection moulding variables are mould temperature, injection pressure, melt (barrel) temperature, and cycle time. The majority of workers consider that mould temperature has the predominant effect on the resulting structure, and this has received most attention. The other variables have received less attention and, of these, injection pressure the least. It was decided therefore to study the effect of injection pressure on structure more closely. In order to do this the cylinder temperature and hence the melt temperature will be kept constant throughout since it has been shown that (53) variations in melt temperature can result in a variation of measured cavity pressure.

A range of mould temperatures will be used and at each one samples will be injected over a range of injection pressures, cycle time being kept constant. Temperature and pressure conditions relevant to the most significant structures will then be selected and the effect of moulding time examined. In this way it is hoped to build up a complete picture of the effect of temperature, pressure and time on the crystalline structure.

Because of heat transfer problems in normal mould cavities it was decided to design and construct a simple mould cavity of a material of low thermal capacity. The cavity also had provision for inserting a thermocouple and pressure transducer.

The injection moulding machine in the laboratory was easily modified for the increased cycle times required.

Standard equipment will be used for microtoming, photomicrography and density determinations.

Dynamic mechanical properties will be determined using the Rheovibron.

3.2. Material used.

"Propathene" LYM 42, natural polypropylene, supplied by I.C.I., Plastics Division, was used throughout. This is a linear homopolymer of very high isotactic content. LYM 42 is a lightly stabilised, easy flowing, injection moulding grade. So that all work could be done on the same batch of material, three 25 kg bags, from the same batch, were supplied. (Batch No. CK No. 3292 N.).

3.3. Injection Moulding of samples.

3.3.1 Injection moulding machine.

The injection moulding was performed using an Edgwick 1214 - HY type 'S' (Mk.II) screw injection moulding machine (67). A general view of the instrument is shown in figure A.1. This machine is fitted with a screw-type injection unit which provides a maximum shot volume of 98 cm³. Water cooling is used to effect a near constant temperature of the hydraulic oil. The plasticising cylinder houses a 41 mm diameter injection screw. The raw polymer is hopper-fed directly onto the screw, and travels to the nozzle end of the cylinder through a non-return valve which allows pressure on the material to be maintained during injection. The cylinder barrel and nozzle are heated by four resistance heater bands which are individually controlled by thermostats.

The amount of polymer fed to the screw is controlled by a plunger cam which trips a microswitch when the screw reaches a pre-set position ensuring a constant volume of melt. This was adjusted initially to a suitable position, and this value used throughout.

The fully automatic cycle is controlled by three relay timers; the pressure timer of range 0 - 30 s, the cooling timer 0 - 30 s, and the dies-open timer 0 - 10 s. After the mould is closed and injection occurs the pressure timer is activated and regulates the time for which the screw remains forward. At the end of this period the screw returns and the cooling timer operates controlling the time for which the mould remains closed and the article cools. Following this the mould opens, the sample is ejected, and the mould remains open for the time set on the dies-open timer. The cycle is then repeated. Under semi-automatic operation, however, the dies-open timer is not used since the opening and closing of the mould is initiated manually.

The machine was modified slightly in order that longer screw forward and cooling times could be achieved. This was done by incorporating on-off toggle switches in such a way that the timer could be isolated until required.

N.B. Care must be taken that the extended times used are not so long that the hydraulic oil becomes overheated.

The injection pressure is produced by hydraulic oil acting on a 152 mm diameter ram. This hydraulic ram is in turn connected to the screw. The injection pressure reading on the dial gauge at the hydraulic pump end of the machine is a measure of the pressure acting on the ram and so is very much smaller than the pressure achieved at the nozzle end by the screw tip. The force on the ram is given by:-

$$\text{Force} = P_1 \times A_1$$

where P_1 = dial gauge reading and A_1 is the cross-sectional area of the ram. This force will be transmitted to the screw producing a pressure at the screw tip given by:-

$$P_{\text{screw}} = \frac{\text{Force}}{A_2}$$

assuming no pressure losses, and where A_2 is the cross-sectional area of the screw.

$$\begin{aligned} \text{So } P_{\text{screw}} &= \frac{A_1}{A_2} P_1 \\ &= 13.7 P_1 \end{aligned}$$

So the pressure at the screw tip is 13.7 times the dial gauge reading assuming no pressure losses. The cavity pressure calculated this way corresponds quite well with the actual cavity pressure reading from the transducer meter, although there is always a loss in pressure which increases as injection pressure increases, (see later).

The maximum pressure attainable is 113 MN/m^2 , (16,400psi).

3.3.2. Mould cavity.

A scale drawing (Appendix) and photograph (Fig.A.2) of the mould is shown.

The important feature to note is the very shallow cavity depth of 1.59 mm. Initial trials were carried out with mould cavities of depths 0.20 mm and 0.30 mm but these were far too small to allow complete mould filling at lower mould temperatures. It was important to ensure complete filling of the cavity otherwise pressure measurements would not have been meaningful. The cavity was made as small as possible so that it could be assumed that any change in the temperature of the mould was immediately transferred to the polymer mass in as short a time as possible. This thickness allows full mouldings to be produced at all temperatures and pressures and at the same time is thin enough to ensure that mouldings achieve the mould temperature throughout their cross section very quickly.

Assuming the polymer sample to be a slab at a particular temperature suddenly brought into contact with two surfaces at another temperature, simple heat transfer calculations show that within 10 - 30 s the centre of the polymer has reached the temperature of the mould. This applies to the incoming polymer melt acquiring the set mould temperature and also to the sample when it is cooled down to room temperature before ejection. Menges (68) has done similar calculations on a 4 mm slab of polyethylene and states that it takes 78s for the centre to reach 21°C from a temperature of 260°C . Gloor (69) has shown that the freeze-off time for a 1.6 mm slab of polyethylene when cooled from 230°C to 80°C is 6s.

As can be seen from fig.A.2. the specimen produced is a simple test piece strip. The mould cavity was originally made by hobbing the shape into one of a pair of copper blocks, but the copper yielded after a few runs and its further use abandoned. It was then decided to machine the cavity into a block of "Duraluminium" aluminium alloy. This was far more successful since the metal could withstand very high clamping pressures without yielding. The two halves of the mould were bolted to blocks of Syndanyo and the latter in turn to steel backing plates through which connection was made to the platens of the machine. Duraluminium has a very low thermal capacity and can thus take up and lose heat very rapidly. To prevent stray heating effects to and from the mould material the mould halves were encased in blocks of good insulating material, Syndanyo. Steel backing plates were introduced to increase the overall strength.

To measure the cavity pressure the pressure transducer was fitted so that the pressure sensitive diaphragm formed part of the moulding surface. An extension of the cavity was cut out to accommodate this (Fig.A.2). The transducer was bolted through its securing holes to a steel plate connected to the back of the platen. The positioning of the transducer was governed by the limited opening in the machine back platen, and because of its position (almost directly behind the sprue puller) and its long length the normal Z-pin ejector system had to be dispensed with. Another sprue pulling device had to be devised and it was eventually decided that the best technique was to use a small undercut around the periphery of the sprue bush.

The sprue bush itself was made of hardened steel and was later modified to allow water to circulate around it through a small channel. This was done so that the cavity could be artificially sealed when very high temperatures were used, but in fact for the present study was not used.

The cooling and heating channels were made as large as strength requirements would allow and as can be seen were drilled as close as possible to the moulding cavity.

Temperature was recorded by a thermocouple situated in the base of the "Dural" block at a slight angle so that the tip was only a millimetre or so away from the surface (Fig.3.1).

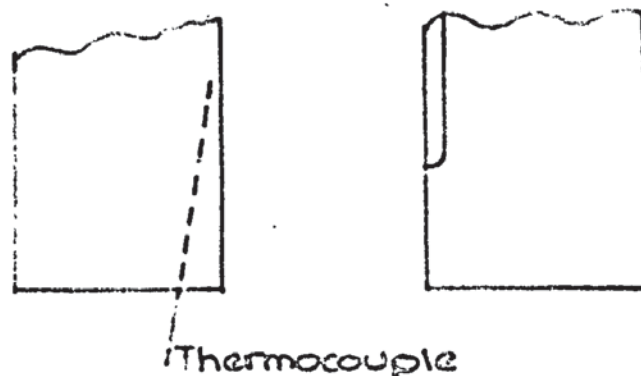


Fig.3.1. Showing thermocouple location.

With the mould materials used and the dimensions used it was assumed that this temperature was representative of both the mould and the polymer.

The standard procedure for setting the moulds described in the machine handbook was followed.

3.3.3. Mould temperature control.

Steam heating was used to heat the mould cavity in the region 100 - 150°C and the Churchill water heater for the range 25 - 100°C. For temperatures below 25°C cold water was passed through the mould.

The steam was generated from an oil-fired boiler, and originally the supply for the mould was taken from another piece of laboratory equipment containing a pressure-reducing valve and was controlled through this valve. However fluctuating demand on the boiler and inaccuracy of the pressure-reducing valve led to poor temperature control. Hence a separate circuit was built for the mould and a very accurate pressure-reducing valve incorporated (70).

The circuit used is shown schematically below (Fig.3.2).

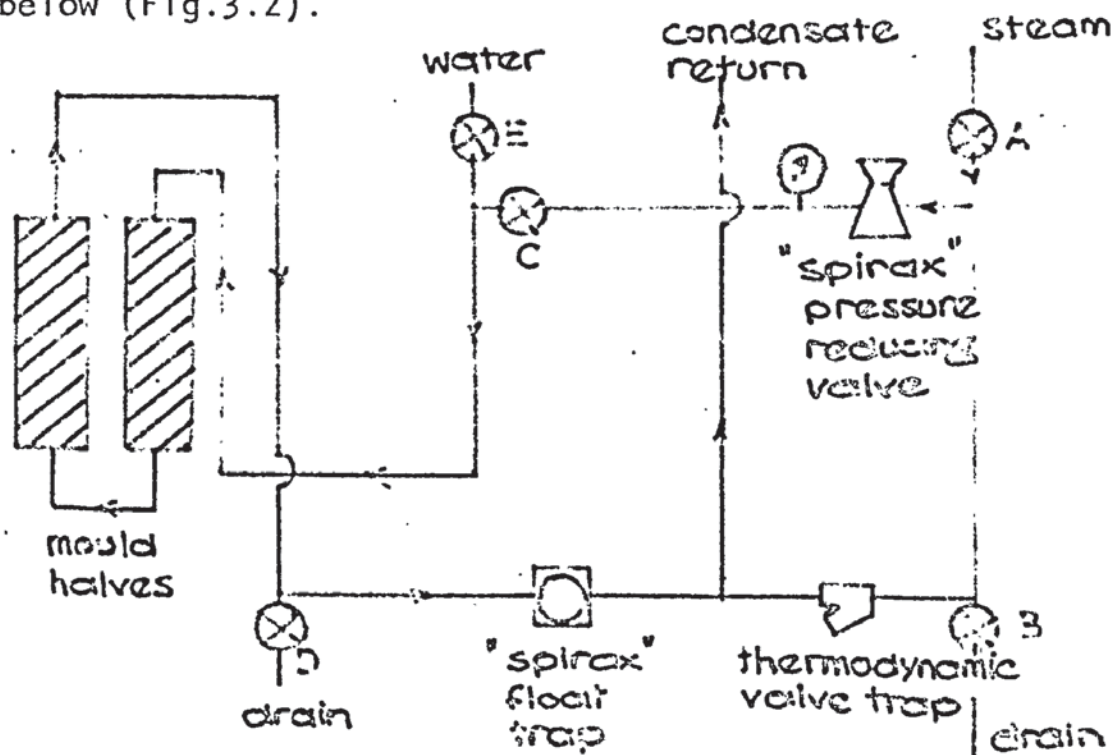


Fig.3 2. Steam heating circuit used for mould.

To heat the mould main steam was turned on at valve A and allowed to run through valve B to drain until live steam appeared, all other valves being closed.

Valve C was then opened and valve B closed and steam passed through the mould and allowed to run through valve D to drain. When live steam appeared here valve D was turned off and the steam allowed to return via condensate return. The temperature was adjusted by varying the steam pressure using the 'Spirax' valve. An approximate calibration curve was constructed relating steam pressure (dial reading) to mould temperature attained and can be found in appendix 1.

Temperature control to an accuracy of $\pm 0.5^{\circ}$ could be achieved using this set-up. In order to cool the mould the steam was turned off at the mains and drain valves B and D opened. Valve C was then turned off and valve E opened to allow water to run through the mould to drain. When cooled the temperature of the mould dropped very rapidly and reached room temperature within 30s, although for samples prepared in this study cooling water was passed for one minute.

The Churchill water heater (71) is shown diagrammatically below (Fig.3.3). Cold water is heated to the set temperature and passed through the mould continuously. If the temperature of the water is raised too high a solenoid valve cuts in and hot water is discharged to drain and replaced by cold water.

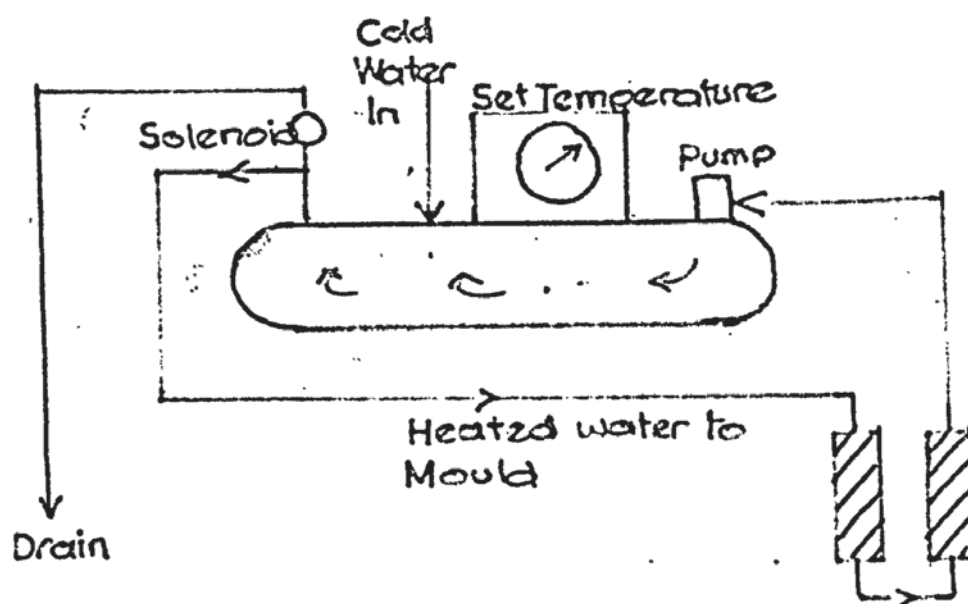


Fig.3.3. Churchill water heater.

3.3.4. Calibration of pressure transducer and thermocouple.

The Dynisco pressure transducer was connected through a C-52 transducer meter (72) to a single channel pen recorder (73). The thermocouple was a "Pyrotenax" chromel-alumel thermocouple and was connected to another single channel pen recorder (see Fig.A.3).

The optimum gauge setting on the transducer meter and the voltage range on the recorder were determined by injecting at the maximum pressure it was envisaged would be used with the meter on the highest range. The range selector was then reduced until the optimum full scale deflection was obtained. By adjusting the recorder range in conjunction with this it was possible to find a combination of settings at which all pressure readings would be on scale without any need to change ranges and with no fear of overscaling. The optimum values were found to be '25' setting on the transducer meter and IV setting on the recorder. Using these settings the recorder chart paper was calibrated and it was found that one division corresponded to 1.7 MNm^{-2} and full scale deflection to 170 MNm^{-2} . The Dynisco was found to be temperature dependent and so

when the mould was heated there was a slight deflection (slight negative pressure reading) on the trace, however after approximately three minutes this had levelled out to a new value slightly lower than the set value as shown (Fig.3.4).

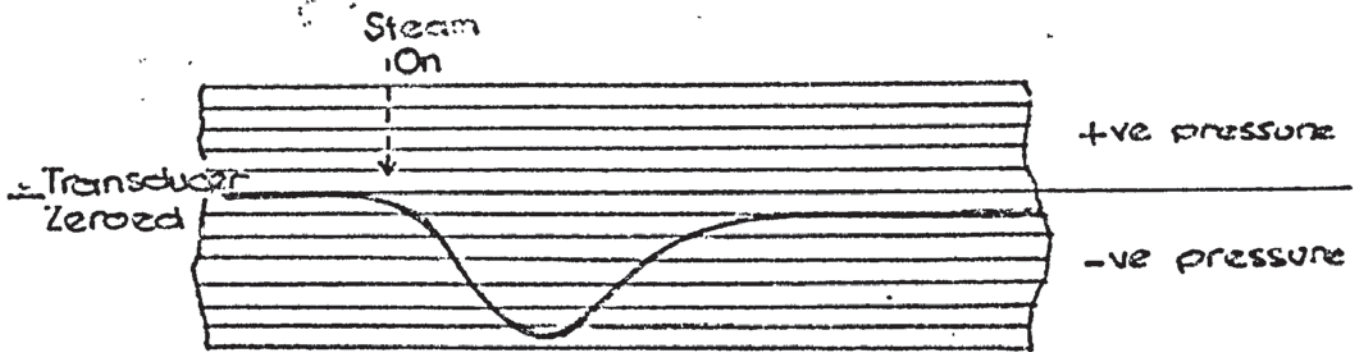


Fig.3.4. Start of a typical pressure trace.

The same effect was shown when the mould was cooled down. It was therefore necessary to allow at least three minutes after equilibrium mould temperature had been attained before commencing to mould to ensure that the pressure transducer had stabilised.

The thermocouple was calibrated by immersing it in crushed ice and water and adjusting the recorder to zero. With a chromel-alumel thermocouple 0mV corresponds to 0°C , and so millivolts could then be read off and converted directly to a temperature without subtracting any room temperature correction.

3.3.5. Preliminary examination of moulding behaviour.

Certain aspects of the moulding behaviour were noted from an examination of the initial pressure traces.

(a) Sealing behaviour.

When the screw was returned before part of the moulding had sealed an instantaneous drop in pressure occurred due to leakage through the molten polymer. This could also be demonstrated by changing the ram pressure and observing the resultant changes in cavity pressure; as soon as the cavity was sealed further changes in

ram pressure caused no change in cavity pressure. Since it was desirable to know how the cavity pressure changed with thermal conditions alone it was decided that the screw should remain forward until at least part of the moulding had sealed, so that on its return no instantaneous pressure drop occurred. It was found that a screw forward time of three minutes was long enough for mould temperatures up to 140°C ; at temperatures above this up to 155°C a slight drop was still produced.

(b) Cavity pressure losses.

Having calibrated the transducer meter pen recorder it was possible to calculate the maximum pressure achieved in the cavity for each set value of injection pressure. This was determined for each injection pressure and compared to the predicted cavity pressure calculated from area considerations. Results are shown in Table 3.1 and it can be seen that values compare quite closely although due to pressure losses the measured value is always less than the predicted value, and this is particularly noticeable at the highest pressures.

Dial gauge reading		Measured cavity pressure	Predicted cavity pressure	Percentage pressure loss
psi	MN \bar{m}^2	MN \bar{m}^2	MN \bar{m}^2	
200	1.3	17.2	18.9	9.6
300	2.1	27.6	28.3	2.8
400	2.8	36.2	37.8	4.4
500	3.5	44.8	47.2	5.4
600	4.1	55.1	56.6	2.8
700	4.8	62.0	66.1	6.6
800	5.5	65.5	75.5	15.4
900	6.2	67.2	85.0	26.5
1000	6.9	67.2	94.4	40.5

Table 3.1. Comparison of measured and predicted cavity pressures

3.3.6. Moulding procedure.

To ensure consistency of mouldings it was essential that a strict sequence of operations should be determined and adhered to. The following routine was used throughout the present study.

- (a) Cooling water to the hopper, hydraulic oil and Dynisco mechanism was turned on and the barrel heaters set to the required melt temperature value and switched on.
- (b) The transducer meter and pen recorder and thermocouple pen recorder were switched on and adjusted to suitable base line values.
- (c) The steam heating to the mould was turned on and a check made to see that all the valves were opened correctly. The steam pressure was adjusted to that required for the particular mould temperatures.
- (d) The machine was then put into action by:-
 - (i) Switching to semi-automatic operation.
 - (ii) Starting the motor.
 - (iii) Switching to hand operation.

- (e) The barrel was filled by opening the feed hopper and rotating the screw. The barrel was thoroughly purged by alternately pressing the "screw rotate" and "plunger inject" buttons until clean polymer appeared.
- (f) When it was checked that the barrel had been purged thoroughly and refilled, and the mould had reached an equilibrium temperature moulding was commenced.
 - (i) The two toggle switches connected to the timers were closed so that the timers were out of circuit.
 - (ii) The mould platens were closed using the starwheel and the floating platen locked.
 - (iii) The mould was then opened and the machine switched to semi-automatic operation.
 - (iv) The mould was closed and injection followed automatically.
 - (v) The pressure was kept on for a predetermined length of time (normally three minutes) and then the first toggle switch was thrown to bring the pressure timer into operation, causing the screw to return.
 - (vi) After a further interval of time (normally three minutes), having passed cooling water for one minute, the second toggle switch was thrown and the cooling timer came into operation. This removed the die locking force and the mould was opened using the starwheel.
 - (vii) The sample was ejected by careful manipulation.

The time for which the sample was held at the mould temperature in the cavity was called the moulding time. The total time for which the sample was held in the cavity or total cycle time was therefore equal to the moulding time plus the cooling time (see Fig.3.5).

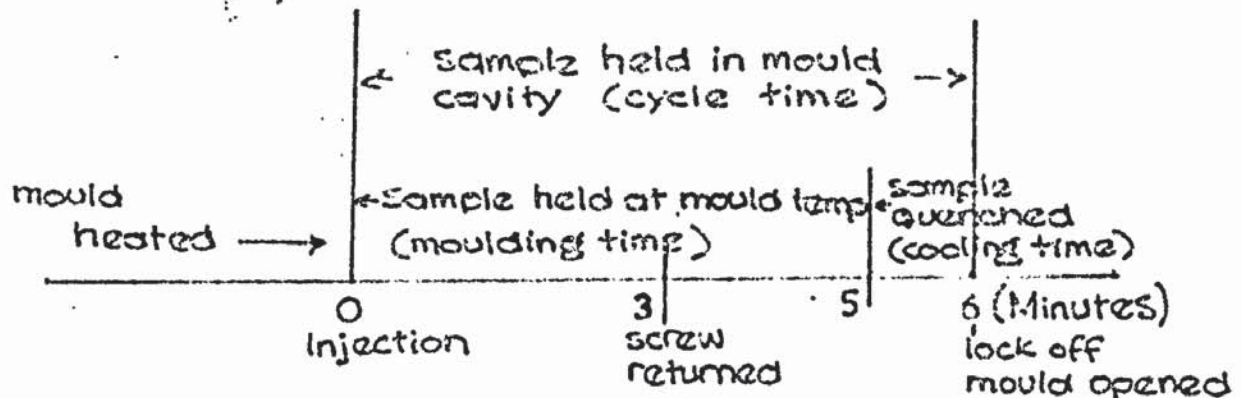


Fig.3.5. Scheme of typical moulding cycle.

After each specimen had been moulded the barrel was purged at least five times before preparing subsequent samples.

Using this procedure it was found that if identical moulding conditions were used then identical pressure profiles were produced.

3.3.7. Samples prepared.

A series of samples were made at various mould temperatures in the range 10 - 150°C and various injection pressures in the range 0.86 - 6.9 MN m⁻² at a constant time held in the mould cavity of five minutes. A constant screw forward time of three minutes was used and cooling water was passed for one minute (Table 3.2).

These samples indicated conditions which produced structures which would be particularly affected by increasing the time for which the sample was held in the mould cavity, so at constant values of mould temperature and injection pressure mould times of 1, 10, 20 and 40 minutes were used (Table 3.3).

The three barrel and one nozzle heater were all set at 225°C and left at these values throughout. In practice however, due to the cooling round the hopper, the rear temperature was always 5 - 10°C lower than this set value.

Tables 3.2 and 3.3 show the conditions under which samples have been prepared and which formed the basis of this study.

Mould temp. °C	Injection pressure									
	125	200	300	400	500	600	700	800	900	1000
	0.86	1.3	2.1	2.8	3.5	4.1	4.8	5.5	6.2	6.9
10		x			x			x		
40		x			x			x		x
63		x			x			x		x
109		x			x			x		x
118	x									
120		x			x			x		x
122	x									
125		x	x	x	x	x	x	x	x	x
127.5		x	x	x	x	x		x		x
130	x	x	x	x	x	x	x	x	x	x
132.5		x	x	x	x	x	x			x
135		x	x	x	x	x	x	x	x	x
137.5			x	x	x	x	x			x
140	x	x	x	x	x	x	x	x	x	x
145		x	x	x	x	x	x	x	x	x
150		x			x			x		

Table 3.2. Samples prepared at constant moulding time of 5 minutes.

	Mould temperature °C								
	130			140			150		
Injection pressure MN m ⁻²	1.3	4.1	6.9	1.3	4.1	6.9	1.3	4.1	6.9
Moulding time (mins)									
1	x	x	x	x	x	x	x	x	x
10	x	x	x	x	x	x	x	x	x
20	x	x	x	x	x	x	x	x	x
40	x	x	x	x	x	x	x	x	x

Table 3.3. Samples held for various moulding times at constant mould temperature and injection pressure.

3.4. Examination of structure.

3.4.1. Preparation of specimens for sectioning.

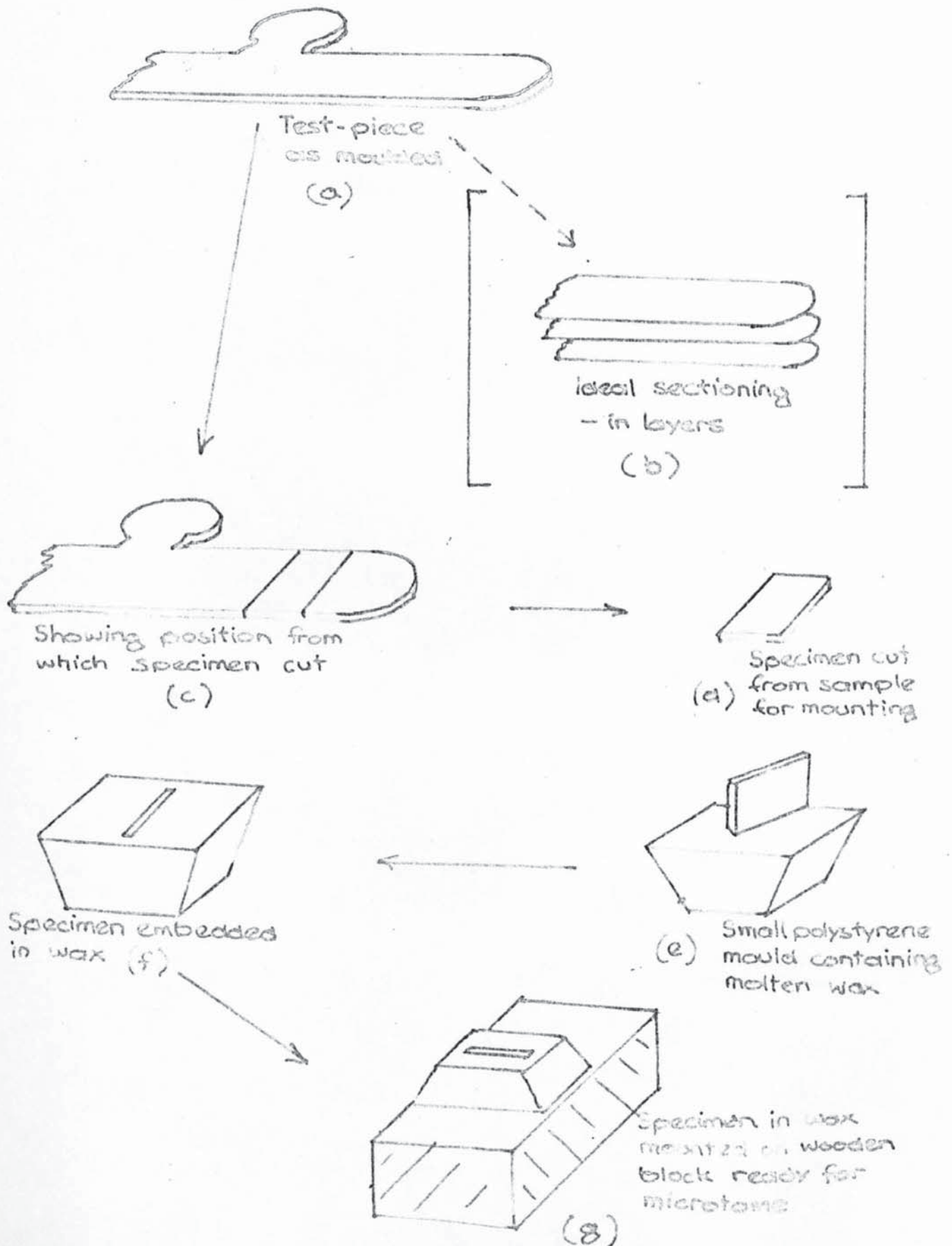
An outline of the procedure for preparing specimens for sectioning is shown in Fig.3.6.

It was desirable to examine the structure profile across the thickness of the moulding, but to section layers length-wise and examine each one separately (b) was difficult because of sample mounting difficulties. Hence it was decided to section across the sample in one particular place (c). Specimens were cut from approximately the same position in each moulding (d). They were then embedded in molten wax (small moulds had been previously filled with molten wax and the wax allowed to almost solidify - specimens were then pushed in) as shown (e and f), and the wax left to harden (one hour at least). The wax blocks containing the specimens were then carefully removed from the moulds and mounted onto small wooden blocks by melting the base of the wax and pushing onto the block. After trimming excess wax away the blocks were then ready for the microtome (g).

3.4.2. Sectioning of samples.

Thin sections of the samples were obtained using a Cambridge rocking microtome (74) (Fig.A.4). Using the procedure outlined in the handbook slides of the specimens were prepared by selecting suitably sectioned slivers and placing them on a glass microscope slide using tweezers. Cover slips were secured using thin strips of adhesive tape. The cutting distance was set at 10 μ m.

Fig.3.6. Outline of preparation of specimens for the microtome.



3.4.3. Microscopy and Photography.

All microscope slides were examined under the ordinary laboratory microscope using polarised light, and sketched. The most significant ones were then photographed using a Carl Zeiss Photomicroscope II (75). This is a highly accurate microscope with a 35 mm camera incorporated in the microscope stand; this ensures consistently perfect adjustment. The film is contained in a cylindrical magazine which is locked in the base of the microscope (Fig.3.7). The advantage of this particular microscope is that specimens can be viewed during exposure with the built-in "Optovar" magnification changer.

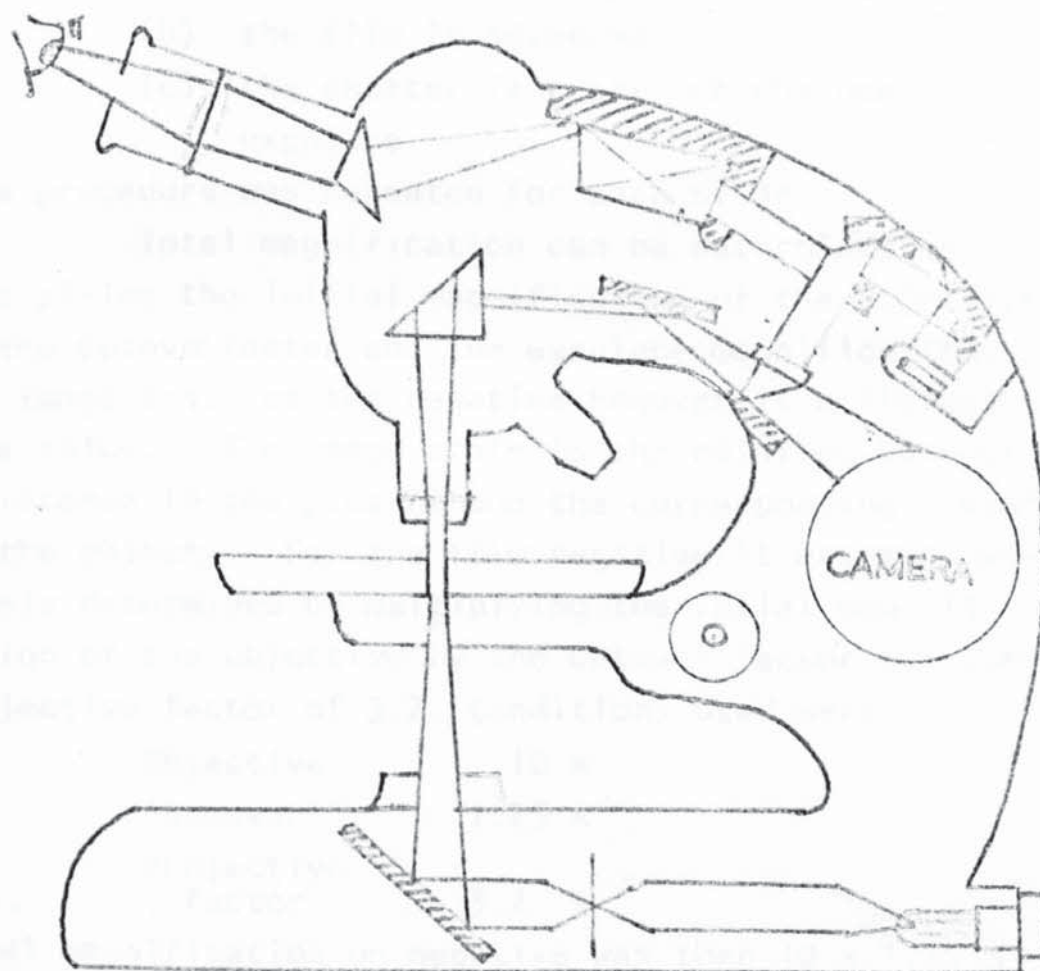


Fig.3.7. Outline of Carl Zeiss Photomicroscope II.

Having set the microscope for polarised light the film (Panatomic-X FX-135 black and white, Kodak Ltd. - 36 exposures) was loaded into the camera and the camera locked into the microscope. When the eyepiece had been focussed accurately the microscope slide was placed on the stage and the specimen located. Suitable magnification was selected by varying the objective lens in conjunction with the Optovar until a well resolved field of view was produced. A knob was pushed to set the field of view ready for photography and this was refocussed and repositioned if necessary. The instrument was then ready for photography and the shutter button was pressed. This single button triggers the following operations:-

- (a) the shutter opens and closes
after automatic exposure timing.
- (b) the film is advanced.
- (c) the shutter is reset for the next exposure.

This procedure was repeated for each slide.

Total magnification can be determined by multiplying the initial magnification of the objective by the Optovar factor and the eyepiece magnification. The image scale on the negative however is different to this value. The image scale is the relation between a distance in the picture and the corresponding distance in the object. For the film negative it was approximately determined by multiplying the initial magnification of the objective by the Optovar factor and the projective factor of 3.2. Conditions used were:-

Objective	10 x
'Optovar'	1.25 x
Projective factor	3.2 x

Total magnification on negative was then $10 \times 1.25 \times 3.2$ or 40 x.

A micrometer slide containing a scale with

inscribed divisions of 0.01 mm and 0.1 mm was also photographed.

3.4.4' Density determinations.

Density was determined by immersing small specimens that had been cut from the mouldings in a density gradient column (76). The column was prepared by carefully mixing two solutions of propan-2-ol and water of different densities in the column and this gave a range of densities from approximately 0.900 g ml^{-1} at the top to 0.920 g ml^{-1} at the bottom. The majority of samples fell within this range of densities. The column was calibrated by carefully lowering floats of different known densities into the column and measuring their heights. A graph of height vs. density was then plotted (Appendix 2). The column was kept in a water jacket maintained at a temperature of 23°C .

Specimens were cut from the same position in each moulded sample - approximately 20 mm from the end of the sample. Different shapes were used for ease of identification in the column, and were approximately $10 - 20 \text{ mm}^2$ in area. Earlier results had shown that a slight variation in density existed along the length of the moulded sample, the density being greater nearer the gate region. It was decided however that since this was a small difference (approximately 0.2%) readings would only be taken from the one position.

Using the equation of Natta (37) percentage crystallinities were determined from the density measurements,

$$\frac{0.983 + 9 \times 10^{-4} (T + 180) - v}{\dots\dots\dots} \dots\dots\dots (3.1)$$

$$X = \frac{4.8 \times 10^{-4} (T + 180)}{\dots\dots\dots}$$

which at 23°C becomes:-

$$X = \frac{1.1657 - v}{0.09744} \times 100\% \dots\dots (3.2)$$

3.5. Dynamic mechanical testing.

The dynamic complex modulus $|E^*|$, and the damping $\tan \delta$, of specimens were measured using the Rheovibron.

3.5.1. Sample preparation.

The dimensions of the test specimen for use on the Rheovibron are limited by the cross-sectional area that can be used, which in turn depends upon the modulus of the sample. A specification of measurement for the instrument drawn on a graph of cross-sectional area vs. modulus can be found in appendix 3.5. In general the size of sample should fall within the following range of dimensions:-

0.2 - 0.3 mm thickness,

2 - 3 mm width,

and 20 - 60mm long.

The mouldings produced in the cavity were too large to be used directly and so test pieces had to be cut from these. As has already been said, sectioning along the length of the specimen to produce layers was difficult due to specimen mounting difficulties, but it was found that if the sample could be clamped securely on its side, then by drawing a scalpel along its edge suitable test specimens were produced. A simple jig was constructed in which the sample could be clamped in the vice (Fig.3.8).

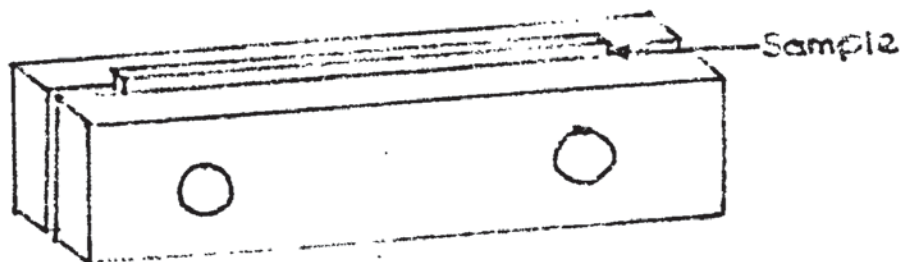


Fig.3.8. Jig for cutting test pieces.

By careful alignment of the sample in this jig a thin sliver could be cut off using a sharp scalpel. In order to eliminate any edge effects the samples were cut in half first and then the section was cut (Fig.3.9).

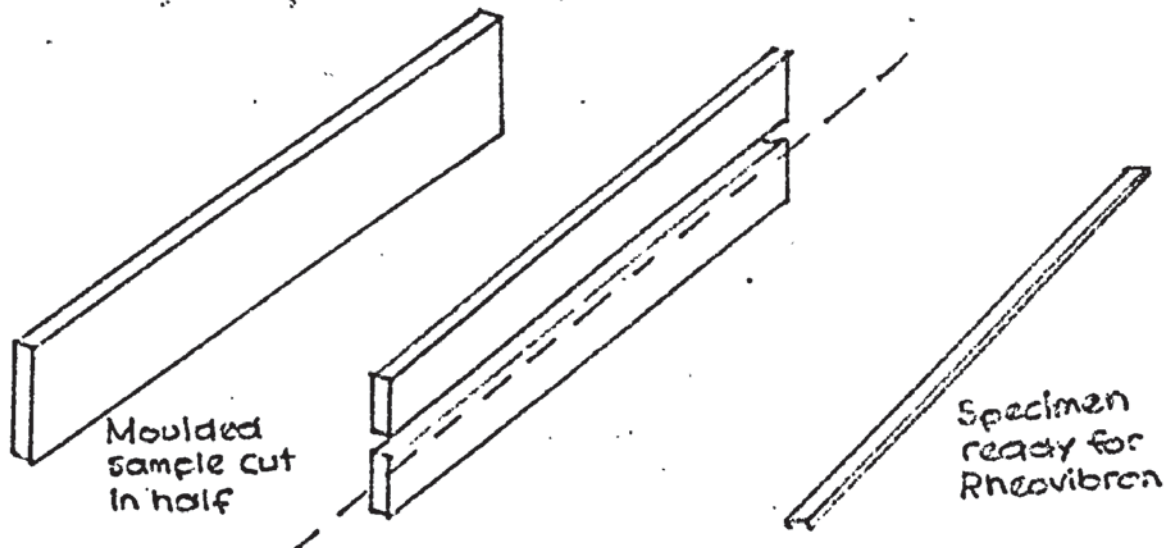


Fig.3.9. Position from which test piece cut. The dimensions were measured using a micrometer. Width and length were obviously fairly consistent; thickness varied slightly from sample to sample but it was checked that there was no variation of more than ± 0.025 mm in thickness along the length in any one specimen. Dimensions of the test specimens used were:-

0.15 - 0.4 mm thickness,
1.59 mm width,
and 40 mm length.

3.5.2. General principles of the Rheovibron.

A general view of the instrument is shown in Fig.A.5.

Sinusoidal tensile strain is applied at one end of the sample, sinusoidal stress is generated at the other end of the sample and the phase angle δ is found between the strain and the stress. Both ends of the sample are fixed to two strain gauges one of which is a transducer of displacement (T-7) and the

other of which is a transducer of generated force (T-1) (Fig.3.10). After the absolute values of the electrical vectors transduced from force and displacement are adjusted to unity (full scale of meter), vector subtraction is made by changing the connection of the output circuit of two strain gauges. $\tan \delta$ is read off directly and the modulus calculated from a knowledge of sample dimensions and the force on the sample.

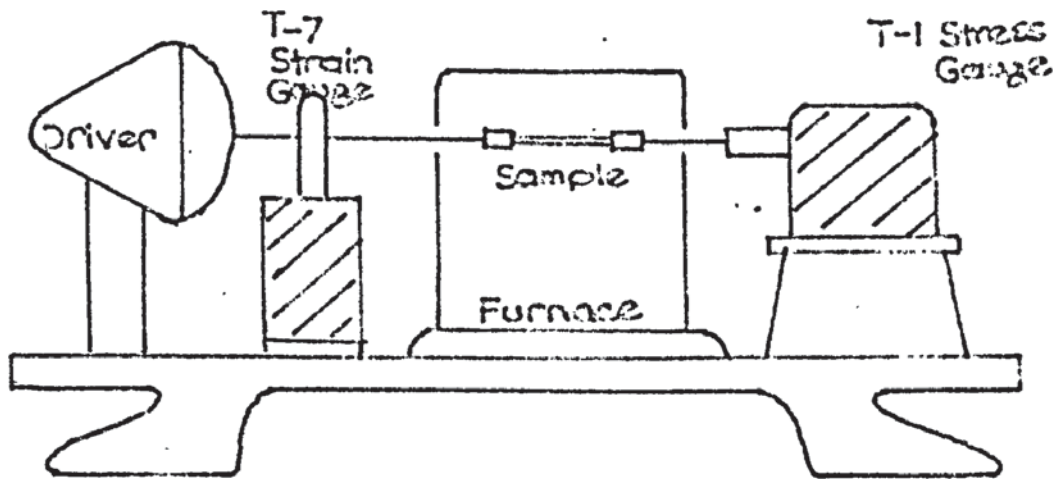


Fig.3.10 Arrangement of apparatus.

3.5.3. Equation of modulus.

The general equation for determining modulus is given by:-

$$\left| \frac{*}{E} \right| = 2.0 \times \frac{1}{A \cdot D - K} \times \frac{L}{S} \times 10^9 \text{ dynes/cm}^2 \dots (3.3)$$

$$\left| \frac{*}{E} \right| = 2.0 \times \frac{1}{A \cdot D - K} \times \frac{L}{S} \times 10^2 \text{ MN/m}^2 \dots (3.4)$$

Where $\left| \begin{smallmatrix} * \\ E \end{smallmatrix} \right|$ is the dynamic tensile complex modulus

A is a constant (see appendix 3.1).

D is the reading from the dynamic force dial

K is a correction factor

L is the total sample length

S is the cross-sectional area.

The derivation of this equation together with the calculation of oscillating displacement and oscillating load can be found in appendices 3.1 - 3.3.

The storage and loss modulus E' and E'' can be determined from a knowledge of $\left| \begin{smallmatrix} * \\ E \end{smallmatrix} \right|$ and $\tan \delta$, since

$$E' = \left| \begin{smallmatrix} * \\ E \end{smallmatrix} \right| \cos \delta \quad \dots\dots\dots(3.5)$$

$$E'' = \left| \begin{smallmatrix} * \\ E \end{smallmatrix} \right| \sin \delta \quad \dots\dots\dots(3.6)$$

3.5.4. Taking readings.

The basic instruction sheet (77) was followed. Basically, the gauges were first balanced and calibrated and then the sample set in the clamps. This was done by clamping the sample at each end in the two clamps and adjusting its length such that there was a slight slackness. Having set the required frequency and adjusted the displacement to full scale, the slack was taken up using the micrometer adjustment. When the maximum scale reading had been obtained the sample was tightened no further. The stress was then adjusted to full scale and then by switching to " $\tan \delta$ " position vectors were subtracted and a direct reading of $\tan \delta$ obtained. The force reading required to give full scale deflection was noted as was the length of the specimen; from these readings the modulus was calculated.

Readings were made at low temperatures by passing air cooled in liquid nitrogen through the furnace. The furnace was then allowed to warm up slowly to room temperature during which time further readings were taken.

For further temperatures above room temperature the furnace was used. By setting a particular value on the variable rheostat a constant heating rate was obtained. For example with 100 V supplied to the furnace the temperature rose by $3^{\circ}\text{C}/\text{min}$. Continuous measurement at each temperature was made with the same test piece. Having read off a value for $\tan \delta$ temperature was read off promptly. Readings were taken at all four frequencies on the instrument but very erratic results were obtained at the lower frequencies due to resonance. For this reason the highest frequency possible 110 Hz was used.

3.5.5. Correction of complex modulus calculation.

When measuring complex modulus oscillating displacement was applied to the sample. However there is also a slight displacement in the chuck rod and the T-1 rod. In order to quote absolute values of modulus a correction for this was made.

Using a specimen of polypropylene the instrument was operated in the normal way while the length of the sample was gradually reduced. Sample length 'L' was then plotted against the value of the dynamic force dial 'D' and the resulting line extrapolated to zero length. The value of D at $L = 0$ was 'K' the correction factor. A value was obtained at each frequency (see Appendix 3.4).

CHAPTER 4 - RESULTS

4.1. Effect of process variables on pressure traces.

4.1.1. General description of pressure traces obtained.

Figure 4.1 shows a typical pressure trace obtained in this study.

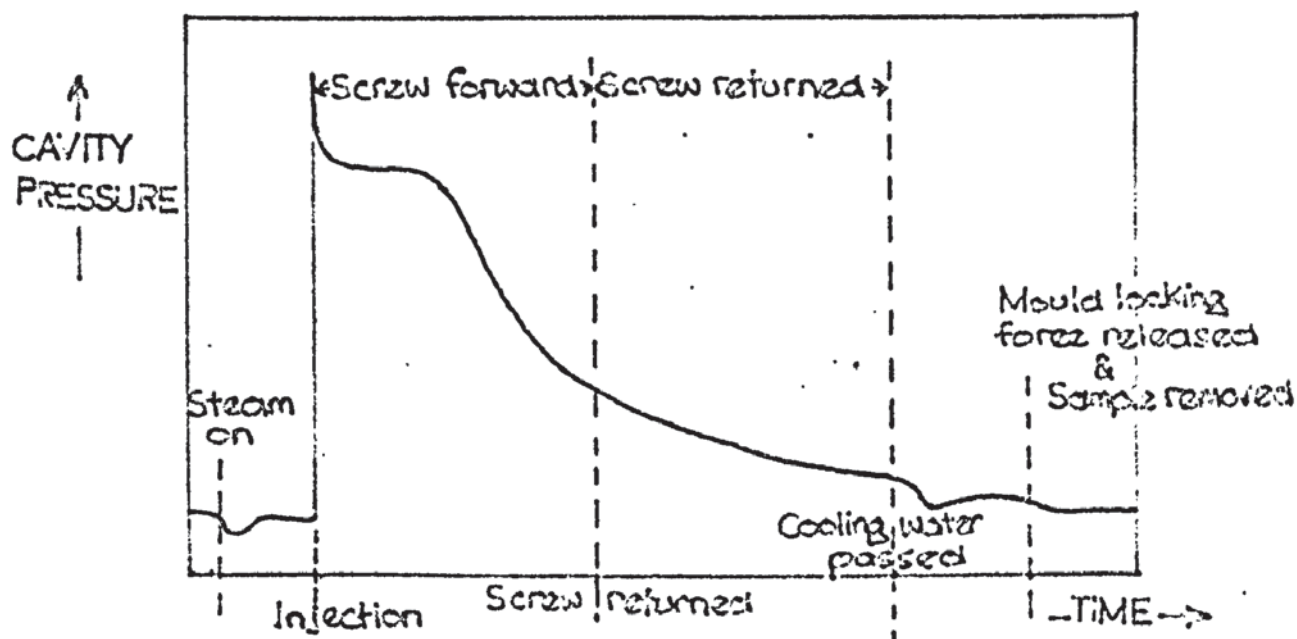


Fig.4.1. Typical pressure trace obtained.

After an initial surge the pressure levelled out for a period of time and then began to drop at a particular rate. If the pressure had not dropped to zero before the cooling water was passed another instantaneous drop in pressure was produced when the cooling water was first turned on. A further slight drop was noted when the die locking force was removed. The slight fluctuations in pressure from the base line value when the steam and cooling water were first turned on was due to the temperature dependence of the pressure transducer, and have been discussed in an earlier section.

The time for which pressure was level before dropping was assumed to be the packing time since it was found that the polymer was still molten during this time.

As a measure of the rate at which the cavity pressure dropped, the time taken for the pressure to drop by a half was noted, $t_{p\frac{1}{2}}$; the faster the rate of pressure drop the smaller $t_{p\frac{1}{2}}$. Since in the majority of cases the pressure had not levelled out before the sample was quenched, it had to be assumed that the level which the pressure would eventually achieve was the level to which the pressure dropped on quenching.

The information obtained from the traces is summarised in Fig.4.2.

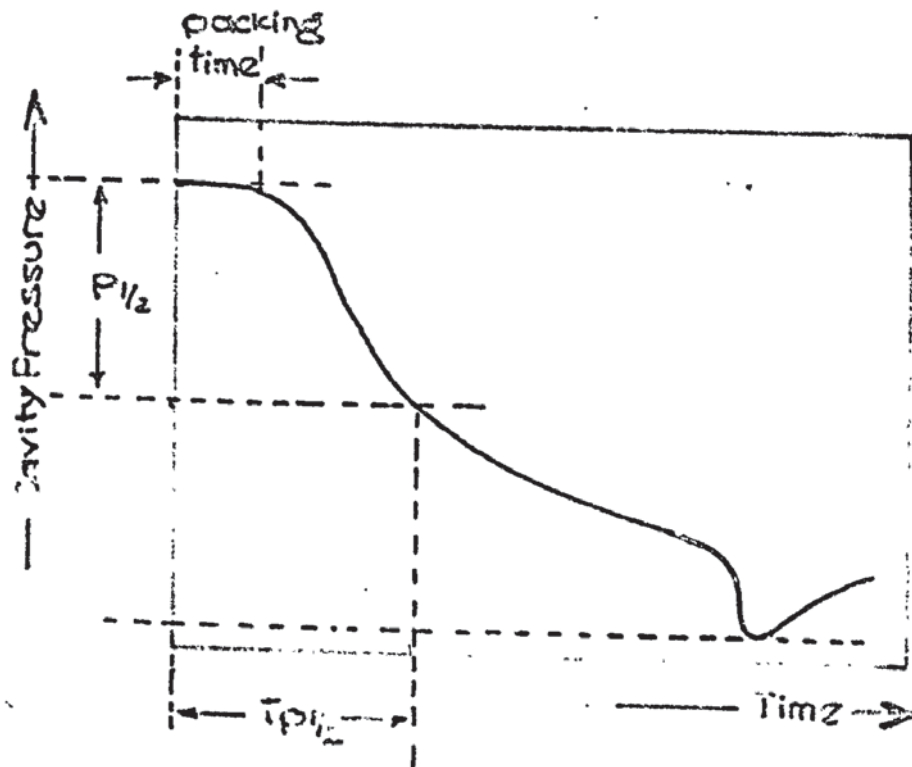


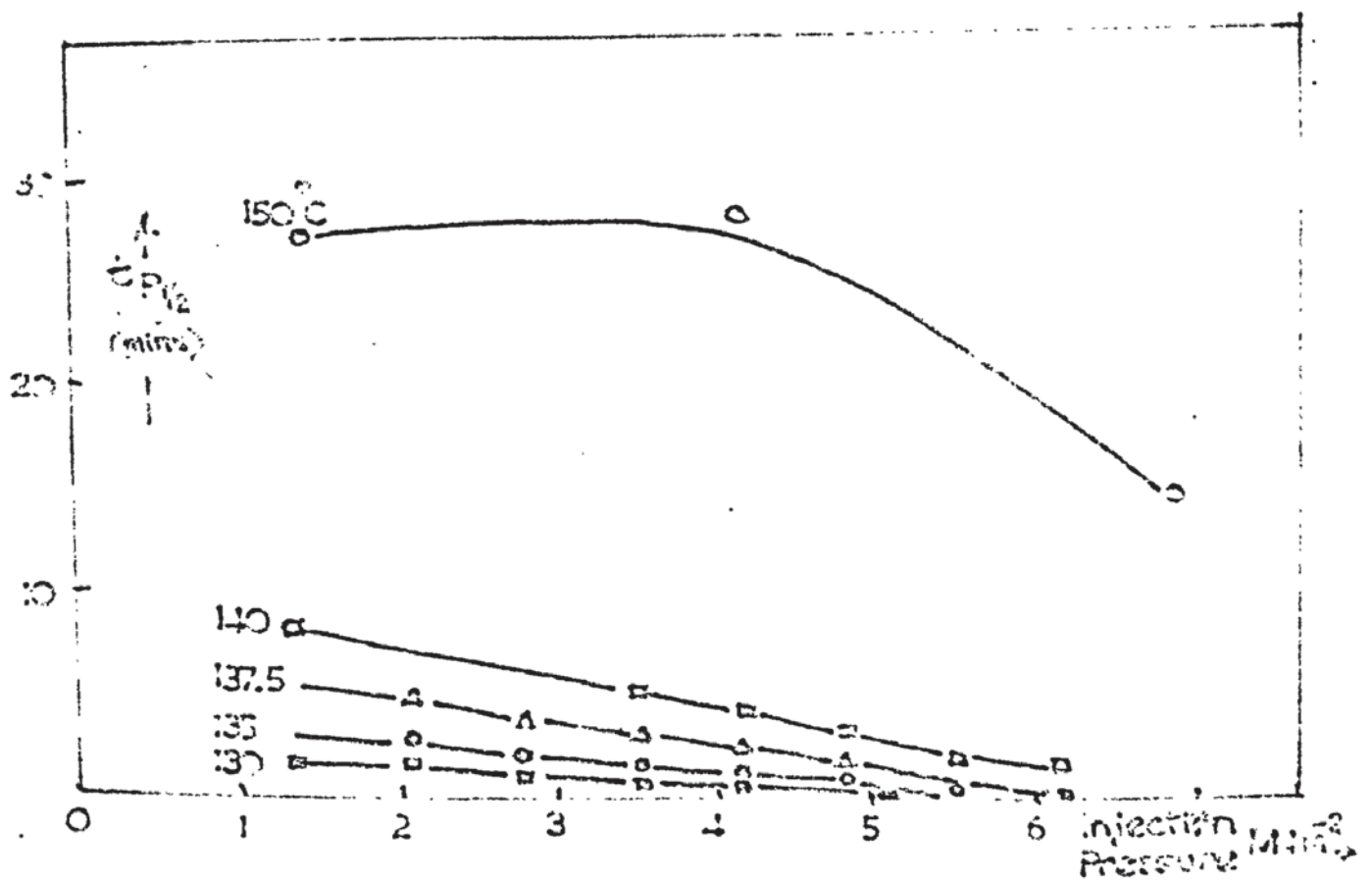
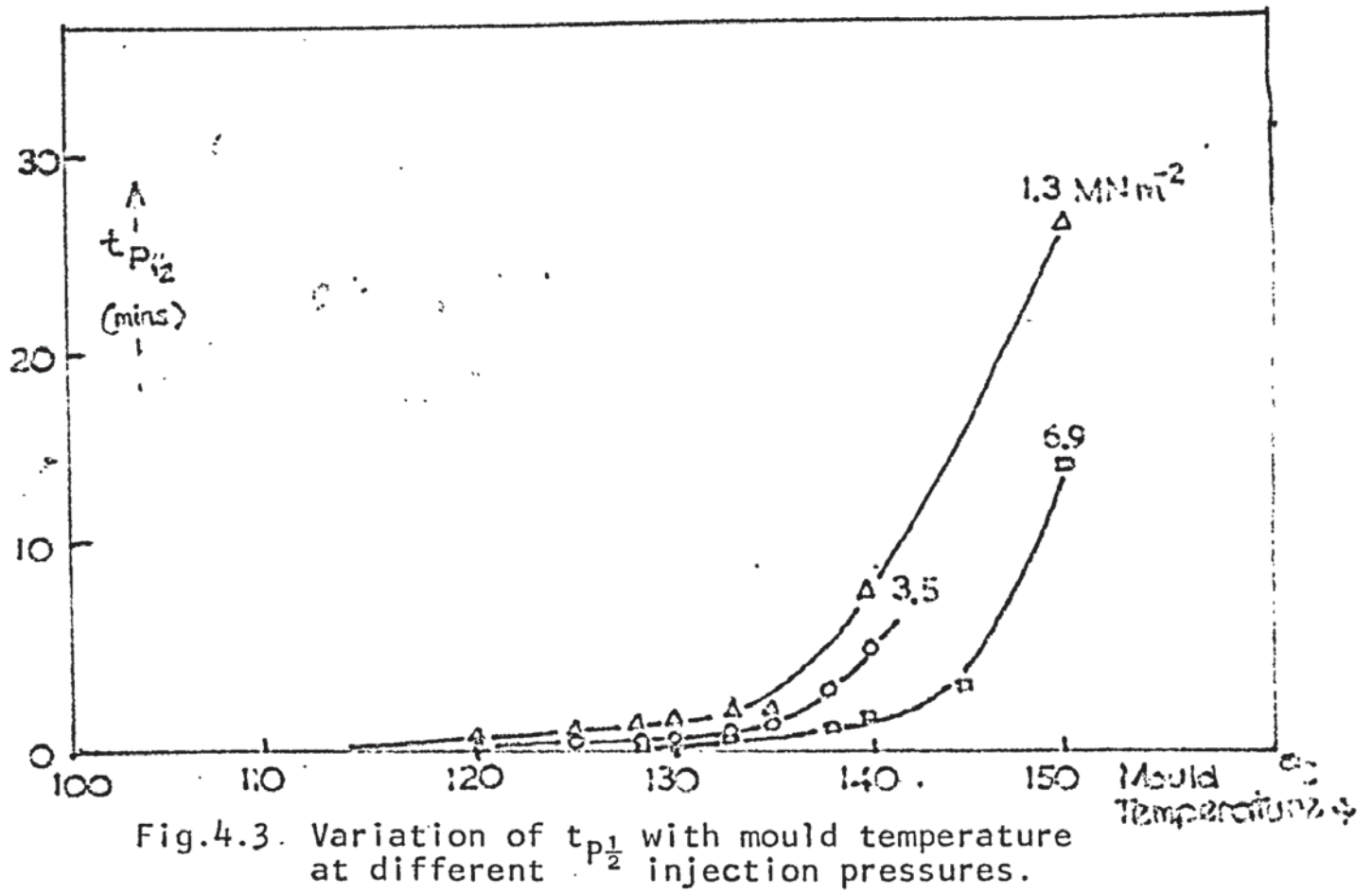
Fig.4.2. Information obtained from pressure traces.

4.1.2. Effect of processing variables on time taken for pressure to drop by a half.

The variation of $t_{p\frac{1}{2}}$ with injection pressure and mould temperature is shown in table 4.1.

Mould temperature °C.	Injection pressure MN \bar{m}^2 .								
	1.3	2.1	2.8	3.5	4.1	4.8	5.5	6.2	6.9
10	<0.1		<0.1			<0.1			
40	<0.1		<0.1			<0.1			
63	0.1		0.1			0.1			
109	0.2		0.2			0.2			
120	0.5		0.3			0.3			
125	0.8	0.7	0.5	0.6	0.5	0.4	0.35	0.4	0.4
127.5	1.5	1.4	1.0	0.8	0.7		0.6		0.7
130	1.4	1.5	1.1	0.9	0.8	0.7	0.6	0.6	0.7
132.5	2.1	2.3	1.7	1.2	1.0	0.9			0.8
135	2.0	2.4	1.9	1.4	1.1	0.9	0.7	0.8	0.8
137.5		5.0	3.5	3.2	2.5	1.6			1.3
140	8.0			5.0	4.2	3.0	2.0	1.6	1.7
145								4.4	3.2
150	27.0				28.0				14.5

Table 4.1. Time taken for pressure to drop by a half in minutes.



As the mould temperature increased at constant injection pressure $t_{p\frac{1}{2}}$ increased. Also, in general, at any particular mould temperature the higher the injection pressure the smaller $t_{p\frac{1}{2}}$. This is shown more clearly in Figures 4.3 and 4.4.

4.1.3. Effect of processing variables on packing time.

Table 4.2 shows the effect of mould temperature and injection pressure on the packing time.

Mould temperature °C.	Injection pressure MN/m ² .		
	1.3	3.5	5.5
63	0.05	0.05	0.05
109	0.10	0.05	0.10
120	0.25	0.10	0.15
125	0.35	0.20	0.20
130	0.50	0.30	0.25
135	0.40	0.40	0.25
140	0.60	0.45	0.50
145	0.75	0.50	0.55
150	0.70	0.60	0.55

Table 4.2. Effect of variables on packing time (in minutes).

These results are shown graphically in fig.4.5. It can be seen that apart from a slight discontinuity in the region 130 to 135°C, the packing time increased with increasing mould temperature and at the lower pressure the packing time was longer.

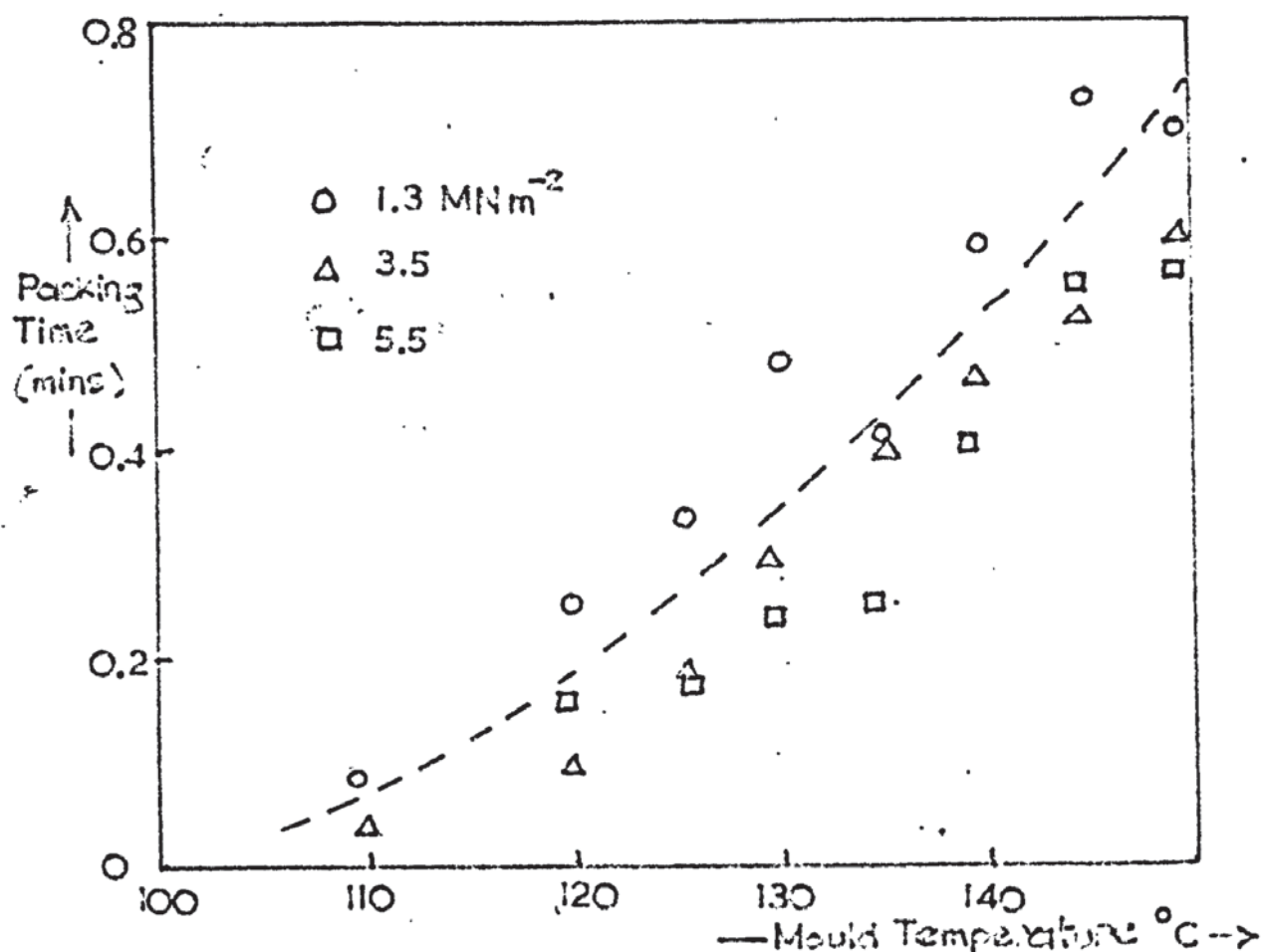


Fig.4.5. Variation of packing time with mould temperature at different injection pressures.

4.2. Crystalline structure of mouldings.

4.2.1. General appearance.

In general the structures consisted of a central spherulitic region surrounded by a thin edge band of different composition. The spherulites in this central region varied in size depending on the moulding conditions used. There was however little variation in spherulite size across the thickness of the moulding and this indicated that the entire central mass had attained the mould temperature in a very short time. The edge band appeared to be a layer of columnar-type crystals lying perpendicular to the direction of flow pointing towards the centre of the moulding. The thickness of this layer varied from approximately 20 to 100 μm , and in general it was found that the larger the

central spherulites the thicker the edge band. Often there was a clear division between the edge band and the central portion of the mouldings but in certain cases there appeared to be an intermediate region between the edge band and the central region which made it difficult to distinguish where one region ended and the other began. A typical structure is shown diagrammatically in Fig.4.6.

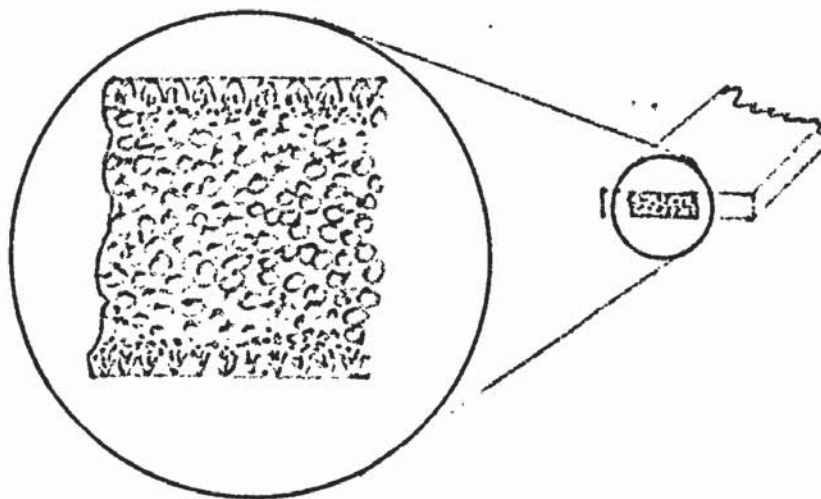
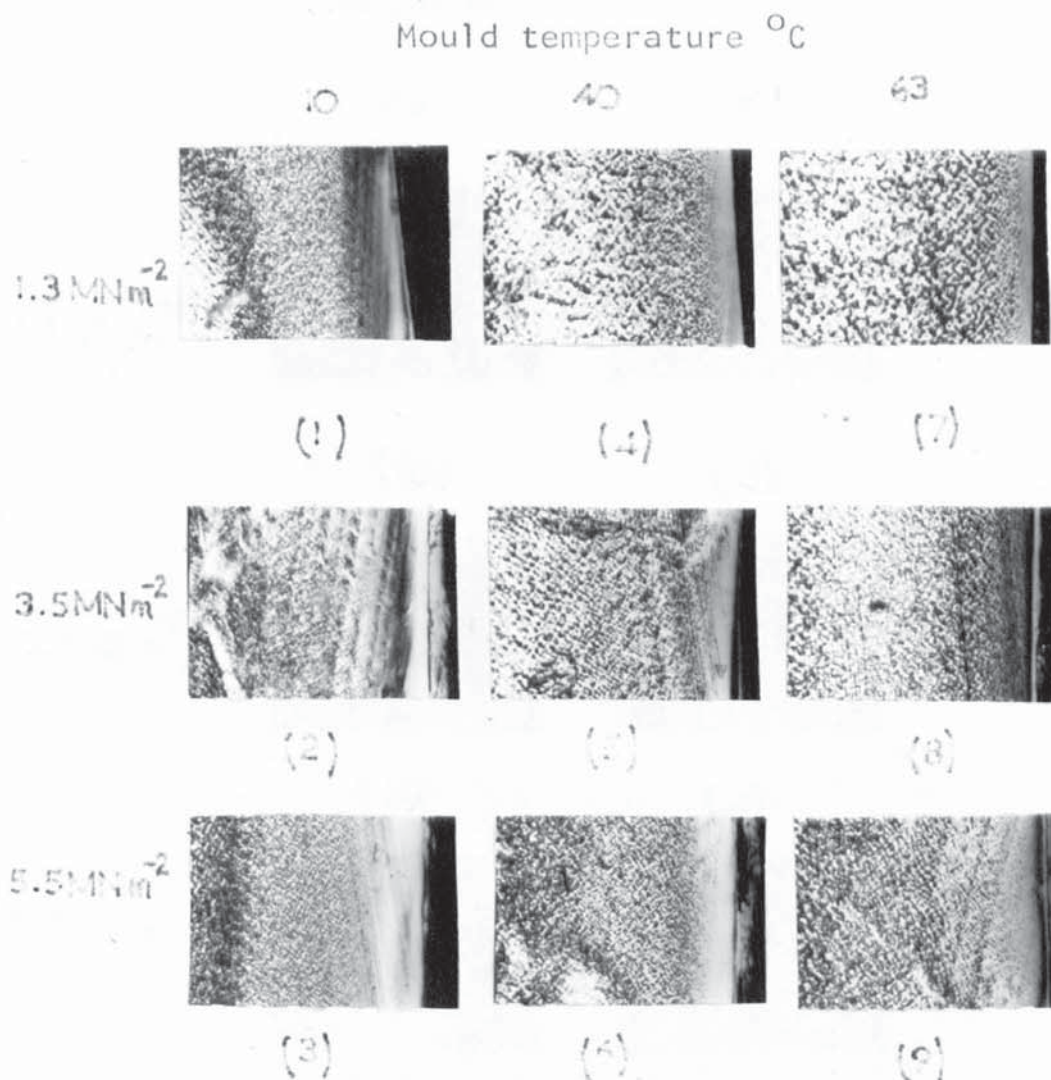


Fig.4.6. Typical structure.

4.2.2. Effect of mould temperature on crystalline structure.

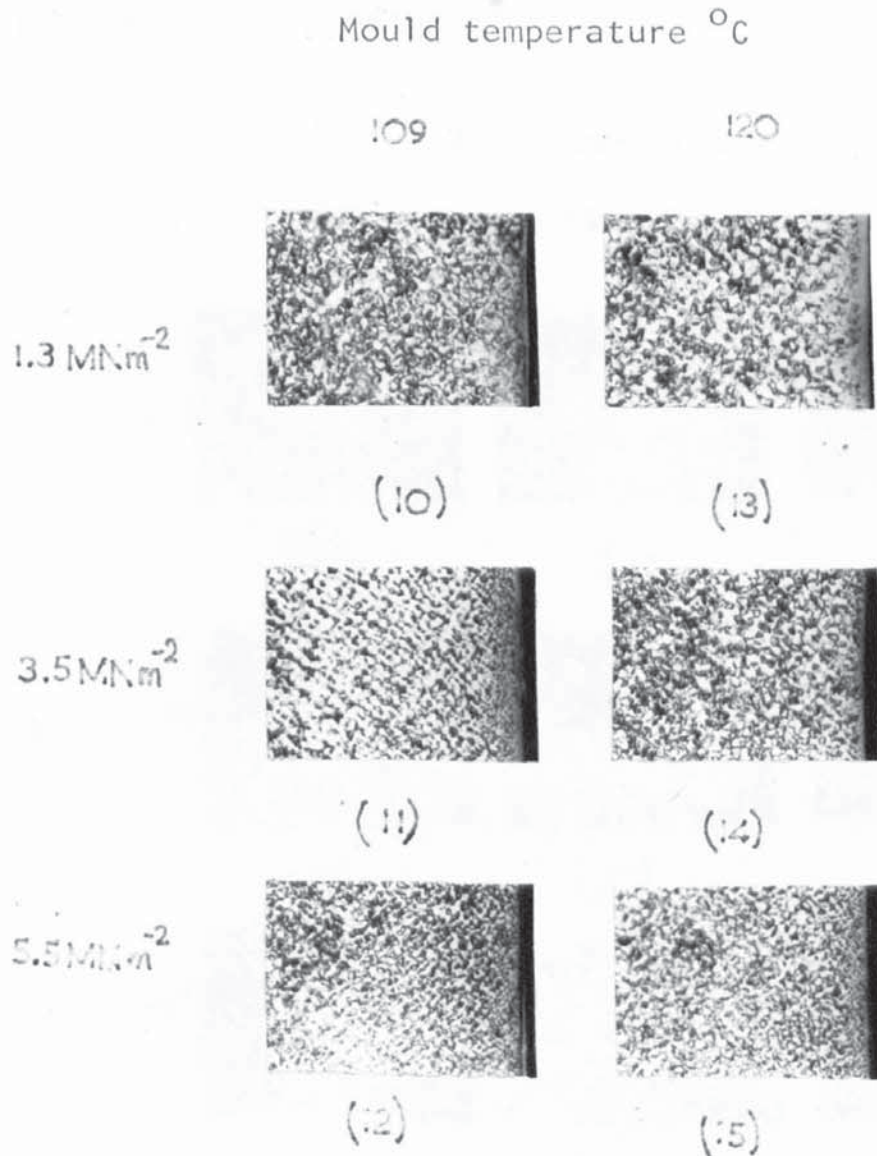
Plates (1) to (9) show the effect of mould temperature in the range 10 to 63°C on structure at three different injection pressures at a constant moulding time of five minutes (magnification 40 X).



Plates (1) to (9)

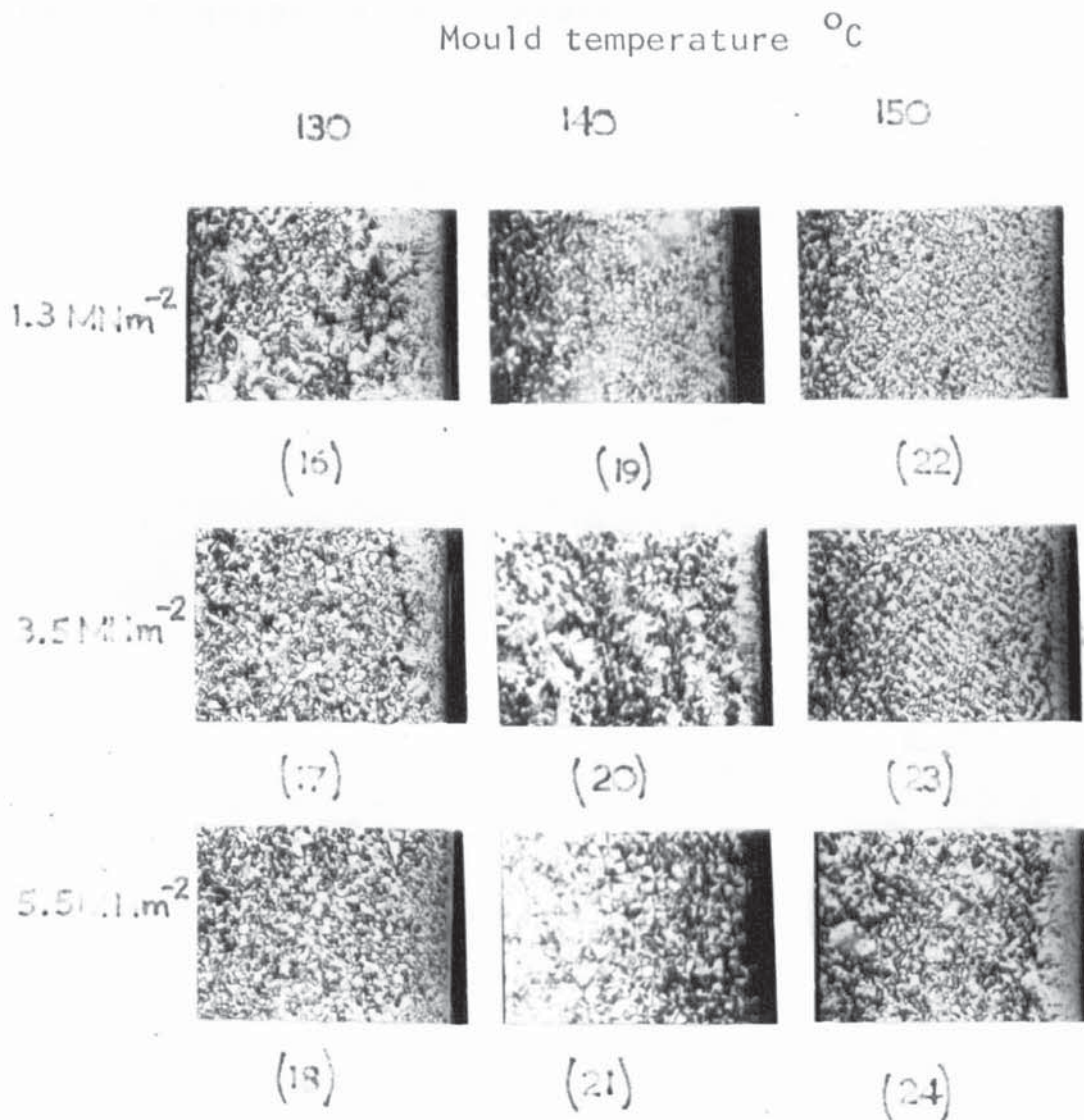
Under these conditions there appeared to be little difference in structure. Very little spherulitic structure was apparent and there was no distinguishable structure in the edge band.

Plates (10) to (15) show the effect of mould temperature in the region 109 to 120°C. These structures were more noticeably spherulitic particularly at the lower injection pressures but the spherulites were still fairly small (20 - 50 μm). The edge band showed more structural features.



Plates (10) to (15).

Plates (16) to (24) show the effect of mould temperature in the region 130 to 150°C. It can be seen that the most distinguishable spherulitic structures were produced in this mould temperature region. Spherulites up to 150 μm in diameter were produced and structure in the edge band became more apparent. Voided samples were also present in this temperature region.



Plates (16) to (24)

4.2.3. Effect of injection pressure on
crystalline structure.

Plates (25) to (39) show the effect of injection pressure on spherulitic structure for various mould temperatures at a constant moulding time of five minutes.

It is noted that the largest spherulites are produced at higher injection pressures as the mould temperature is increased.

Mould temperature °C

INJECTION
PRESSURE
MN m⁻²

125

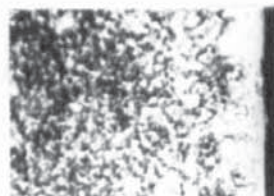
135

145

1.3



(25)

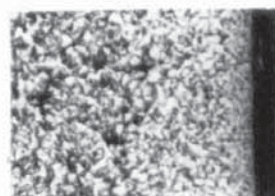


(30)

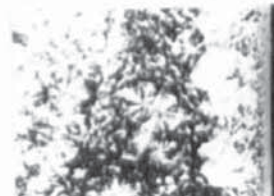


(35)

2.8



(26)



(31)

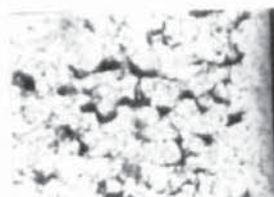


(36)

4.1



(27)

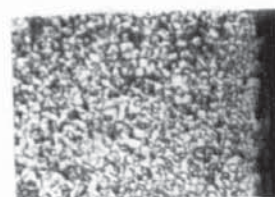


(32)

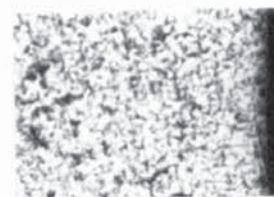


(37)

5.5



(28)

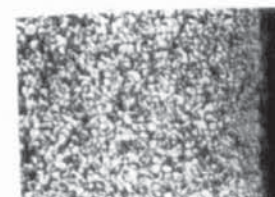


(33)



(38)

6.9



(29)



(34)



(39)

Plates (25) to (39).

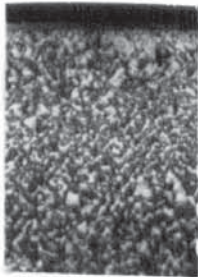



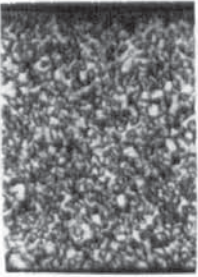
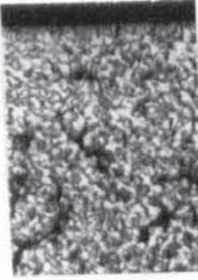

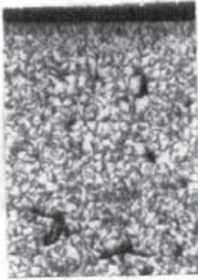

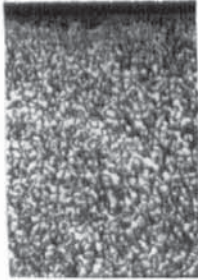
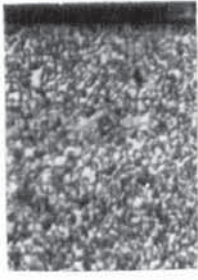
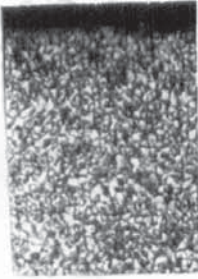
4.2.4. Effect of moulding time on crystalline structure.

Plates (40) to (75) show the effect of time held in the mould cavity on structure at various injection pressures and mould temperatures.

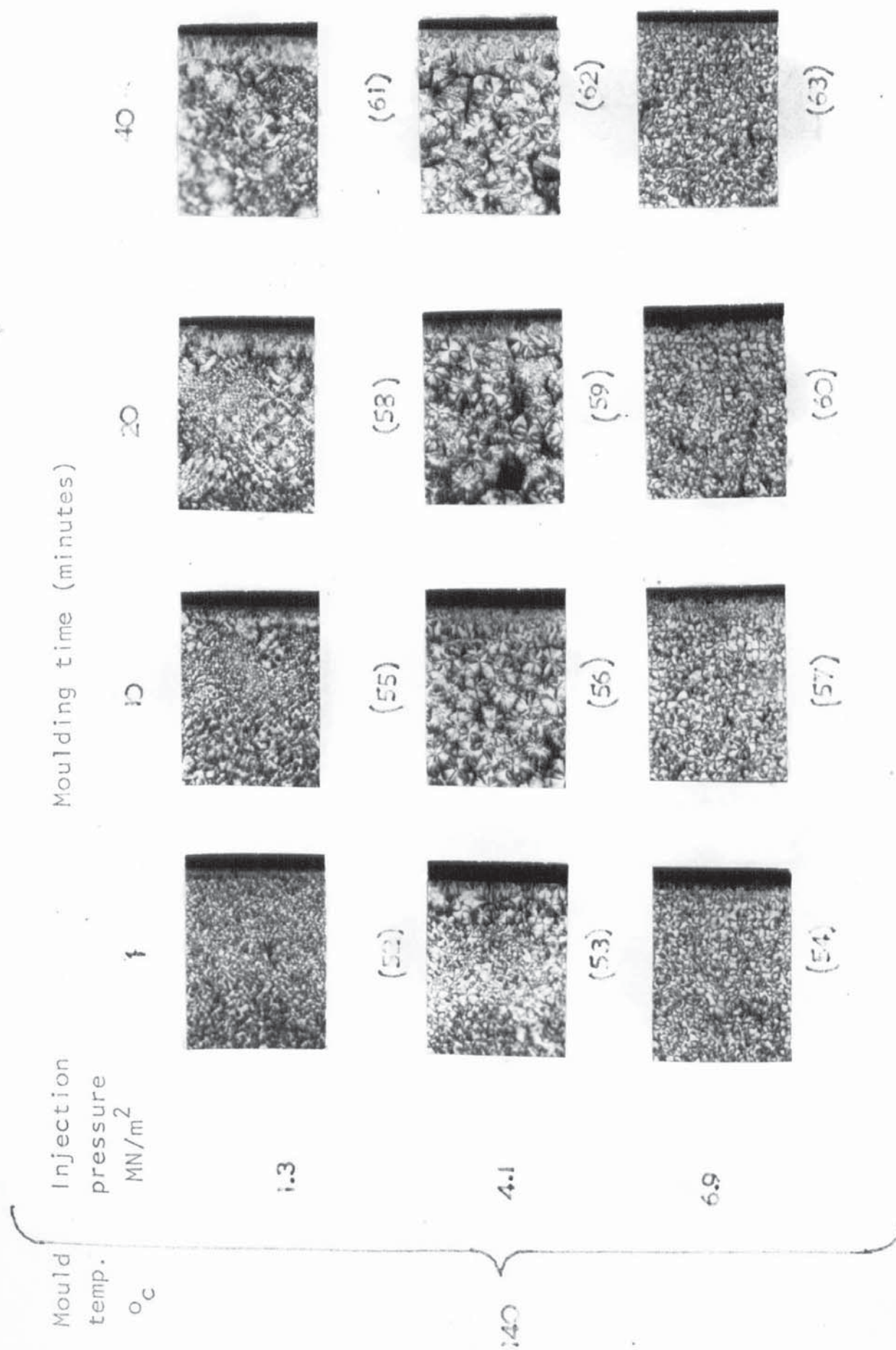
Measurements of the spherulite diameters were taken from these photographs and are tabulated in Table 4.3.

Mould temp.	Injection pressure	Moulding time (mins)			
		1	10	20	40
130°C	1.3 MNm ⁻²	20	120	150	100
	4.1	30	30	30	30
	6.9	20	20	20	20
140	1.3	20	70	80	120
	4.1	40	100	120	100
	6.9	30	50	50	50
150	1.3	30	30	30	30
	4.1	20	50	100	120
	6.9	50	150	120	100

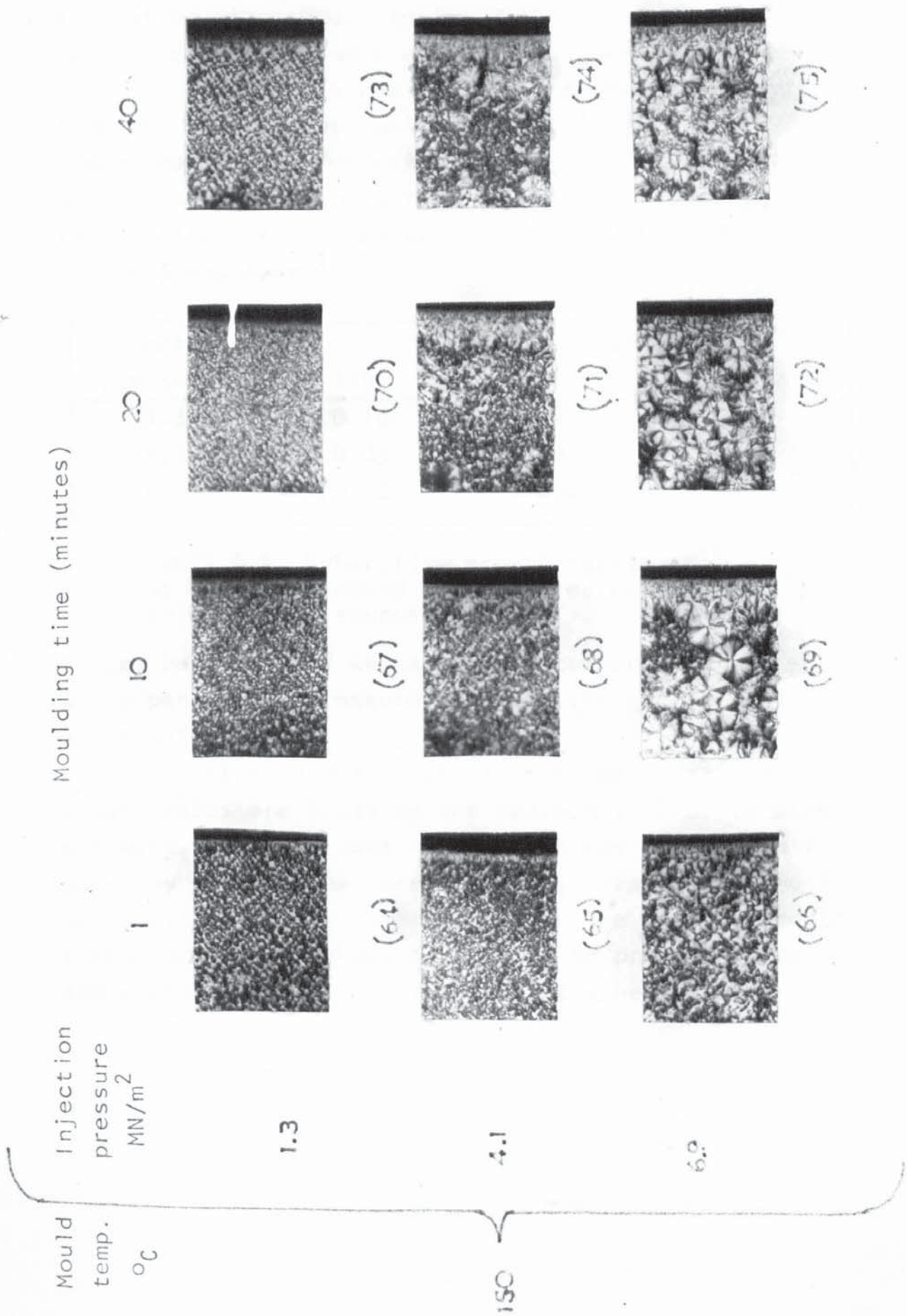
Table 4.3 Showing approximate spherulite diameters taken from photographs in μms under different processing conditions.

Mould temp. °C	Injection pressure MN/m ²	Moulding time (minutes)			
		1	10	20	40
130	1.3				
	4.1				
	6.9				
		(40)	(43)	(46)	(49)
		(41)	(44)	(47)	(50)
		(42)	(45)	(48)	(51)

Plates (40) to (51) showing the effect of moulding time on structure



Plates (52) to (63) showing the effect of moulding time on structure



Plates (64) to (75) showing the effect of moulding time on structure

Spherulite size tended to increase with time, although certain conditions were established where this was not so.

Spherulite radii (μm) were plotted against time (S) at constant mould temperature (Fig.4.7).

Growth rates were determined from the slopes of these graphs and are shown in table 4.4.

(N.B. since graphs deviated at longer times the slope at 500 S was taken).

Injection pressure MN m^{-2}	Mould temperature $^{\circ}\text{C}$		
	130	140	150
1.3	0.10	0.06	0.03
4.1	0.03	0.09	0.05
6.9	0.02	0.046	0.14

Table 4.4. Spherulite growth rates μms^{-1} at different mould temperatures and injection pressures.

It can be seen that at each mould temperature there was a particular pressure at which the growth rate was greatest.

It should be noted that these so-called growth rates are based on the maximum spherulite size achieved, and so growth rates which may appear small here may in fact have been very fast leading to small spherulites in a very short time. The largest growth rates in this study are assumed to be produced under those conditions giving the largest spherulites.

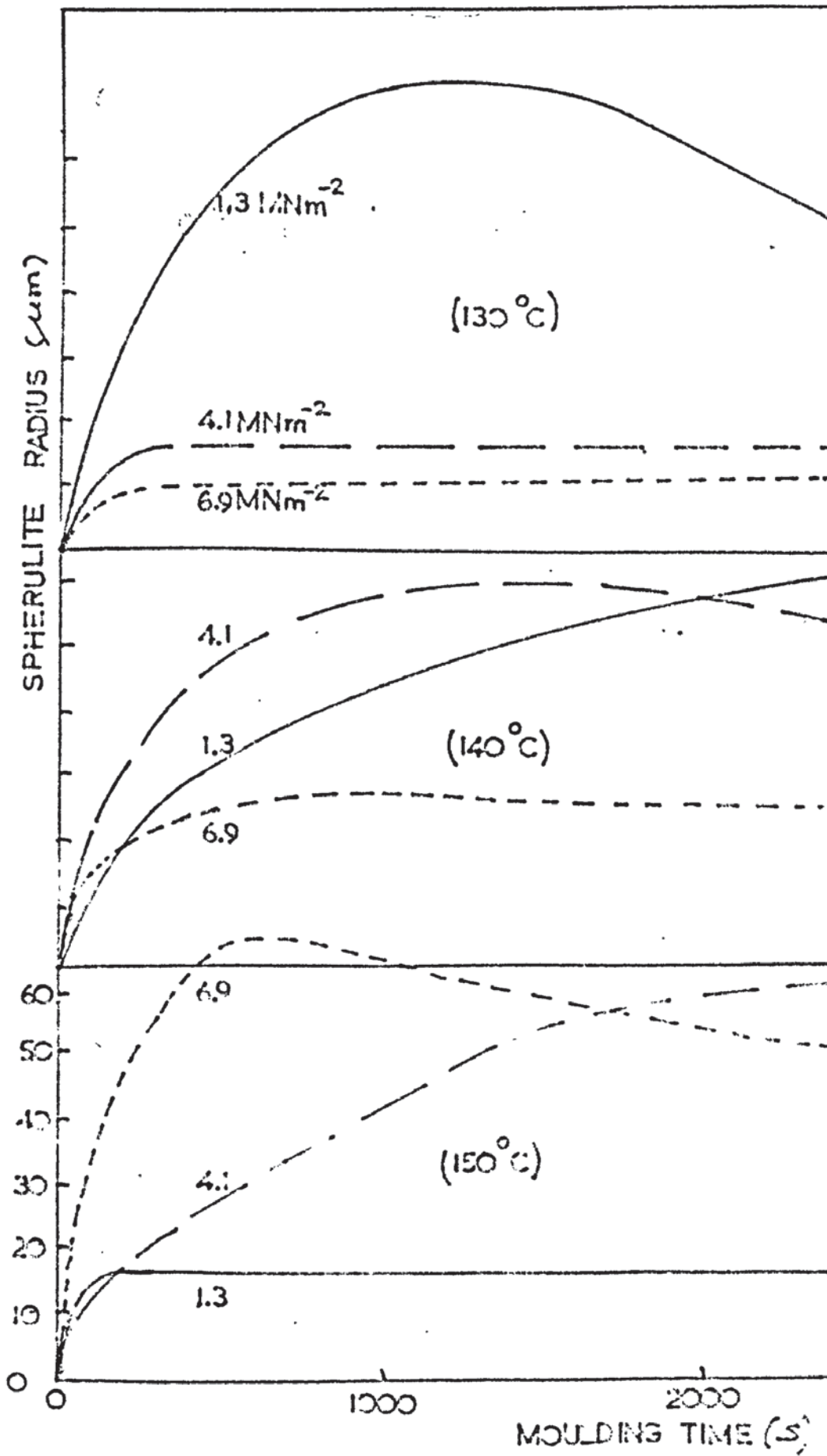


Fig.4.7. Variation of spherulite size with time.

4.2.5. Variables producing voided structures.

Under particular conditions of temperature, pressure and time voided structures (see fig.A.6) were produced. This was particularly noticeable in the mould temperature region 125 to 135°C. For example, at a constant moulding time of five minutes the following conditions of temperature and pressure led to voided structures (Table 4.5).

Mould temperature °C	Injection pressure MN m ⁻²								
	1.3	2.1	2.8	3.5	4.1	4.8	5.5	6.2	6.9
125	v	sv	c	c	c	c	c	c	c
127.5	c	sv	v	sv	c		c		c
130	c	sv	v	v	sv	c	c	c	c
132.5	c	c	sv	v	sv	c			c
135	c	c	sv	v	v	sv	c	c	c
140	c	c	c	c	c	c	c	c	c
150	c			c			c		

Table 4.5. Conditions producing slightly voided (sv), voided (v) and clear (c) structures.

An increase in moulding time produced voids in samples which, prepared under the conditions above, were clear. This is shown in table 4.6.

It can be seen that voiding rarely took place at the higher pressures, and only occurred at the highest pressure at a mould temperature of 150°C for the longer times.

Mould temp. °C	Injection pressure MNm ⁻²	Moulding time (minutes)			
		1	10	20	40
130	1.3	c	v	v	v
	4.1	c	v	v	v
	6.9	c	c	c	c
140	1.3	c	c	c	sv
	4.1	c	sv	v	v
	6.9	c	c	c	c
150	1.3	c	c	c	c
	4.1	c	c	sv	sv
	6.9	c	c	sv	v

Table 4.6. The effect of moulding time on voiding.

4.3. Percentage crystallinities.

4.3.1. Effect of mould temperature and injection pressure on percentage crystallinity.

The variation of percentage crystallinity with mould temperature and injection pressure is shown in Table 4.7.

Mould temp. °C	Injection pressure MNm ⁻²								
	1.3	2.1	2.8	3.5	4.1	4.8	5.5	6.2	6.9
10	< 56 ¹			< 56			< 56		
40	< 56			< 56			< 56		
109	63.8			62.7			62.2		62.6
120	66.2			66.0			63.9		64.9
125	v ²	67.3	67.0	66.9	66.7	66.8	65.6	64.9	64.6
127.5	62.2	63.7	v	66.6	66.4		66.2		64.6
130	61.2	64.4	v	v	66.8	66.6	65.6	66.0	65.5
132.5	60.0	60.5	63.9	v	v	66.4			66.1
135	60.1	61.3	62.6	v	v	67.0	66.8	66.4	66.2
137.5		58.9	61.3	61.8	65.9	66.6			66.4
140	59.2	59.2	60.6	61.7	62.0	66.0	67.5	67.5	67.2
145	59.2	58.3	59.2	60.0	60.1	61.3	62.9	66.6	67.2
150	58.9			59.2			61.3		60.9

Table 4.7. The effect of mould temperature and injection pressure on percentage crystallinity.

- N.B.
1. Samples prepared under these conditions had densities too low for the column used.
 2. It was shown that voided samples gave erroneous results in the density gradient column and so these were omitted.

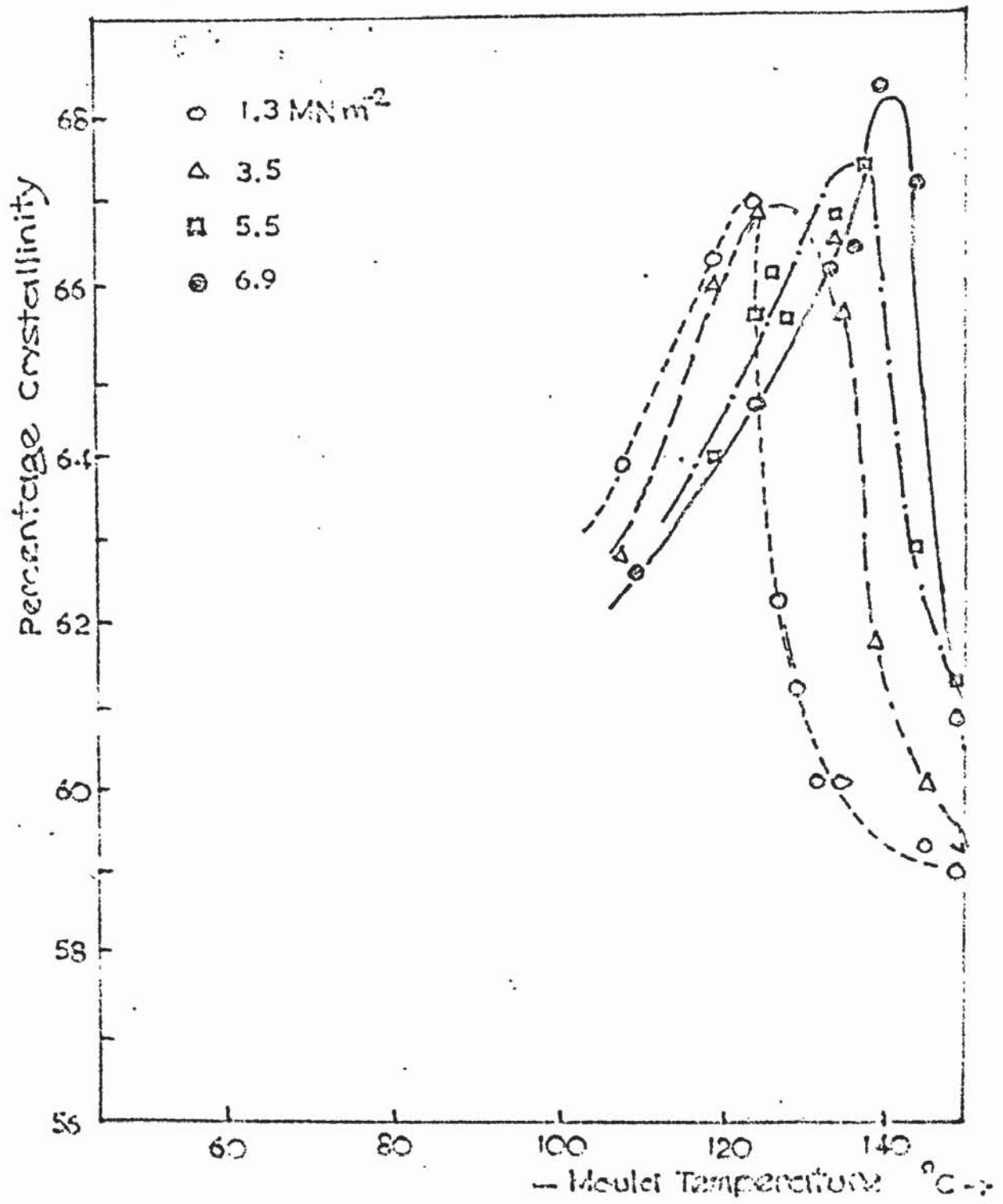


Fig.4.8. Variation of percentage crystallinity with mould temperature.

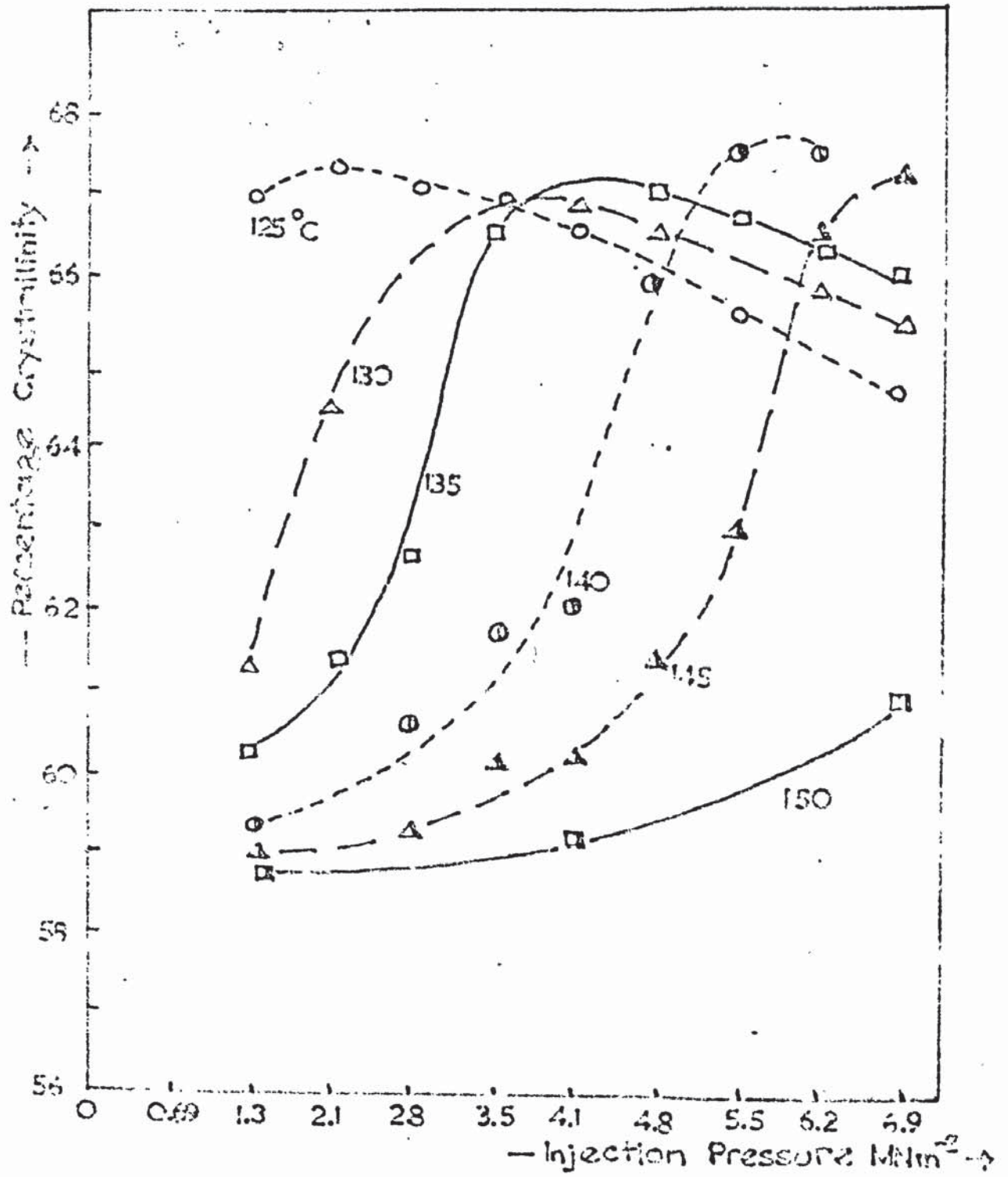


Fig.4.9. Variation of percentage crystallinity with injection pressure.

The variation of percentage crystallinity with mould temperature at constant injection pressures and the variation with injection pressure at constant mould temperatures is shown in figures 4.8 and 4.9.

It can be seen that at low injection pressures the highest percentage crystallinities were produced at lower mould temperatures, while at the higher injection pressures they were produced at higher mould temperatures.

4.3.2. Effect of moulding time on percentage crystallinity.

The variation of percentage crystallinity with moulding time at various conditions of mould temperature and injection pressure is shown in Table 4.8. (again voided samples shown as 'v').

Mould temp. °C	Injection press. MNm ⁻²	Moulding time (minutes)			
		1	10	20	40
130	1.3	61.5	v	v	v
	4.1	65.7	v	v	v
	6.9	64.9	66.0	66.2	66.7
140	1.3	60.3	61.0	62.2	62.1
	4.1	61.3	67.3	v	v
	6.9	65.6	67.4	67.9	68.6
150	1.3	< 56	60.3	60.0	61.0
	4.1	56.9	61.3	61.7	65.0
	6.9	61.8	66.0	68.1	v

Table 4.8. Variation of percentage crystallinity with moulding time.

An increase in moulding time led to an increase in percentage crystallinity. At each injection pressure there was a temperature at which this increase with time was greatest.

4.4. Mechanical Properties.

4.4.1. Dynamic mechanical properties - general.

Results have either been shown as temperature dispersion curves with modulus and $\tan \delta$ plotted as a function of temperature of testing, or have been expressed as point values at one particular test temperature. Early samples were tested throughout the complete range of testing temperatures (approx. 0 - 150°C) and it was noted that the curves obtained for the modulus were very reproducible; the curves obtained for $\tan \delta$ on the other hand were much less consistent. This was probably due to the fact that there was a large temperature region over which the curve changed from a maximum to a minimum since $\tan \delta$ is very sensitive in this transition region. However, since it was thought that for this study the determination of the dynamic modulus would be most useful, it was decided that it would be justified to make measurements of the modulus at one particular test temperature. In this way far more samples were tested and it was far easier to compare point values of different samples rather than the complete dispersion curves.

The temperature dispersion curves of dynamic tensile complex modulus ($|E^*|$) and mechanical damping $\tan \delta$ were found to follow the normal pattern (fig.4.10); that is as temperature of testing was increased from 0 - 120°C there was an approximately ten-fold drop in modulus. $\tan \delta$ over this same range of temperatures was found to go first through a maximum at approximately 15 - 20°C and then through a minimum at approximately 60 - 70°C.

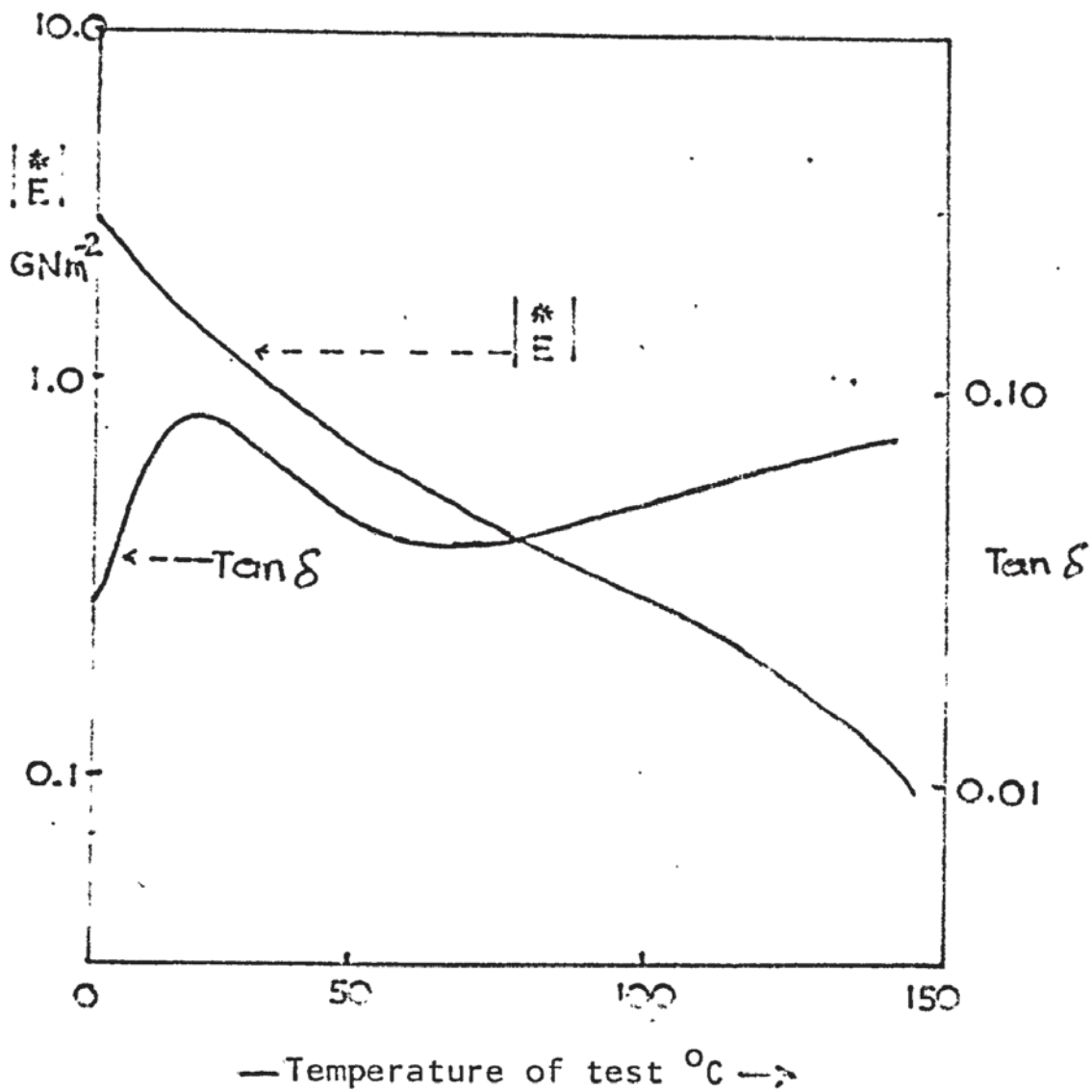


Fig.4.10 Typical temperature dispersion curves obtained in the present study.

4.4.2. Effect of mould temperature on dynamic mechanical properties.

The variation of $|\dot{E}|^*$ and the mechanical damping $\tan \delta$ with mould temperature in the range 0 - 120°C is shown in figure 4.11. The properties have been plotted against temperature of testing such that a complete dispersion over the useful temperature range was obtained. Frequency of testing was 110 Hz.

Under these conditions it was noted that the modulus increased (and $\tan \delta$ decreased) as the mould temperature was increased to 120°C. At mould temperatures above 120°C these trends were reversed.

The same effect was shown but not so clearly for samples prepared at an injection pressure of 5.5 MNm⁻² (Fig.4.12).

4.4.3. Effect of injection pressure on dynamic mechanical properties.

By comparing figures 4.11 and 4.12 it can be seen that in general the higher the injection pressure the lower the modulus and the higher the damping in the mould temperature range 10 - 120°C. Above a mould temperature of 120°C however the higher the injection pressure the higher the modulus. This is shown in fig.4.13.

The variation of $|\dot{E}|^*$ over the complete range of mould temperatures and injection pressures is summarized in table 4.9.

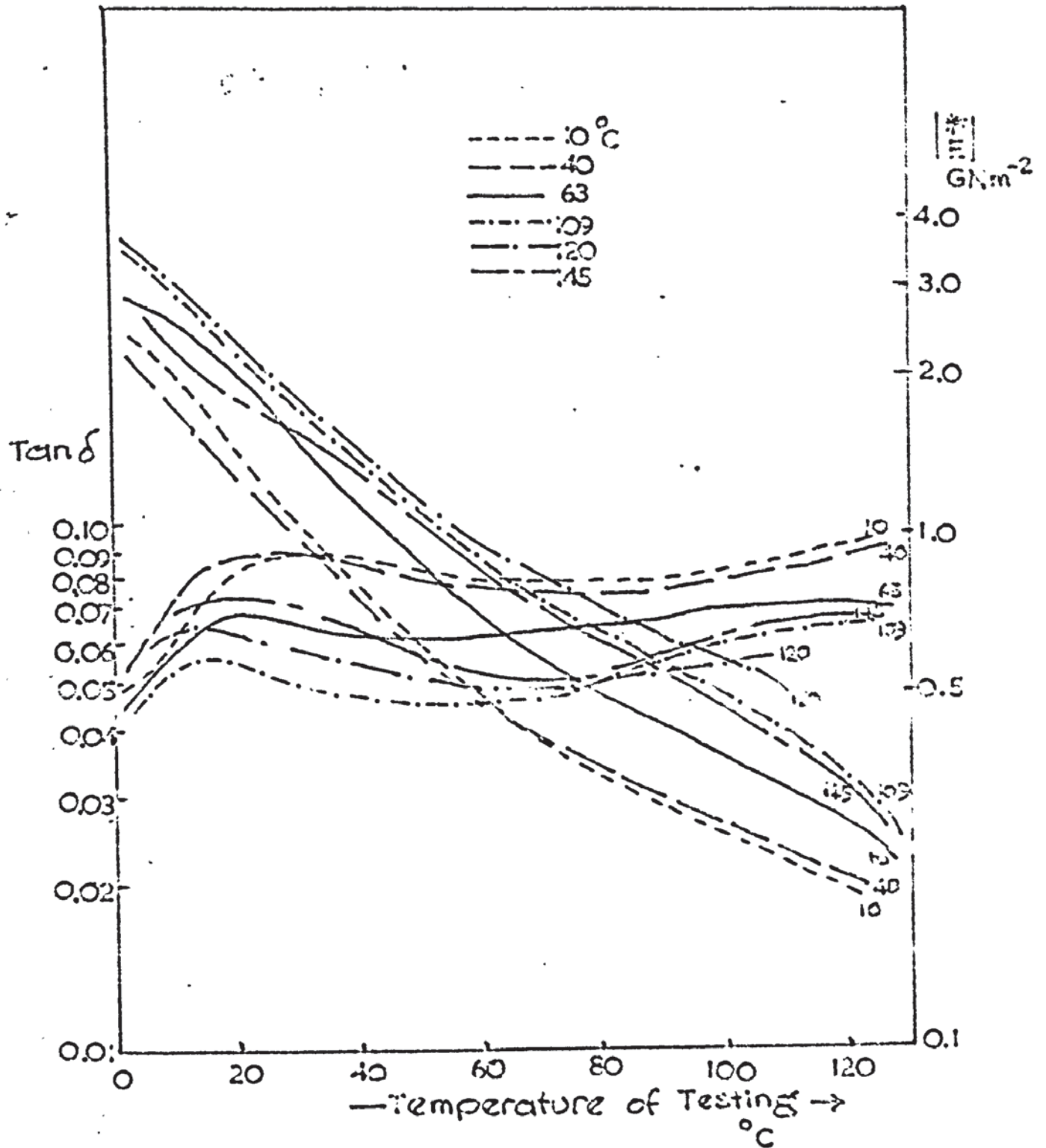


Fig.4.12. Dynamic mechanical properties of samples prepared at different mould temperatures at a constant moulding time of 5 minutes and injection pressure 5.5 MN m^{-2} .

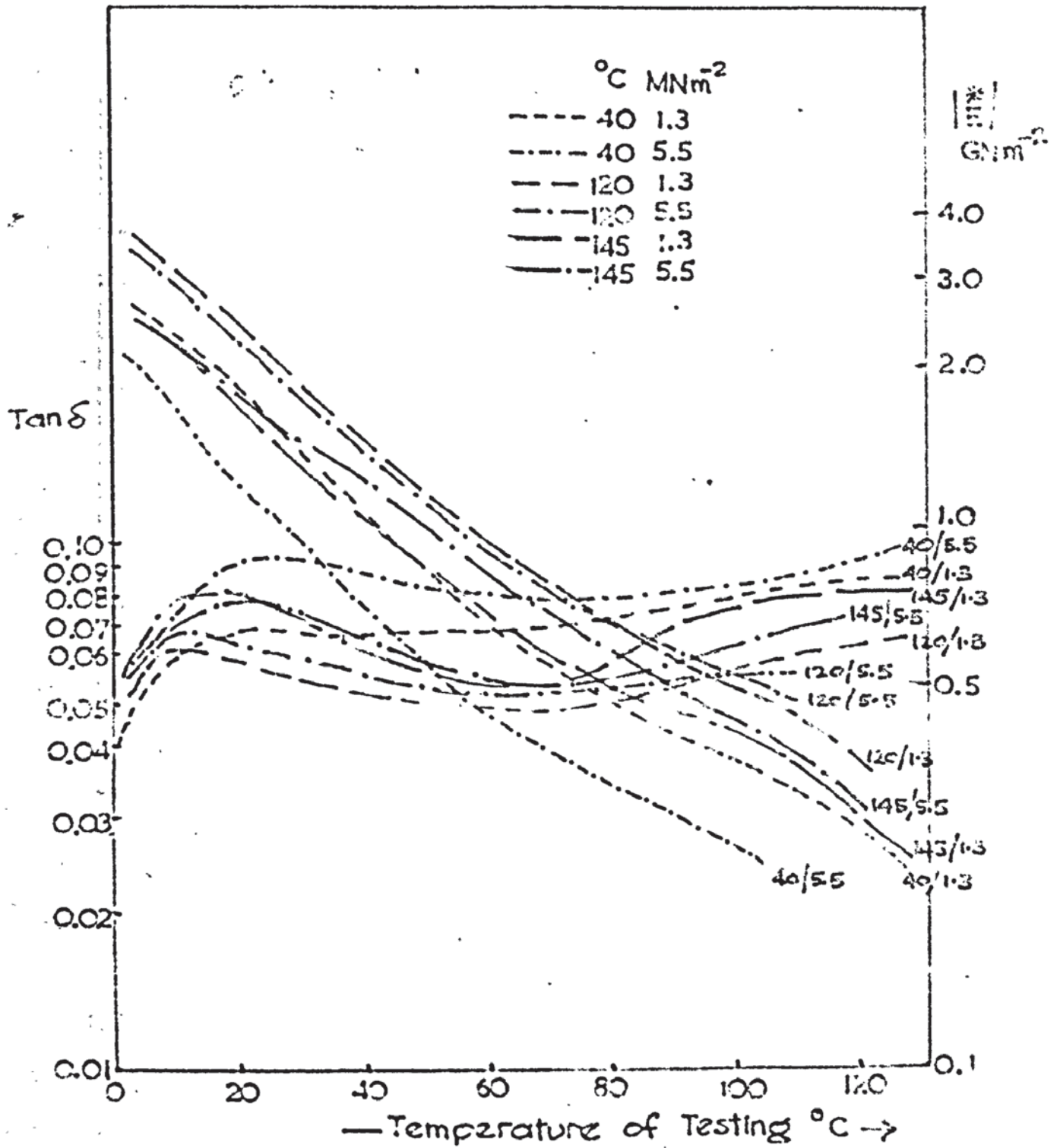


Fig.4.13. Dynamic mechanical properties of samples prepared at different mould temperatures and injection pressures at a constant moulding time of 5 minutes.

Mould temp. °C	Injection pressure MN m ⁻²			
	1.3	3.5	5.5	6.9
10	1.50		1.40	
40	1.85	1.78		1.84
63	2.00	1.97	1.85	1.98
109	2.15	2.22	1.95	2.06
120	2.30	2.24	2.17	2.00
125	1.96	2.09	2.00	2.07
127.5	2.03		2.10	2.04
130	2.10	1.95	2.12	2.00
132.5	2.11			2.15
135	2.00	2.08	2.15	2.15
137.5				2.24
140		2.15	2.03	2.13
145		2.00	1.80	2.17
150	2.00	2.12	2.00	2.10

Table 4.9. Effect of mould temperature and injection pressure on modulus at constant moulding time of 5 minutes. Values are point values at 22°C (E, 22) and units are GN m⁻². Frequency of testing was 110 Hz.

These results are presented graphically in fig.4.14.

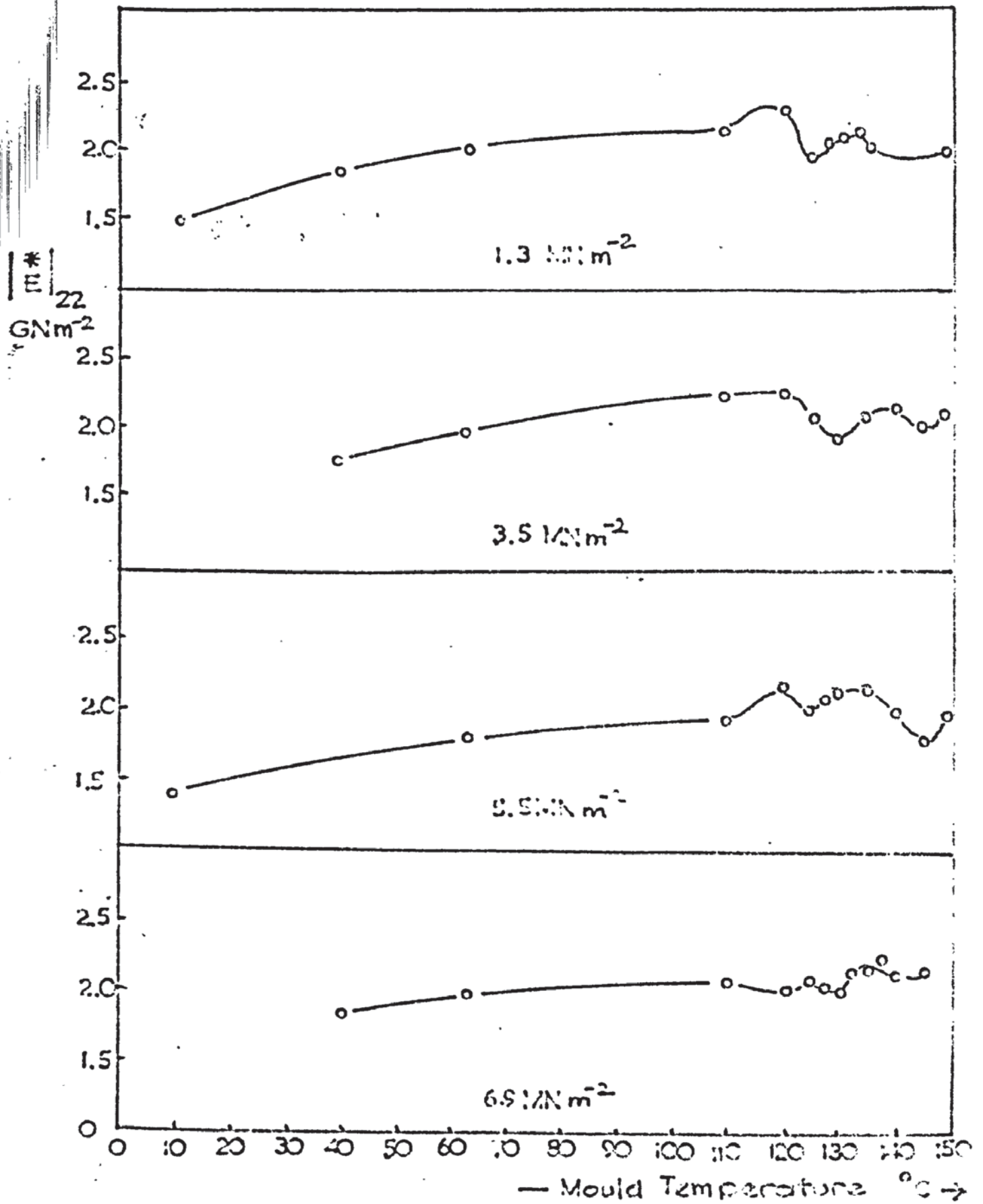


Fig.4.14. Variation of $|*E|_{22}$ with mould temperature at different injection pressures.

It was seen that an increase in mould temperature up to 120°C produced an increase in modulus. Above 120°C the modulus showed no consistent behaviour with mould temperature (although in general it was lower than the value at 120°C). At lower injection pressures a minimum in the value of $|E^*|_{22}$ was produced and the temperature at which this occurred varied depending on the injection pressure.

Although values have not been shown $\tan \delta$ generally varied in the opposite manner to the modulus.

4.4.4. Effect of moulding time on dynamic mechanical properties.

The variation of $|E^*|_{22}$ with moulding time is shown in table 4.10.

It can be seen that in general there was little variation of modulus with time. The biggest variation was noted at 130°C at an injection pressure of 1.3 MN m^{-2} where a minimum was produced at about 20 minutes.

Mould temp. $^{\circ}\text{C}$	Injection press. MN m^{-2}	Moulding time (minutes)			
		1	10	20	40
130	1.3	2.06	1.60	1.36	1.81
	4.1	2.34	2.32	2.18	2.22
	6.9	2.35	2.44	2.26	2.37
150	1.3	2.02	1.80	1.94	2.11
	4.1	1.87	1.70	2.00	1.90
	6.9	2.14	2.00	2.40	2.30

Table 4.10 Effect of moulding time on $|E^*|_{22}$, point values of modulus taken at 22°C , units GN m^{-2} .

CHAPTER 5 - DISCUSSION

5.1. Experimental techniques used for preparing samples:

Under normal conditions of injection moulding the bulk of the polymeric material injected into the cavity has little opportunity of achieving equilibrium conditions. This is because of the poor thermal conductivity of polymers combined with the fact that the mould cavities are normally large and the moulds are made over large to withstand long production runs; also moulding times are short. Consequently polymer structure is usually non-uniform across the section of the moulding. With the simple mould cavity used in the present study reproducible structures were prepared under constant conditions. The materials from which the mould was made and dimensions of the cavity used ensured that changes in the temperature of the heating/cooling medium were immediately experienced by the mould cavity itself and by the bulk of the polymer within a very short space of time. This was important since the structure that was produced during a particular run was immediately "sealed in" when the cooling water was passed, without producing any further major spherulitic structure which may have been misleading. This also had the effect that at high mould temperatures, where little growth had taken place, quenching the mould produced a uniform quenched structure throughout the sample similar to that produced at lower mould temperatures.

Also with this mould the assumption that a density measurement taken from one position in the moulding represented the density of the entire moulding was reasonable since, the reasons that density varies throughout the moulding under normal conditions, were overcome. First the melt density will normally vary as the pressure drops along the cavity (3), whilst packing pressure will increase the density in the gate region. This was overcome since the length of the moulding was relatively short.

More significantly, under normal conditions the ability of different parts of the mould to remove heat will vary owing to differing metal thicknesses and distances of mould faces from the cooling channels. Further, the gate region of the mould is hotter than the extremities since the former is heated by the passage of the incoming material. Under these normal conditions mould temperature differences of 50 - 100°C are quite possible. These were overcome by the small and uniform dimensions of the mould cavity and mould halves and the efficiency of the cooling system particularly in the sprue region.

5.2. Analysis of pressure traces obtained.

The traces obtained in this present study compared very well with those presented in the literature. It is generally accepted (3) that as the cooling and thermal contraction take place in the mould cavity the cavity pressure steadily falls until a point is reached where residual pressure ceases. Results in this study have confirmed that the rate of pressure drop is related to thermal contraction since at any particular injection pressure the rate of pressure drop is faster at lower mould temperatures. The packing time is also reduced.

Since the polymer used, polypropylene, was semi-crystalline there was a possibility that the rate of pressure drop was increased somewhat due to the greater change in specific volume on crystallising. An indication that this may be so was gained by moulding some amorphous polymer (Styrene-acrylonitrile 'SAN' 'Tyril') of similar thermal properties as polypropylene (Thermal conductivities $2.8 \times 10^{-4} \text{ cal S}^{-1} \text{ cm}^{-1} \text{ deg C}^{-1}$ for PP and 2.9×10^{-4} for SAN) under identical conditions as the polypropylene and comparing the pressure traces obtained. This is shown in Fig.5.1.

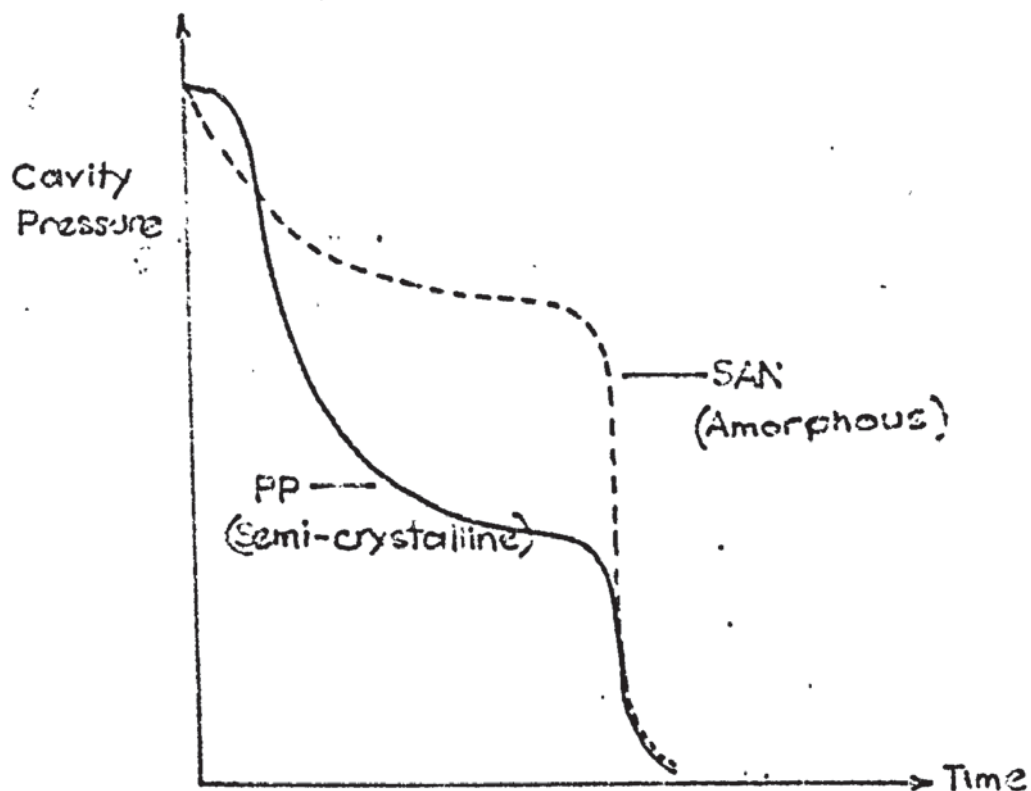


Fig.5.1. Pressure profiles for PP and SAN, at 140°C and 6.9 MN m^{-2} injection pressure.

It will be noted that the pressure drop for the amorphous polymer was very much slower than that for the semi-crystalline polymer, and it showed little or no packing time. And so the thermal contraction of the semi-crystalline polymer was far greater than for the amorphous material; this suggests that the crystallisation of the polymer is affecting the rate of pressure drop. It has been shown theoretically by Spencer and Gilmore (78) that the loss of volume and resulting drop in pressure is markedly higher with a semi-crystalline polymer than with an amorphous polymer.

As a measure of the rate of pressure drop values of the time taken for pressure to drop by a half, $t_{p\frac{1}{2}}$, were plotted against mould temperature for various injection pressures. This was shown in figure 4.3. From this it was noted that the temperature at which the "half-life" suddenly began to rise very steeply was dependent on the injection pressure and was slightly higher the higher the injection pressure. Since it had been noted that the pressure traces obtained were very similar to those traces obtained from dilatometric observations it was decided to compare these 'pressure half-life' curves with those obtained from dilatometer experiments under normal crystallisation conditions. Using the values of $t_{\frac{1}{2}}$ for polypropylene crystallised at various temperatures at atmospheric pressure obtained by Keller (12) and Hybart (79) the comparison of the curves is shown in Figure 5.2.

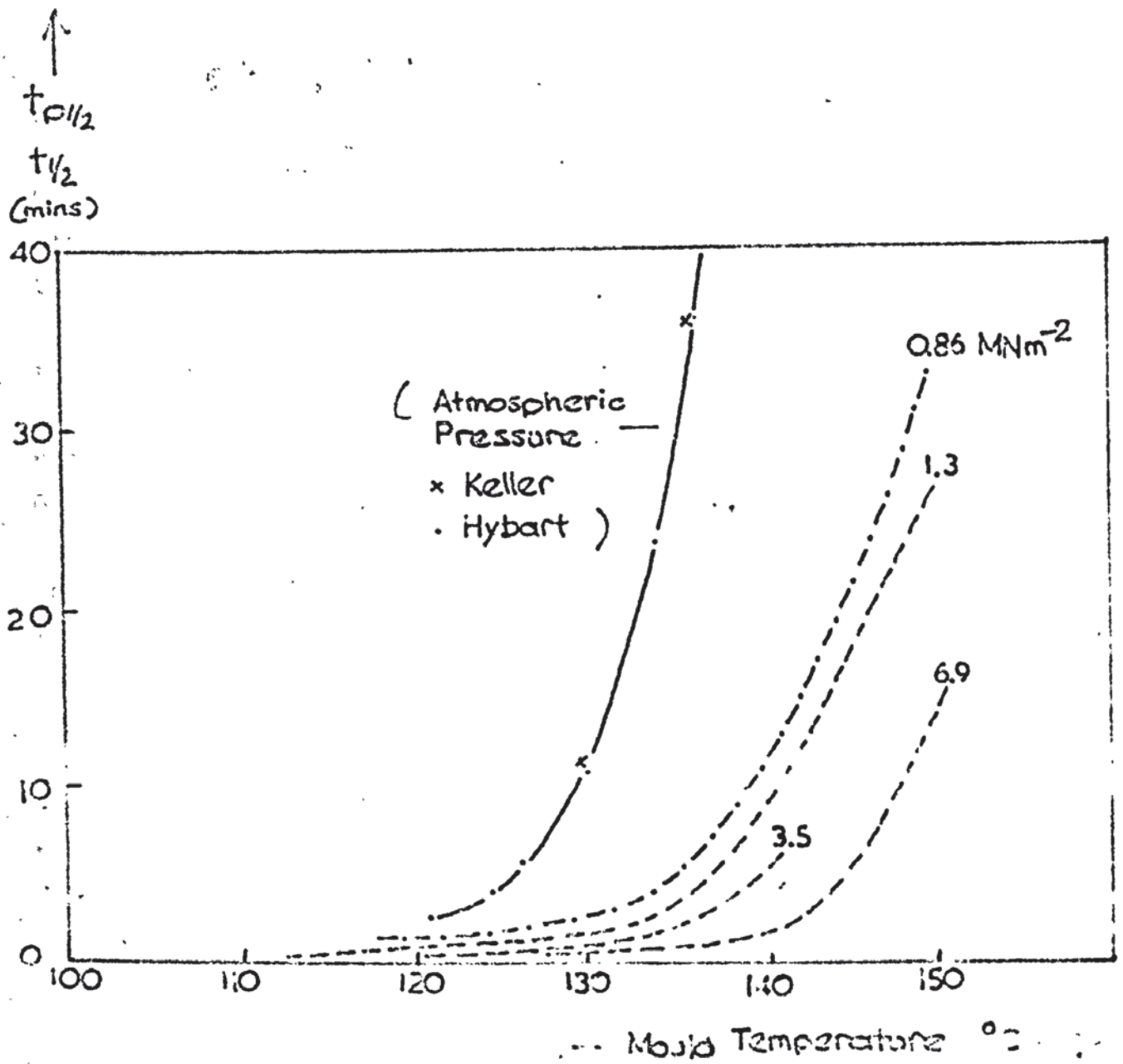


Fig.5.2. Comparison of $t_{p1/2}$ values with $t_{1/2}$ values from normal crystallisation conditions.

The curves obtained were very similar and to check this further some samples were moulded at the lowest practicable injection pressure. This was at 0.86 MN m^{-2} and this curve is also shown in figure 5.2. It can be seen to follow the same trend.

This then suggests that the rate of pressure drop does contain a contribution from the crystallisation process. At any particular mould temperature the "half-life" under pressure is very much shorter than at atmospheric pressure. This faster drop could be due to crystallisation which occurs much faster under pressure.

Assuming that the pressure drop is related to the rate of crystallisation then the rate of drop might be expected to obey a relationship linking the rate of crystallisation with crystallisation temperature. One of the many relationships derived is that by Mandelkern, Quinn and Flory (20) in which they show that the temperature dependence of the crystallisation rate is given by an equation of the form:

$$\ln(\text{rate}) = A - B \left(\frac{T_m^2}{T \Delta T^2} \right) \dots (5.1)$$

where T is the crystallisation temperature, T_m is the thermodynamic melting point of the polymer and ΔT is the value $T_m - T$. A and B are constants.

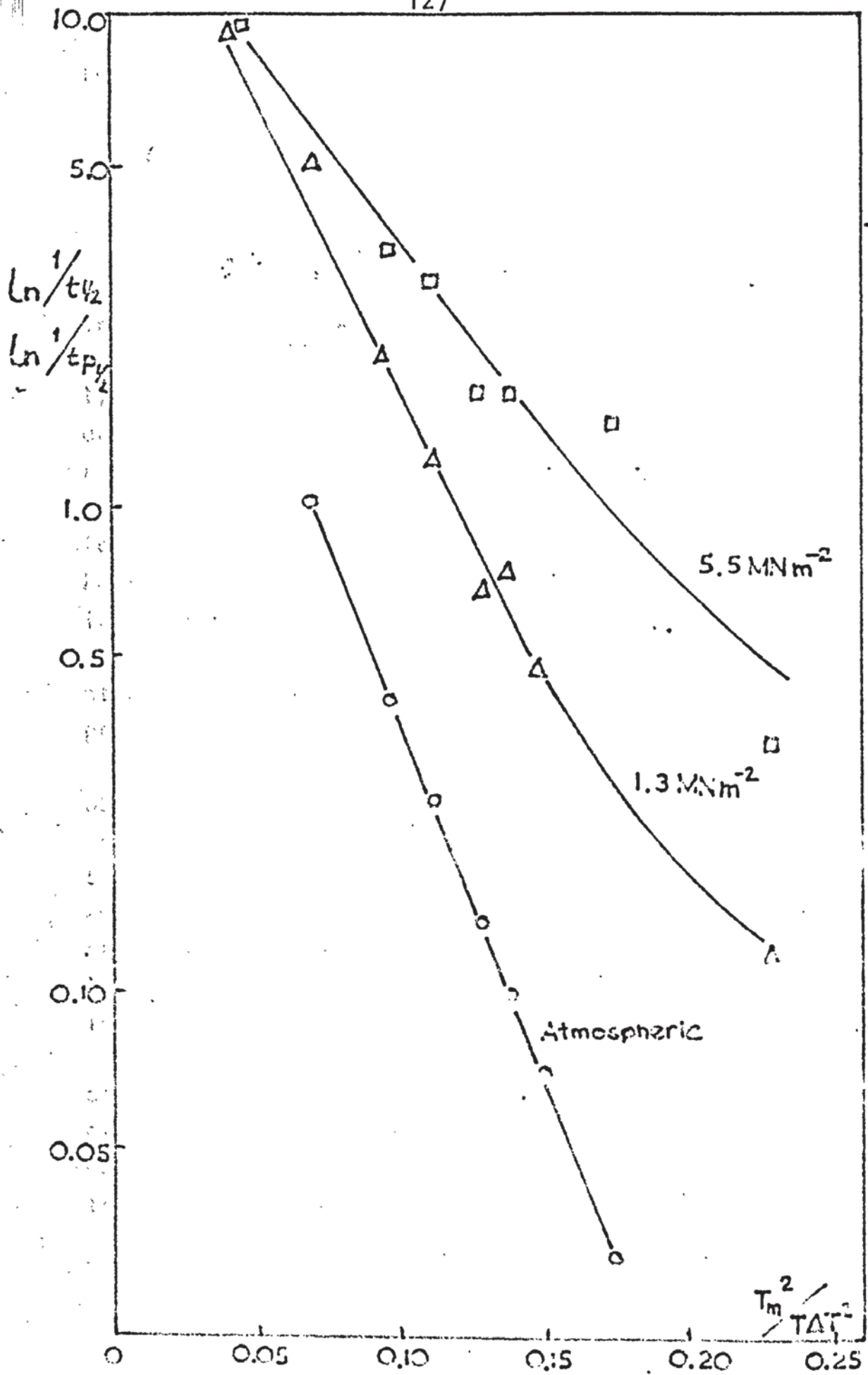


Fig.5.3. Temperature dependence of crystallisation and rate of pressure drop.

In terms of the half-life the equation becomes:

$$\ln \frac{1}{t_{\frac{1}{2}}} = \frac{A - \ln \ln 2}{n} - \frac{B}{n} \left(\frac{T_m^2}{T \Delta T^2} \right) \dots \dots (5.2)$$

In other words a graph of $\ln 1/t_{\frac{1}{2}}$ against $T_m^2/T \Delta T^2$ should result in a straight line. Assuming a melting point of 170°C the results are shown in figure 5.3. for both the crystallisation at atmospheric pressure and the $t_{p\frac{1}{2}}$ results at two injection pressures.

It can be seen that a very good straight line resulted for crystallisation rates at atmospheric pressure. Reasonable straight lines were obtained at the two injection pressures. A possible discrepancy may have resulted here in assuming that the melting point at atmospheric pressure was the same as that under varying pressures.

Further consideration shows that the pressure drops obtained with polypropylene must predominantly be due to crystallisation. The pressure drop can only be due to thermal contraction while the polymer is cooling and achieving the mould temperature. The drop in pressure after this time must therefore be due to either crystallisation or leakage. The latter can be ruled out since long screw forward times were used.

Results tend to show then that the crystallisation of the polymer is the predominant contribution to the rate at which the cavity pressure drops, and at any particular mould temperature an increase in injection pressure leads to an increase in the rate of crystallisation.

5.3. Effect of processing variables on crystalline structure.

5.3.1: General appearance.

The general appearance of the structures obtained compares well with those previously discussed in the literature. The edge-band and central spherulitic structure has been discussed by Clark (48) with injection moulded polyoxymethylene and he found the edge-band to have a thickness of $125\mu\text{m}$. In the present study there appeared to be little correlation between the edge-band thickness and the processing conditions, although it appeared to have more structure at the higher mould temperatures particularly where large central spherulites were appearing.

At mould temperatures in the region 10 to 60°C the structure appeared as a mass of small spherulites with injection pressure having little effect. In the region 60 to 120°C the structures were more noticeably spherulitic particularly at the lower injection pressures. At higher injection pressures in this temperature range the spherulites appeared smaller. In the region 120 to 150°C the most distinguishable spherulitic structures were produced. The predominant feature however was the effect of injection pressure. In general samples made at the highest injection pressures gave a mass of small well-defined spherulites while at lower injection pressures much larger spherulites were generally present.

5.3.2. Explanation of observed structures.

At the lower mould temperatures nucleation is assumed to be rapid irrespective of injection pressure, although in fact there appeared to be slightly more spherulites at the higher pressures. It is proposed that at these temperatures nucleation predominates over spherulite growth. So after a short length of time all available space is filled with a mass of small spherulites with little room for further growth. At the lowest injection pressures it is possible that less nuclei are produced and slightly more room is available for subsequent growth. This is illustrated in fig.5.4.

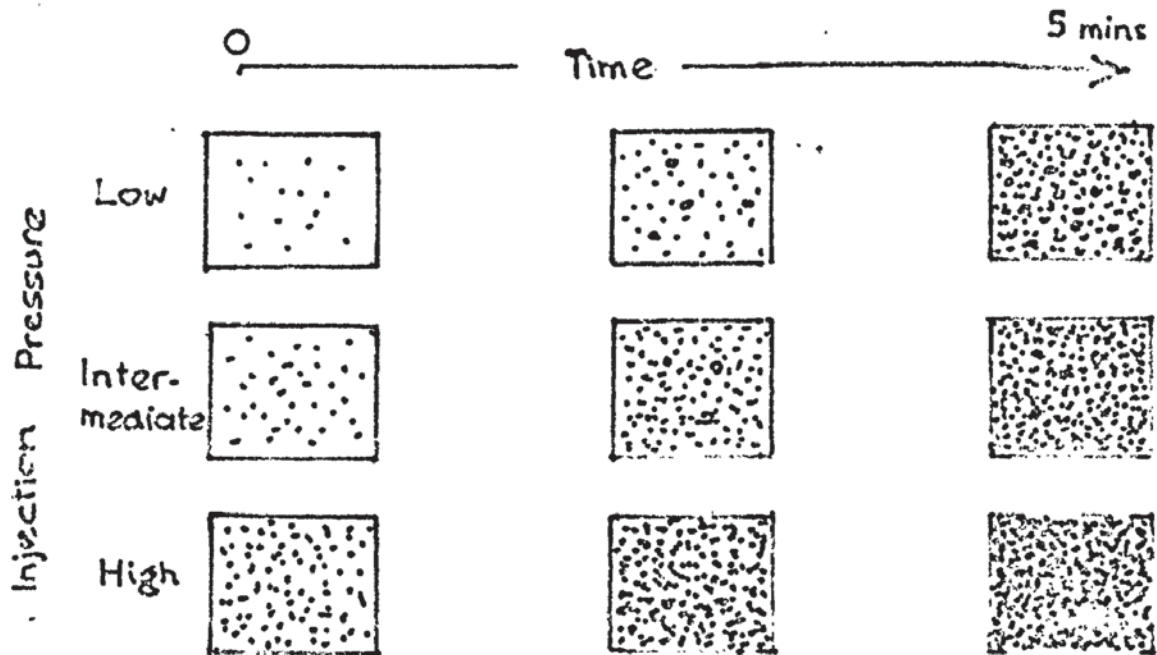


Fig 5.4. Structures produced at low mould temperatures.

This has assumed sporadic growth with time and the final structure produced on quenching after five minutes would therefore expect to contain a variation of spherulite sizes. It was difficult, however with spherulites of this size to say whether this was in fact

the case; but it can be confirmed that in general at the lower injection pressures the spherulites were slightly larger than at the higher pressures.

At temperatures in the region 120 to 140°C the predicted effect of injection pressure on structure is illustrated in fig.5.5.

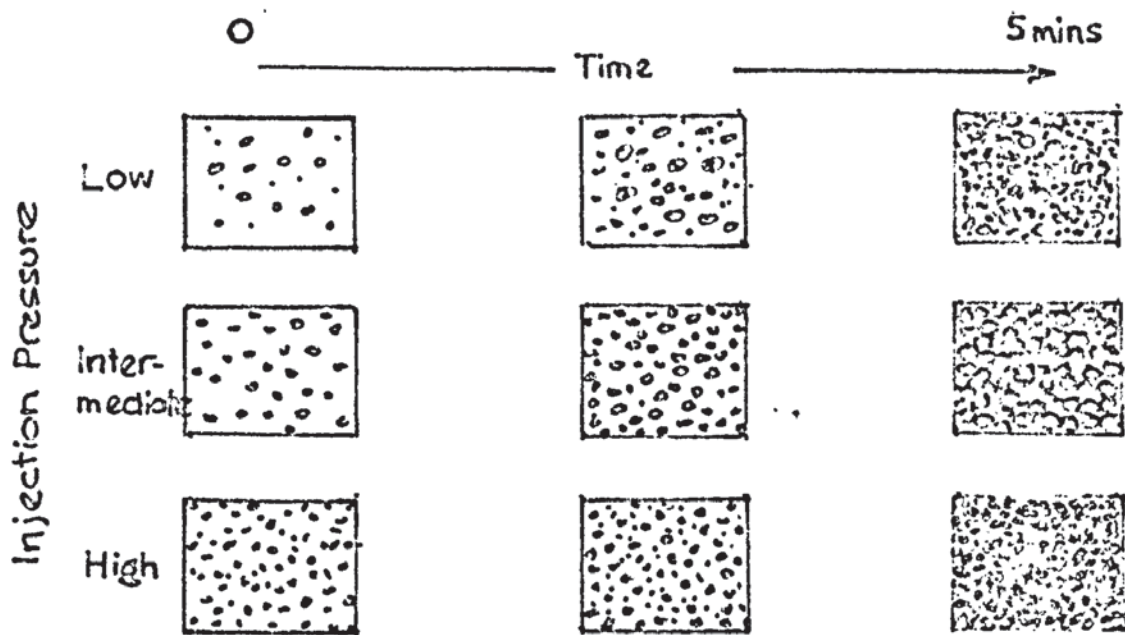


Fig.5.5. Structures produced in mould temperature range 120 - 140°C.

It is proposed that in this temperature region the effects of nucleation and spherulite growth have approximately equivalent effects. It is in this region that the maximum rate of overall crystallisation for polypropylene has been quoted (27, 29, 32). The rate of nucleation is assumed to be considerably lower than at the low mould temperatures. At high injection pressures however, this rate is still thought to be fairly high and although growth rate is high the available space is soon filled with little chance for further growth to occur. A mass of small spherulites results. At low injection pressures, nucleation, it is proposed, occurs to a far less extent and since spherulite growth is significant the presence of large spherulites

is expected. If sporadic nucleation is the mechanism by which new nuclei are formed then large spherulites randomly distributed in a matrix of smaller ones are expected to be present. At intermediate injection pressures a set of conditions is achieved where nucleation and growth occur at just the right levels to give fairly large spherulites of uniform size throughout the moulding.

By examining the photographs (plates 16 to 21) of samples prepared in this region it can be seen that the experimental results compare quite closely to those predicted. It is interesting to note also that it is in this region that voided structures were produced (this will be discussed later).

At very high mould temperatures i.e. greater than 145°C - the rate of nucleation is very low and the rate of growth is very much lower than at the lower temperatures. It is assumed that the majority of nuclei are produced during the quenching stage at the end of the cycle. At the very high pressures however, some nuclei may be produced initially and these will be allowed to grow. So at most injection pressures in this range one would expect to find a mass of small spherulites and at higher injection pressures the occasional large spherulite dispersed in a matrix of smaller ones. This is illustrated in fig.5.6.

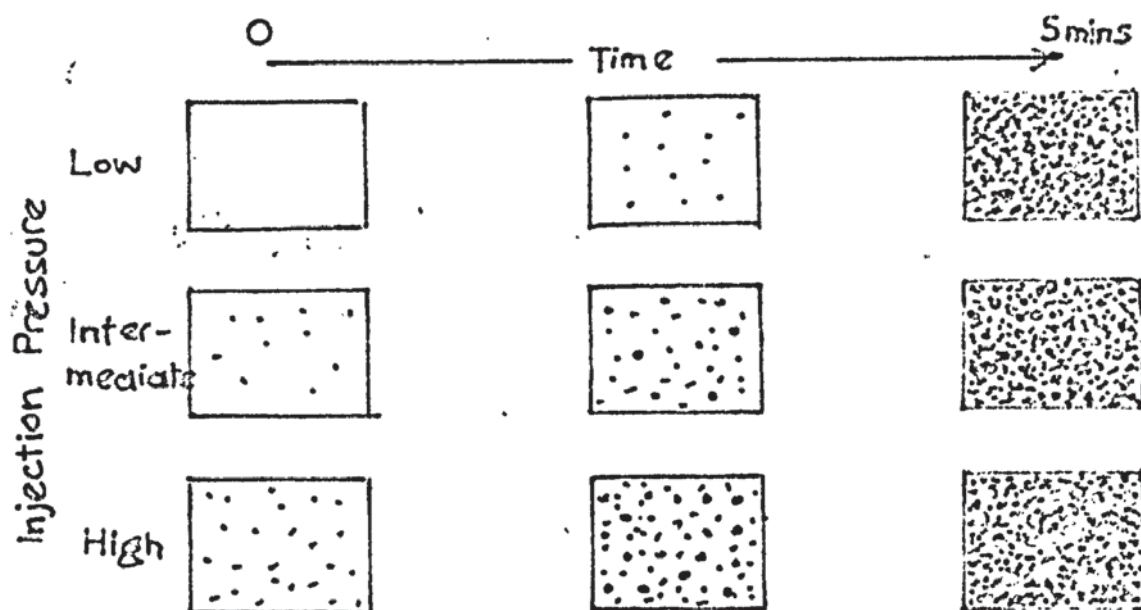


Fig.5.6. Structures produced at mould temperatures greater than 145°C .

Again the photomicrographs (plates 22 to 24) agree closely with the proposed theory.

Maxwell (26) has previously shown the effects of pressure on a polymer while it is cooling. He stated that pressure could induce crystallisation and suggested that this was because the melting point was pressure dependent, and at higher pressures the lower energy crystalline state is reached at higher temperatures. Matsuoka (22) too has found that the melting point is considerably affected by pressure.

It is proposed then that pressure is inducing nucleation and subsequent crystallisation. At high injection pressures nucleation is greater than at low injection pressures. This idea is illustrated diagrammatically in fig.5.7. which shows the proposed level of nuclei at any particular time at three different injection pressures for three regions of mould temperature.

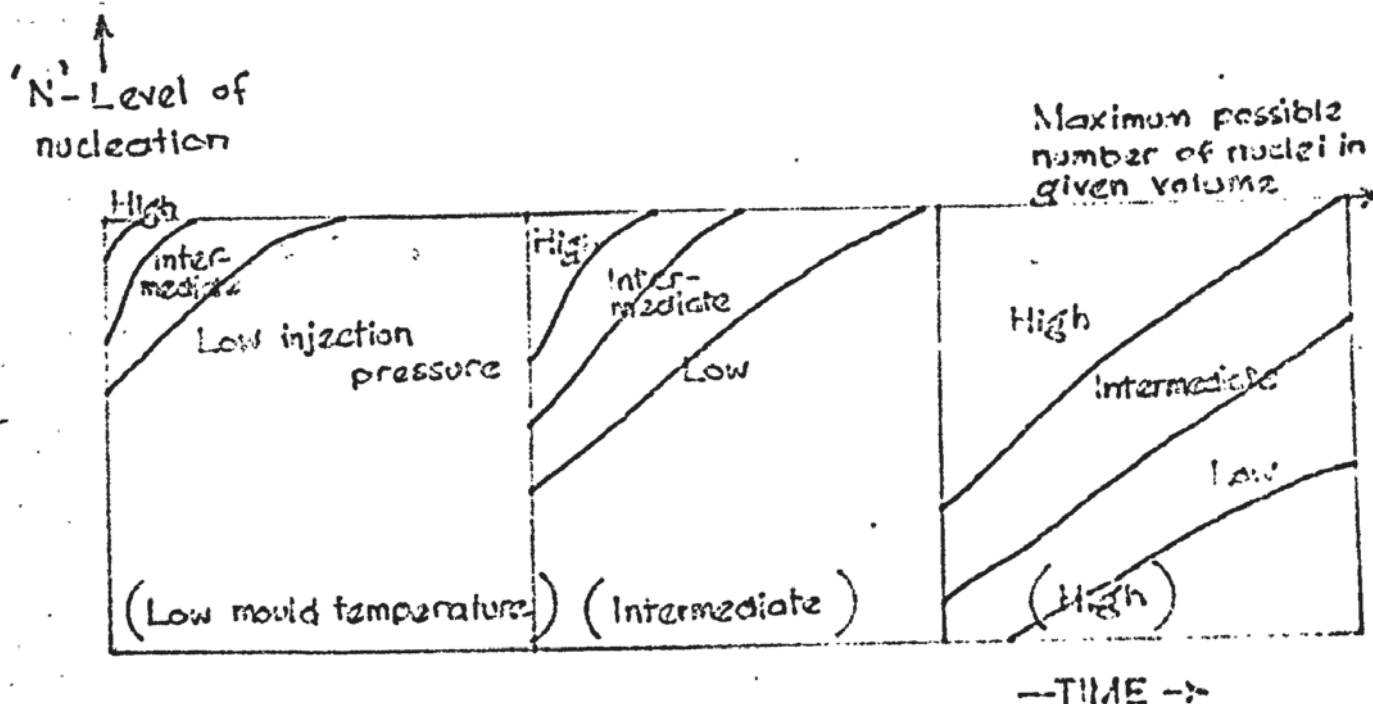


Fig.5.7.

These predicted graphs assume that nuclei are appearing with time. It can be seen that at the lower and intermediate mould temperatures the greater majority of nuclei are produced instantaneously and the higher the injection pressure the more nuclei there are produced. As can be seen, at high temperatures it is expected that some time will elapse before any nuclei are produced at the lowest injection pressures. As injection pressure is reduced this lag might be expected to increase and so at atmospheric pressure quite a time will elapse before nuclei begin to appear. This corresponds to the induction time which has been discussed in the literature. It would appear that there is little time dependence of nucleation at the low and intermediate temperatures except at the low pressures, whereas at high mould temperatures one might expect time dependence of nucleation at all injection pressures.

Sharples (10) has stated that the relation between nucleation rate and the temperature of crystallisation has been determined in a limited number of cases for the temperature range just below the melting point, and such data that do exist confirms that this will increase very rapidly once the degree of super-cooling exceeds a certain value.

The graphs in fig.5.7. have been predicted assuming no growth to take place, so that eventually the maximum possible number of nuclei will result under all conditions. When growth is considered together with nucleation, however, the maximum number of nuclei in that same volume will be lower leading to spherulites of larger dimensions. The predicted relationship of overall growth with time at various mould temperatures and injection pressures is illustrated in fig.5.8.

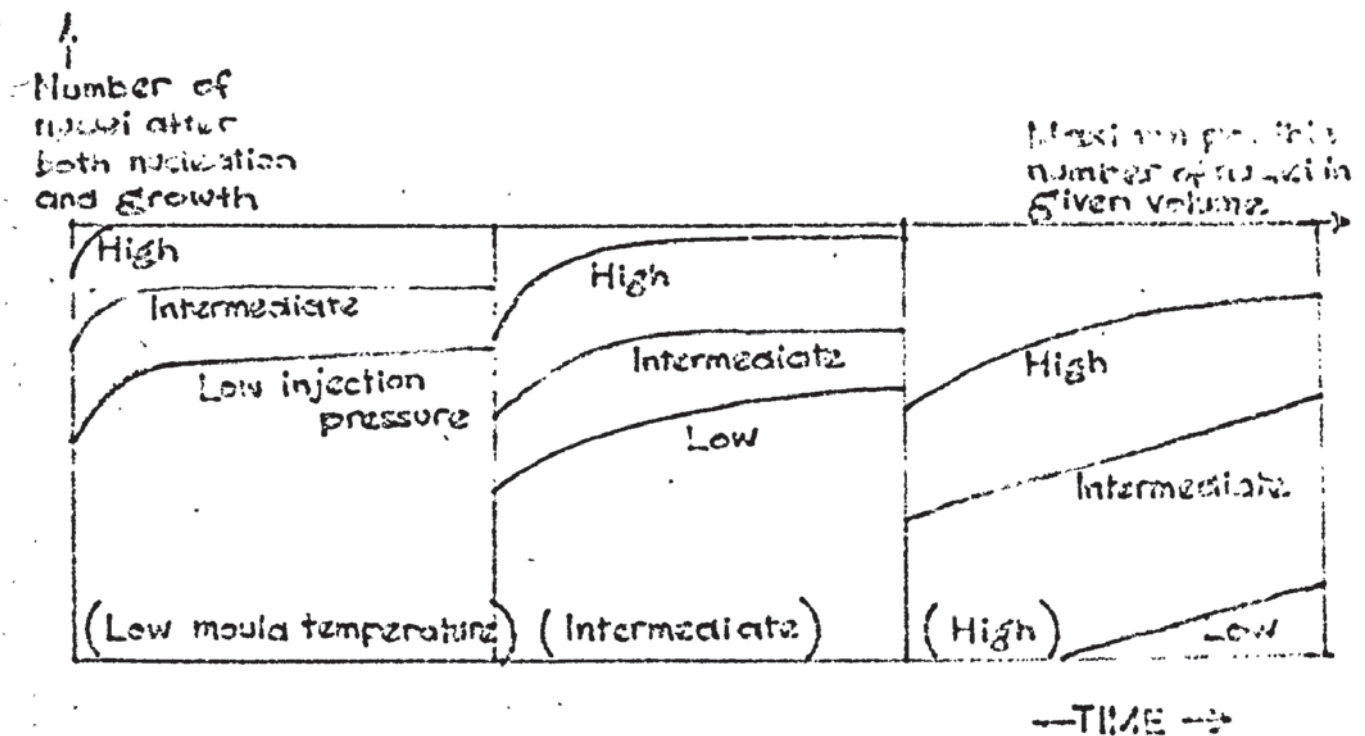


Fig.5.8.

5.3.3 Effect of moulding time on crystalline structure.

This proposed theory is confirmed from an examination of the samples made at various moulding times (plates 40 to 75).

At 130°C it can be seen that the greatest time dependence of nucleation and growth occurred at the lowest of the injection pressures used. After one minute a few reasonably large spherulites were present while after ten minutes the entire area was filled with large spherulites of fairly constant size. At the higher pressures little variation in size was noted with time, and at the highest pressure the smallest spherulites were produced.

At 140°C time dependence of growth was noted at both low and intermediate injection pressures. At the lowest pressure new spherulites appeared throughout the forty minutes and after forty minutes there was still room for more nucleation and subsequent growth. At the intermediate pressure a similar situation existed as occurred at a mould temperature of 130°C and injection pressure 1.3 MNm⁻² (130/1.3) whereby after ten minutes almost all of the area was filled with large spherulites, but their size was slightly smaller suggesting a higher rate of nucleation. At the highest injection pressure little variation in size with time was noted, but the size of the spherulites appeared slightly larger than those produced at 130/6.9 again suggesting that nucleation was less.

At 150°C there was no time dependence at the lowest injection pressure, but spherulites appeared at the intermediate injection pressure and after forty minutes under these latter conditions there was still room for further nucleation and subsequent growth to take place. The greatest time dependence was shown at the highest injection pressure where, as at 130/1.3 and 140/4.1, almost the entire area was filled with large spherulites after ten minutes.

Analysis of the spherulite growth rates (see table 4.4) confirms the above observations. The spherulite growth rate at 130°C based on maximum diameter achieved was a maximum at the lowest injection pressure of the pressures used, and the maximum growth rates at 140 and 150°C occurred at the intermediate and highest injection pressures used respectively.

So the photographic evidence agrees with the predicted behaviour quite well assuming 130 , 140 and 150°C to be low, intermediate and high mould temperatures respectively which have been discussed earlier. From the photographs then, an idea of the actual overall rate of crystallisation including both nucleation and growth can now be obtained and fig.5.8, the predicted curves, can be estimated more accurately. In fig.5.9 the overall growth is plotted on an arbitrary scale against time at different injection pressures at the three mould temperatures considered. This can be done since it has been shown that the rates of growth at $130/1.3$, $140/4.1$, $150/6.9$ are similar as are those at $130/4.1$ and $140/6.9$, and those at $140/1.3$ and $150/4.1$. It can be seen that these graphs compare very well with those predicted earlier in fig.5.8.

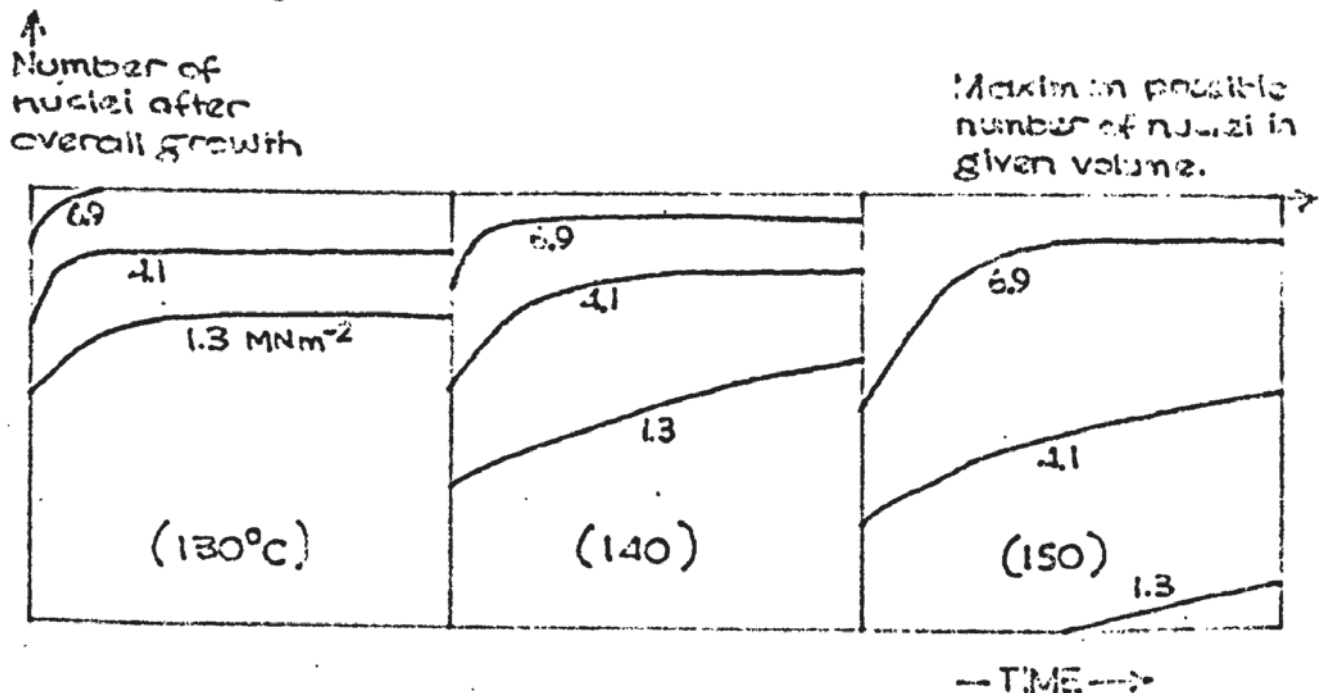


Fig.5.9

This variation in number and size of spherulites with temperature and time has been discussed in the literature by various workers. Magill (30) has shown that the number of spherulites per unit volume decreases while their size increase, as the isothermal crystallisation temperature is raised. Beck and Ledbetter (34) using DTA found that at relatively low cooling rates the spherulitic growth rate predominates over the nucleation rate and a few large spherulites are obtained. At more rapid cooling rates the large dependency of the nucleation rate predominates over the spherulitic growth rate and many small spherulites result. Marker and Hay (29) used microscopy to study the kinetics of crystallisation of polypropylene in the region 120 to 160°C, and found that the lower the temperature of crystallisation the faster the rate of growth, and also that the number of spherulites produced in a certain volume increased initially with time, but gradually reached a constant value as the spherulites began to touch each other.

5.3.4. Nucleation levels.

The temperature dependence of the growth rate for spherulites has been determined for several systems, and in all cases a pronounced maximum is observed. The dependence of the nucleation rate has received far less attention, although again it is assumed that the nucleation rate passes through a maximum (10).

Examination of the photographs shows similarity of structures made under different processing conditions. The particular structures and the conditions under which they were made are tabulated in table 5.1.

Figure 5.10 illustrates this more clearly.

<p>'Quenched' structures- designated 'No'- produced by high mould temperatures followed by quenching prior to ejection.</p>	<p>Large spherulites</p> <p>'N'₁</p>	<p>Voided structure</p> <p>'N'₂</p>	<p>Mass of small spherulites (not due to quenching)</p> <p>'N'₃</p>
<p>130°C/0.86MNm⁻²</p> <p>135/1.3</p> <p>137/2.1</p> <p>140/2.8</p> <p>145/3.5</p>	<p>118/0.86</p> <p>128/1.3</p> <p>130/2.1</p> <p>132/2.1</p> <p>135/2.8</p> <p>137/3.5</p> <p>140/4.1</p> <p>145/5.5</p>	<p>125/1.3</p> <p>127.5/2.8</p> <p>130/3.5</p> <p>132/4.1</p> <p>135/4.8</p>	<p>120/3.5</p> <p>125/4.8</p> <p>135/6.2</p> <p>137.5/6.9</p>

Table 5.1

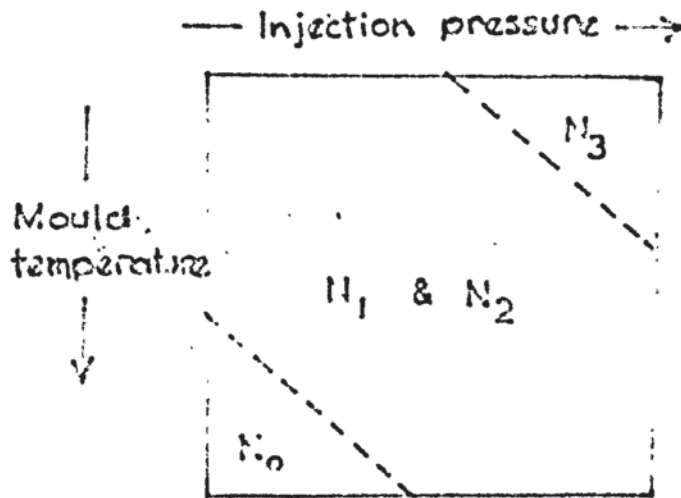


Fig.5.10 Nucleation levels expected under conditions of mould temperature and injection pressure.

In this figure injection pressure is increasing across the page and mould temperature down the page. The areas in which one might expect to find the respective levels of nucleation are shown.

So it will be assumed that $N_3 > N_2 > N_1 > N_0$. If these conditions are now plotted on a graph of level of nucleation (or number of nuclei) against mould temperature fig.5.11 results when points of equal injection pressure are joined. From this empirical graph it is confirmed that a decrease in mould temperature leads to an increase in nucleation level and also that an increase in injection pressure produces an equivalent level of nucleation at a higher mould temperature. This would suggest that at atmospheric pressure under normal conditions equivalent extents of nucleation to those produced in the present study would be produced at much lower temperatures. This would then be in agreement with previous workers (32) who have shown that the temperature of maximum overall crystallisation rate is in the region 114 to 121°C.

It will be shown in a later section that maximum overall crystallisation will normally result in a nucleation level somewhere between N_2 and N_3 .

The influence of injection pressure is to cause nucleation and subsequent crystallisation to take place at much higher temperatures than normally expected; a similar effect to that of nucleating agents.

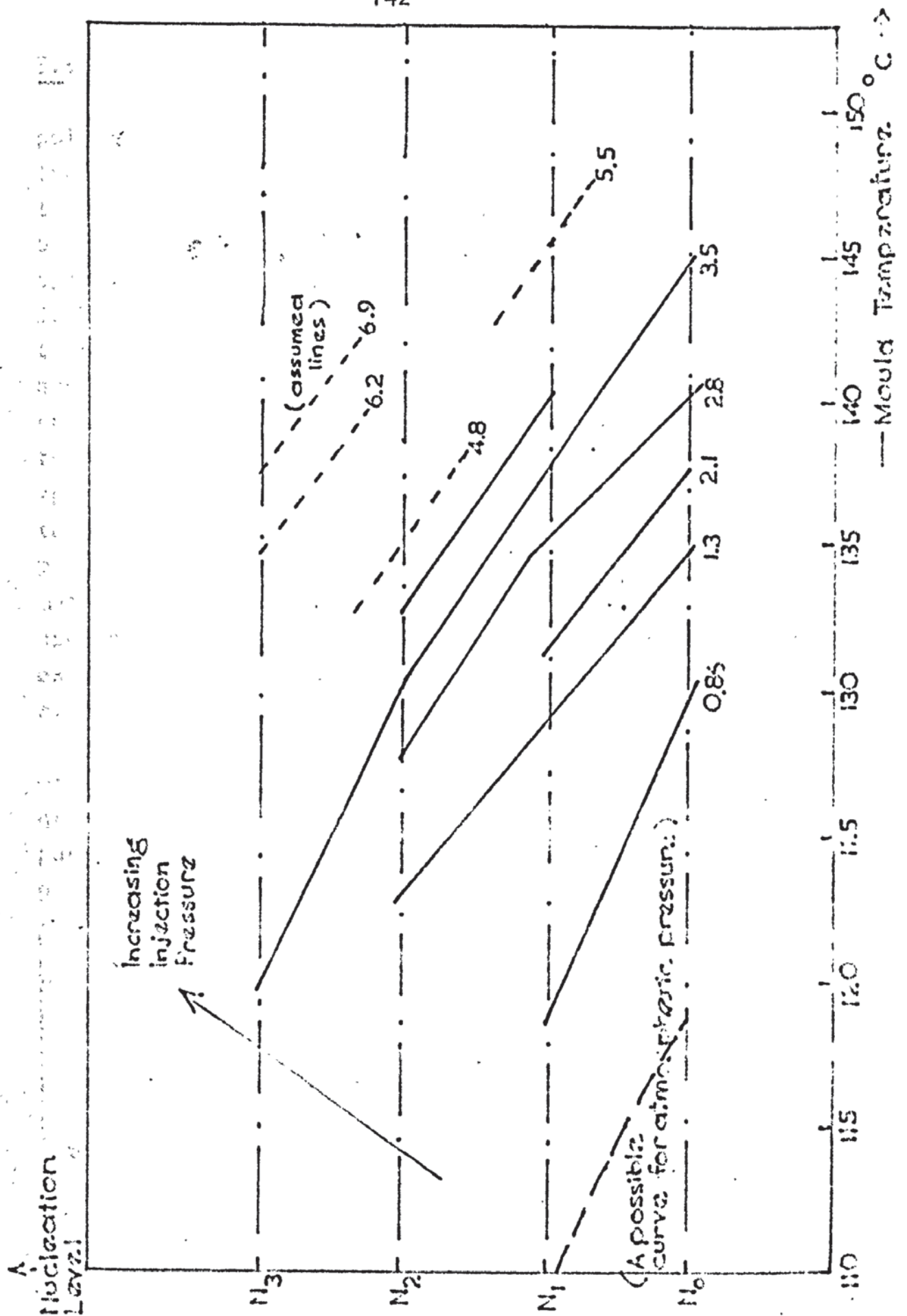


Fig. 5.11

5.3.5. Type of nucleation.

The type of nucleation that occurs when polypropylene is crystallised has been discussed in the literature by various workers. Examination of the photographs obtained in this study gave some idea as to whether the nucleation was simultaneous or sporadic. Examination of specimens made at constant moulding time under different conditions of mould temperature and injection pressure showed that below about 125°C nucleation was instantaneous since spherulite size variation was very slight. At temperatures above this however under certain conditions sporadic nucleation appeared to occur. At mould temperatures in the region 125 to 135°C at low injection pressures large spherulites were present dispersed in a matrix of smaller ones suggesting that nuclei were appearing sporadically with time. The same situation existed at mould temperatures in the range 140 to 150°C at higher injection pressures.

Samples made at varying moulding times gave more insight into the type of nucleation and subsequent growth occurring. The type of nucleation under particular conditions of mould temperature and injection pressure is summarised in table 5.2.

	130	140	150°C
1.3 MNm ⁻²	Sporadic	Sporadic	Instantaneous (produced on quenching)
4.1	Instantaneous	Sporadic	Sporadic
6.9	Instantaneous	Instantaneous	Sporadic

Table 5.2.

If this trend is followed throughout the complete mould temperature range it can be assumed that at temperatures below these (irrespective of injection pressure) nucleation is instantaneous. At temperatures above 150°C nucleation is sporadic although at short moulding times and low injection pressures the structure appears as a mass of small uniform size spherulites produced on quenching.

This disagrees however with the findings of Magill (30) who has shown that at atmospheric pressure under the polarising microscope nuclei are produced simultaneously above about 115°C . Below this nuclei are sporadically formed although he could not completely resolve the precise morphology of structures crystallised below 115°C . He based his conclusions on the values he obtained for the Avrami exponent. The sporadic nucleation discussed in this present paper does not necessarily imply homogeneous nucleation. Indeed it would seem unlikely that the nucleation mechanism would suddenly change with a sudden change in conditions. What is probably happening in the cases where sporadic nucleation was observed is that heterogeneous centres were being brought into play successively, and so resulted in a time dependent or sporadic process. This has been discussed by Sharples (10).

The nature of the heterogeneities is a little uncertain. Nucleating agents are ruled out in this present study since it was confirmed by the suppliers that none had been added to the batch used. It is still possible however that particles of other additives that may have been used e.g. stabiliser could act as nucleating centres. Heterogeneities taking the form of particles containing crevices capable of being wetted by the molten polymer has been advanced (80). This seems a very possible source of centres for nuclei to be formed when one considers the machined surface of the mould cavity. Microscopic examination would show this to be a very

uneven surface with many crevices. This would lead to rapid nucleation at the surface and is the probable explanation of the edge band formation. Evidence from the photomicrographs obtained suggests that this edge band can give rise to a type of 'self-seeding' nucleation for the bulk of the material. The photograph (plate 76) below shows this, where it can be seen that spherulites are appearing at the boundary between the edge band and the bulk of the polymer.

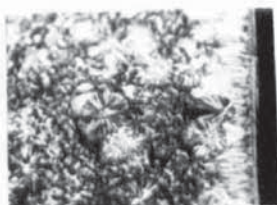


Plate (76)

It is interesting to note also that this region between the edge band and central spherulites may correspond to a region of maximum orientation as discussed by other workers (3,45), and this may also initiate growth in the bulk of material.

5.3.6. Voiding.

Examination of tables 4.5 and 4.6 shows the conditions under which voided structures were produced. It can be seen that these conditions correspond closely with those conditions where fairly large spherulites were produced, that is where the overall combination of growth and nucleation was a maximum. It is possible that these voids are produced by contraction of the polymer. Since the outer surface of the moulding is rapidly crystallised it hardens quickly and forms a type of "envelope" and so contraction cannot be taken up at the surface in the form of sink marks. The reason for the contraction is either due to further

thermal contraction or is possibly due to imperfect rapidly grown spherulites perfecting themselves and at the same time leaving voids between the new slightly smaller spherulites. Low pressure favoured this voiding and in fact voiding was not produced at the higher injection pressures. Table 4.6. shows the voiding process to be time dependent, and so the voided samples made at a moulding time of five minutes must be made under conditions of near maximum nucleation and growth. This reduction in spherulite size with time could be due to secondary crystallisation, as discussed by Remaly & Schultz (59) since the two stages (primary and secondary) of crystallisation have been shown to produce a distinct break when crystallised under pressure (22). By using processing conditions known to produce voiding it was shown that the voiding could be destroyed by increasing the mould temperature to 175°C for a period of time prior to quenching and ejection, while the actual spherulitic structure remained the same. It appears that this temperature is enough to cause mobility of spherulites and hence destroy the voiding but not to melt them and so change the structure.

Voids are very common in thick sections of polypropylene and it seems possible that because of heat transfer problems conditions at the centre are close to those of maximum nucleation and growth. The slow cooling of thick sections and the rapid stiffening of the material on cooling can result in cavitation (81). If the outside skin of the moulding cools and solidifies rapidly further shrinkage takes place in the inside and bubble-like voids are formed. The earlier freezing of the outside surfaces of the moulding in thicker sections is the reason for the internal voiding according to Glanvill (3) since the hot core can only take up its further cooling contraction by forming such voids. Kuhre (32) found that voids in thick sections were reduced by the addition of nucleating agents again showing that voiding is associated with larger spherulitic structures.

5.4. Effect of processing conditions on percentage crystallinity

At the very low and very high mould temperatures the percentage crystallinity was less than 60%. For mould temperatures in the range 110 to 145°C the value varied from 60 to 68%. So in general the more 'spherulitic' (having regard to their size and concentration) the structure the higher the percentage crystallinity. Typical values for the percentage crystallinity quoted in the literature of commercial polypropylene are between 60 and 80% (82).

It was noted that at a particular mould temperature there was an injection pressure at which the percentage crystallinity was at a maximum. The higher the mould temperature the higher the pressure at which this maximum occurred. This is shown in table 5.3.

Mould temperature °C	Maximum percentage crystallinity at this temperature	Injection pressure at which maximum is produced MN m ⁻²
109	63.8	1.3
120	66.2	1.3
125	67.3	2.1
127.5	66.6	3.5
130	66.8	4.1
132.5	66.4	4.8
135	67.0	4.8
140	67.5	5.5/6.2
145	67.2	6.9

Table 5.3.

By referring to the photomicrographs it can be seen that the highest percentage crystallinity achieved did not always correspond to the structure containing the largest spherulites. It did correspond however to a particular level of nucleation shown in fig.5.11 and was somewhere between the nucleation producing a voided structure (N_2) and the nucleation producing a mass of small spherulites (N_3). Presumably this allows the right number of nuclei to grow to a size which results in the most efficient packing. The samples containing large spherulites (i.e. based on nucleation level N_1) had percentage crystallinities in the region 61 to 63%. Samples with the quenched structures (i.e. those based on nucleation level N_0) had percentage crystallinities in the region 59 to 60%. This tends to back up the assumptions that were made in the production of fig.5.11 regarding the relative positions of the levels of nucleation.

The effect of injection pressure is again reflected in the values of the percentage crystallinities. Examination of figures 4.8 and 4.9 shows that maximum values for the degree of crystallinity occurred at the higher mould temperatures at the higher injection pressures. This correlates well with the discussion in section 5.3.

It is interesting too to note that the voided structures were produced under the conditions corresponding to the peaks of these curves (figs.4.8 & 4.9). The actual value of the density was not known for the voided samples since the density gradient column is an unsuitable technique for voided samples, but it can be assumed that the highest density samples were those made under conditions of maximum combination of nucleation and growth.

This follows since from a fixed volume of melt, a higher density in the final component must infer a greater volumetric contraction.

The same correlation is found for samples made for varying moulding times. Under conditions of maximum time dependence of growth i.e. $130^{\circ}\text{C}/1.3\text{MN m}^{-2}$, 140/4.1, 150/6.9, voided samples were produced. Under all conditions there was always an increase in percentage crystallinity with moulding time. At high injection pressures it can be seen that the largest increase occurred between 1 and 10 minutes suggesting that it was during this time that the majority of crystallisation took place, and that little followed from 10 to 40 minutes. Also at the high injection pressures the samples made for 1 minute had a fairly high value compared with those prepared at lower injection pressures for the same time. This suggested that nucleation and growth had occurred in one minute under the prior conditions whereas under the latter conditions little growth appears to have taken place and the majority of the structure was produced during the quenching stage.

5.5. Effect of processing conditions on dynamic mechanical properties.

5.5.1. General

The general curve for $|\dot{E}|$ against temperature of testing was very reproducible and compared well with those appearing in the literature. The temperature dispersion for $\tan \delta$ was far less reproducible and although the curve followed the expected shape the value and position of the maxima were inconsistent which is to be expected since $\tan \delta$ is very sensitive in the region of T_g .

The value of the dynamic tensile complex modulus ($|\dot{E}|$) at 22°C was in the range 1.40 - 2.30 GN m⁻². The maximum in the damping curve occurred in the range of 15 - 20°C and its value was in the range 0.06 - 0.09.

Little has appeared in the literature on dynamic mechanical tests at higher frequencies, the majority of work on polymers having been done using the torsional pendulum in the frequency range 0.1 - 1.0 Hz. Workers using the torsional pendulum (40, 65) have found that $\tan \delta$ is a maximum at about 5 - 10°C and has a value of approximately 0.1. The room temperature dynamic shear modulus using the same technique was approximately 0.1 GN m⁻². Takayanagi (83) has measured $|\dot{E}|$ at 100 Hz using the rheovibron and quotes a room temperature value for polypropylene of 2.0 GN m⁻².

It is difficult however to make direct comparisons with literature values since it is generally accepted that dynamic properties are dependent on the physical structure.

5.5.2. Effect of processing conditions on dynamic mechanical properties.

It can be seen that in general the variation of room temperature modulus with processing conditions is small but consistent. Modulus increased with mould temperature up to 109°C which corresponded with the onset of formation of some distinguishable crystalline texture, but above this mould temperature modulus was fairly constant irrespective of the nature of the crystalline texture. This has been shown previously by Gumen et al (58). Generally speaking at the lower mould temperatures the modulus was higher at the lower injection pressures, and at the higher mould temperatures modulus was generally greater at the higher injection pressures. These results follow the same trend as the previous discussion in that the mould temperature at which the maximum modulus was achieved increased with increasing injection pressure.

A better correlation that can be made between modulus and processing conditions is via the percentage crystallinity or density. The higher the percentage crystallinity the higher the modulus. This has previously been shown by Neilsen (61). The variation of both with mould temperature is shown in fig.5.12.

It is noted that the two curves correspond quite closely, except for the minimum present in the modulus curve. However, closer examination shows that this minimum occurred under the same conditions which produced voided specimens. Under conditions where no voiding was produced, i.e. high injection pressures, then no minimum in the modulus was produced. It was also noted that although the voided samples were weaker than the other crystalline structures they still had a slightly higher modulus than the samples with no distinguishable crystalline structure.

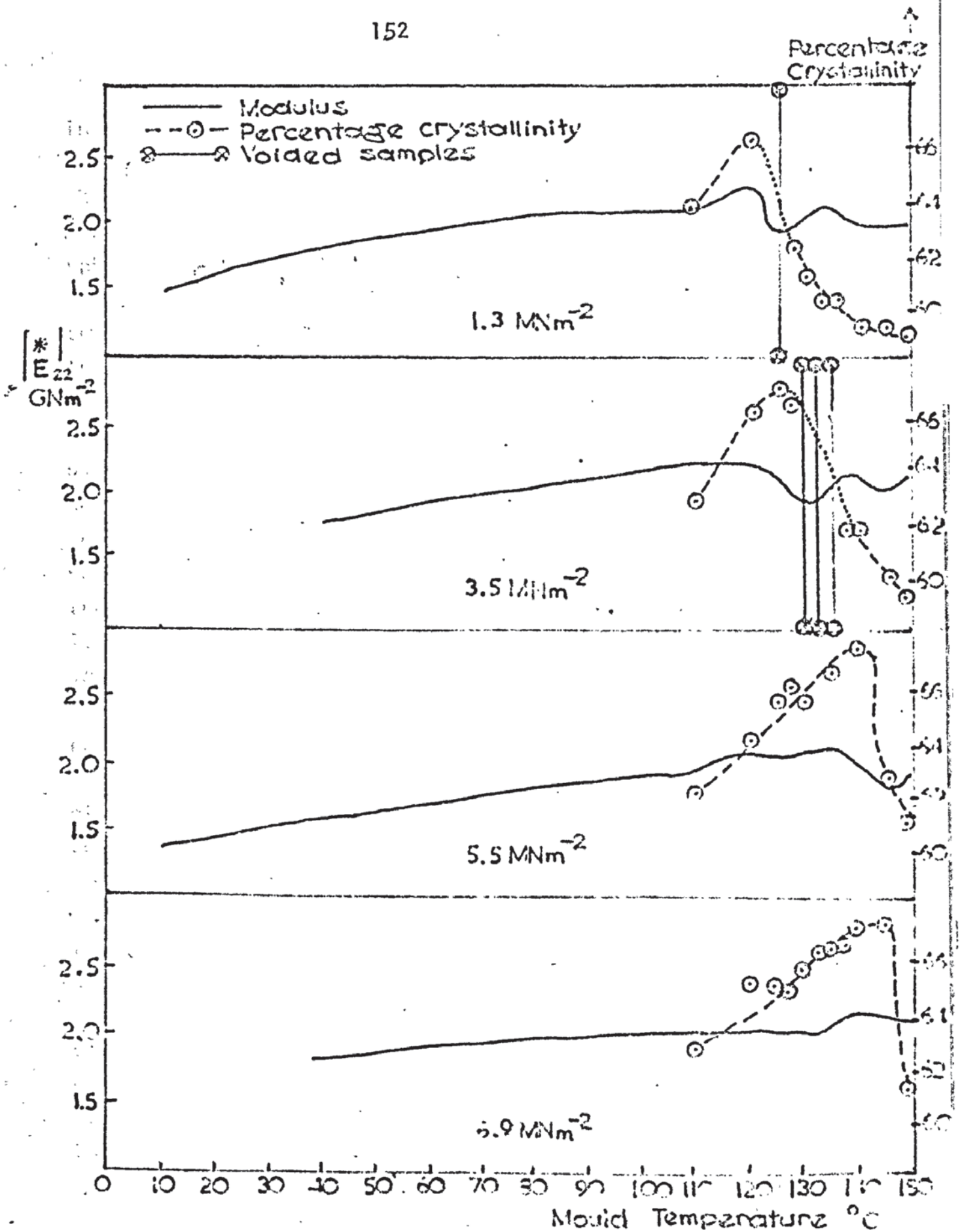


Fig.5.12. Variation of $|E_{22}^*|$ and percentage crystallinity with mould temperature at different injection pressures.

As has already been discussed, an increase in the percentage crystallinity does not always correspond to an increase in spherulite size, in fact the maximum normally corresponds to conditions of maximum nucleation and growth rather than the largest spherulites.

Examination of the photomicrographs shows that specimens with a room temperature modulus lower than 1.9 GN m^{-2} have a fairly indistinguishable structure and were those made at the low mould temperatures, while those with higher moduli have some sort of crystalline structure. It appears that the presence of finite sized spherulites generally produces a higher modulus, but that variations in spherulite size do not greatly affect the value. The edge band appeared to contribute little to the overall strength of the sample. This was demonstrated by testing a voided sample in the normal manner and then again with the edge band removed. The traces obtained were very similar.

The moulding time also appeared to have little effect on the dynamic tensile modulus. It might have been expected that since percentage crystallinity increased with increasing moulding time then so should the modulus. However, although in general modulus was fairly constant throughout the range of moulding times, at any particular moulding time the higher the percentage crystallinity the higher the modulus. The biggest variation occurred at 130°C at the lowest injection pressure used. Under these conditions, at a moulding time of ten minutes and longer, the samples were voided and so one expects the modulus to be lower. The increase at the longest moulding time of forty minutes is probably due to perfection of spherulites and this is borne out by the reduction in spherulite diameter at this time. So under constant conditions of mould temperature and injection pressure an increase in moulding time produces little improvement in the dynamic tensile modulus and in fact under certain conditions can be detrimental.

5.5.3. Stress-strain measurements.

Stress-strain properties were briefly examined. Results have not been quoted since only one specimen was available from each set of conditions, and with a destructive test such as the tensile stress-strain test, where scatter is very large, results are only significant when averaged out over a series of identical samples. However, the indications were that samples containing a mass of small spherulites were tougher (measured approximately from area under the stress-strain curve) than those containing larger spherulites in that the former yielded when stretched while the latter broke. This has been generally accepted as the usual case, but again variation in spherulite size appeared to have little effect on the modulus (taken to be slope of stress-strain curve).

CHAPTER 6 - CONCLUSIONS

6.1. Effects of processing on structure and properties.

It has been shown that crystallisation of the polymer contributes to the rate at which the cavity pressure drops. At any particular mould temperature an increase in injection pressure leads to an increase in the rate of crystallisation.

The photographic evidence has shown that mould temperature and injection pressure can affect the resulting crystalline structure. At low mould temperatures nucleation predominates and a mass of small spherulites are produced irrespective of injection pressure. As the mould temperature is increased nucleation rate becomes lower and the growth process becomes more significant and so larger spherulites are produced; the higher the mould temperature the higher is the injection pressure required to give these. At high mould temperatures and low injection pressures where both nucleation and growth are small quenched structures result when the moulding is cooled. An increase in injection pressure under these conditions increases the nucleation and growth and larger spherulites result. This is summarised diagrammatically in fig.6.1. This shows that at intermediate mould temperatures there is a region where the combination of nucleation and growth is a maximum, and this region is shifted to higher temperatures at higher injection pressures.

Under the majority of conditions nucleation is instantaneous and final spherulite size is uniform.

Voided samples are produced under conditions of maximum nucleation and growth and their production is favoured at lower injection pressures.

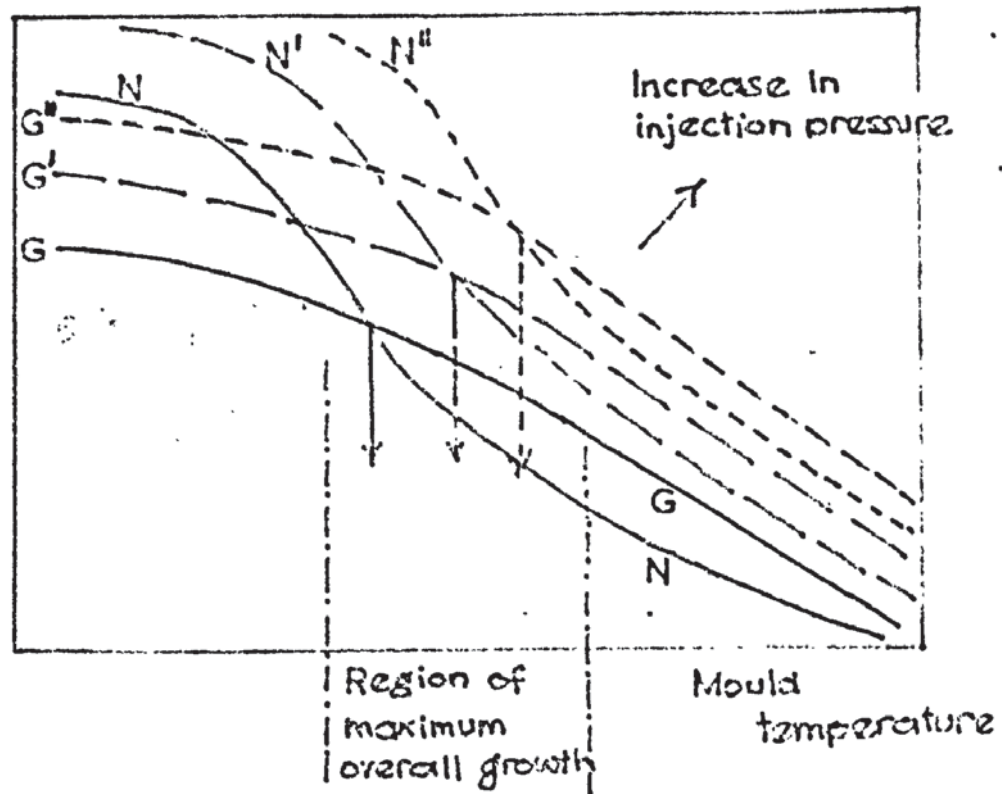


Fig.6.1.

The more spherulitic the structure the higher was the percentage crystallinity. The maximum percentage crystallinity did not correspond to the structure containing the largest spherulites but did correspond to a particular level of nucleation and occurred under conditions of maximum overall growth.

Modulus of crystalline structures was higher than the rapidly quenched structures produced at low mould temperatures, but variation in actual spherulite size had little effect on modulus. The variation of modulus showed better correlation with percentage crystallinity - an increase in percentage crystallinity leading to an increase in modulus. Voided samples had lower moduli than the ordinary crystalline structures but slightly higher moduli than the indistinguishable crystalline structures produced at low mould temperatures.

6.2. Practical implications.

Information is now available on the effects of processing conditions on crystalline structure, percentage crystallinity and dynamic mechanical properties. The conclusion of this study must then include a combination of all this information such that an overall picture can be given of the outcome of processing the polymer under certain conditions as regards its properties and eventual service life.

A disappointing result has been the relatively poor correlation between mechanical properties and crystalline structure, since it is not easy to say now which particular crystalline structure gives improved properties. This however seems to have confirmed previous work which has shown that the percentage crystallinity or the density has the dominant effect on modulus. As a general rule it has been said in the literature that the larger the spherulites the higher the stiffness or modulus and the lower the strength or toughness. However, it seems possible that due to the ambiguity of the word "crystallinity" it has been assumed that an increase in "crystallinity" has necessarily meant an increase in spherulite size. This has been shown not always to be the case. The non correlation between structure and dynamic mechanical properties may be in itself significant too, since it has been shown that any distinguishable crystalline structure gives similar values for modulus irrespective of spherulite size.

Conditions which are normally used for production runs during injection moulding would probably tend to give the lowest values for modulus, since the study has shown that samples moulded at temperatures below about 100°C have the lowest modulus.

The question must therefore be asked - is it worth changing processing conditions to gain an improvement in properties?

The best improvement possible in the present study as regards the room temperature modulus was from 1.40 to 2.30GN m^{-2} and this was achieved by increasing the mould temperature from 10 to 120°C and reducing the injection pressure from 5.5 to 1.3 MN m^{-2} with a moulding time of five minutes. Almost as good improvement was made from 1.40 to 2.17GN m^{-2} by just increasing the mould temperature to 120°C and keeping injection pressure constant at 5.5 MN m^{-2} . An increase of modulus of 50% can therefore be achieved simply by changing the mould temperature from 10 to 120°C. However, to do this steam heating of the mould must be used and so a steam heating circuit must be installed and, since the mould must be cooled before ejection, production rate will be lowered. However, by simply increasing the mould temperature to 60°C a modulus of 1.85GN m^{-2} (or 30% increase) can be achieved. Better still, by raising the mould temperature to 60°C and reducing the injection pressure from 5.5 to 1.3 MN m^{-2} a modulus of 2.00GN m^{-2} (or 40% increase) can be achieved. These latter changes in processing variables can be done relatively simply and cheaply with a water heater and mouldings too can be simply ejected with no extra mould cooling.

The examples presented above have resulted from fairly long moulding times. (i.e. five minutes with a screw forward time of three minutes) and, it must be stressed, using this particular mould geometry with fairly artificial conditions; but they give an indication of improvements that may be possible with simple adjustment of the processing variables.

The pressure induced nucleation noted in this work could be an advantage where toughness is required and many small spherulites desirable. The full benefit however probably would not be achieved under certain conditions unless fairly lengthy screw forward times were used; under the majority of conditions however it has been shown that instantaneous nucleation occurs within a very short time (say one minute) and little further growth was noted with an increase in moulding time. Pressure then can be useful in controlling structure but again for production purposes it may be necessary to use specific pressures for filling reasons. Again it has been shown that if very high injection pressures are used in conjunction with very high mould temperatures some large spherulites are produced.

Voiding has been shown to occur under certain conditions of fast crystallisation leading to rapid contraction and rapid cavity pressure drop. It would seem necessary therefore to use as high a mould temperature as possible to eliminate rapid crystallisation and contraction. It was shown too that voiding did not occur with high injection pressures. Voiding is a particular problem with thicker sections of polypropylene when moulded in cold moulds. Under normal conditions polypropylene cannot be quenched to a completely amorphous state without some crystallisation occurring. Consequently when thick sections are injected into a cold mould the central region may still be at a much higher temperature at which crystallisation can take place at conditions of maximum combined nucleation and growth. This central large spherulitic region would be particularly prone to produce voids.

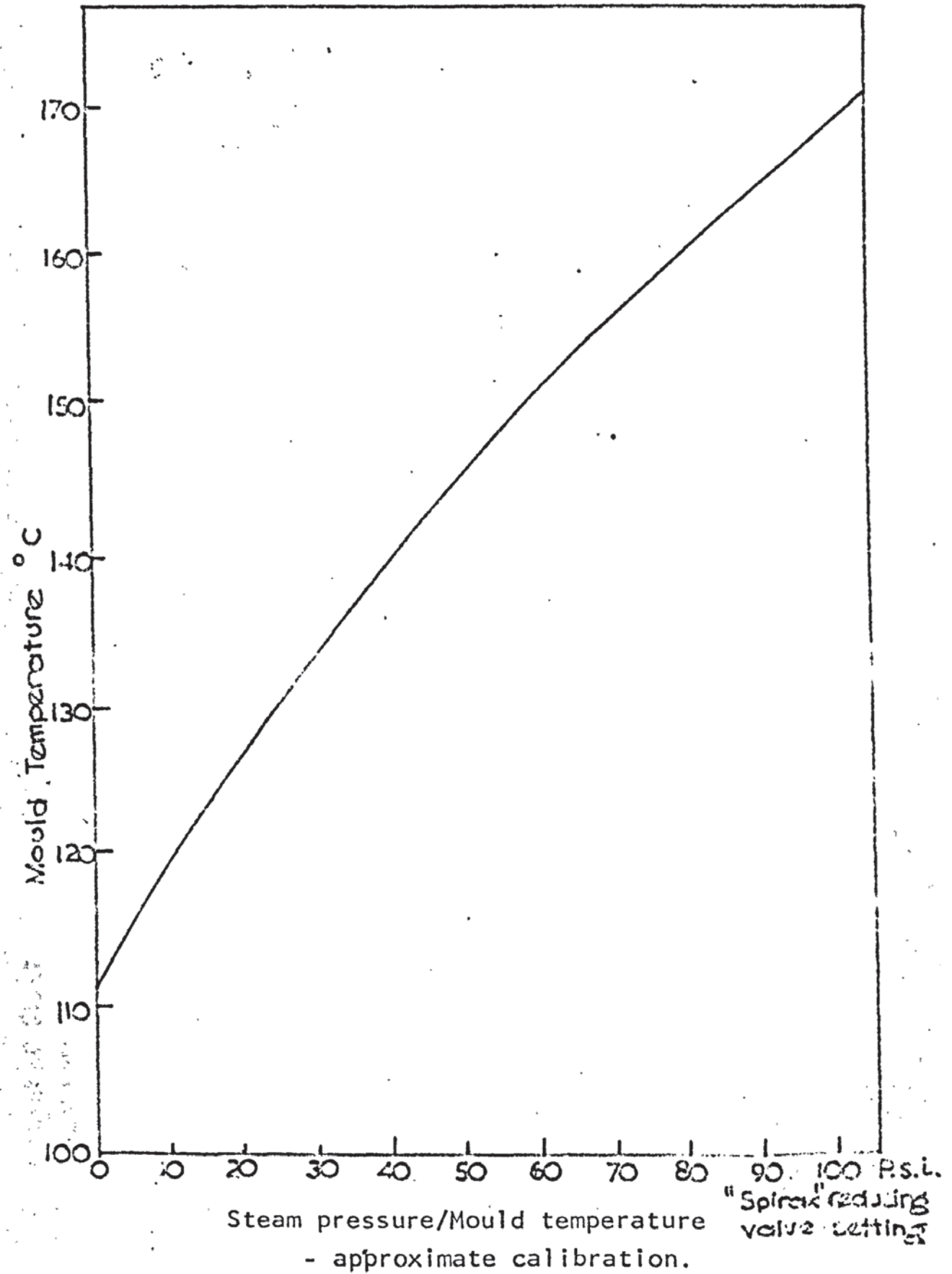
Finally, even at the early processing stage some insight can be gained into the type of structure expected by careful monitoring of cavity pressure and temperature.

6.3. Suggestions for further work.

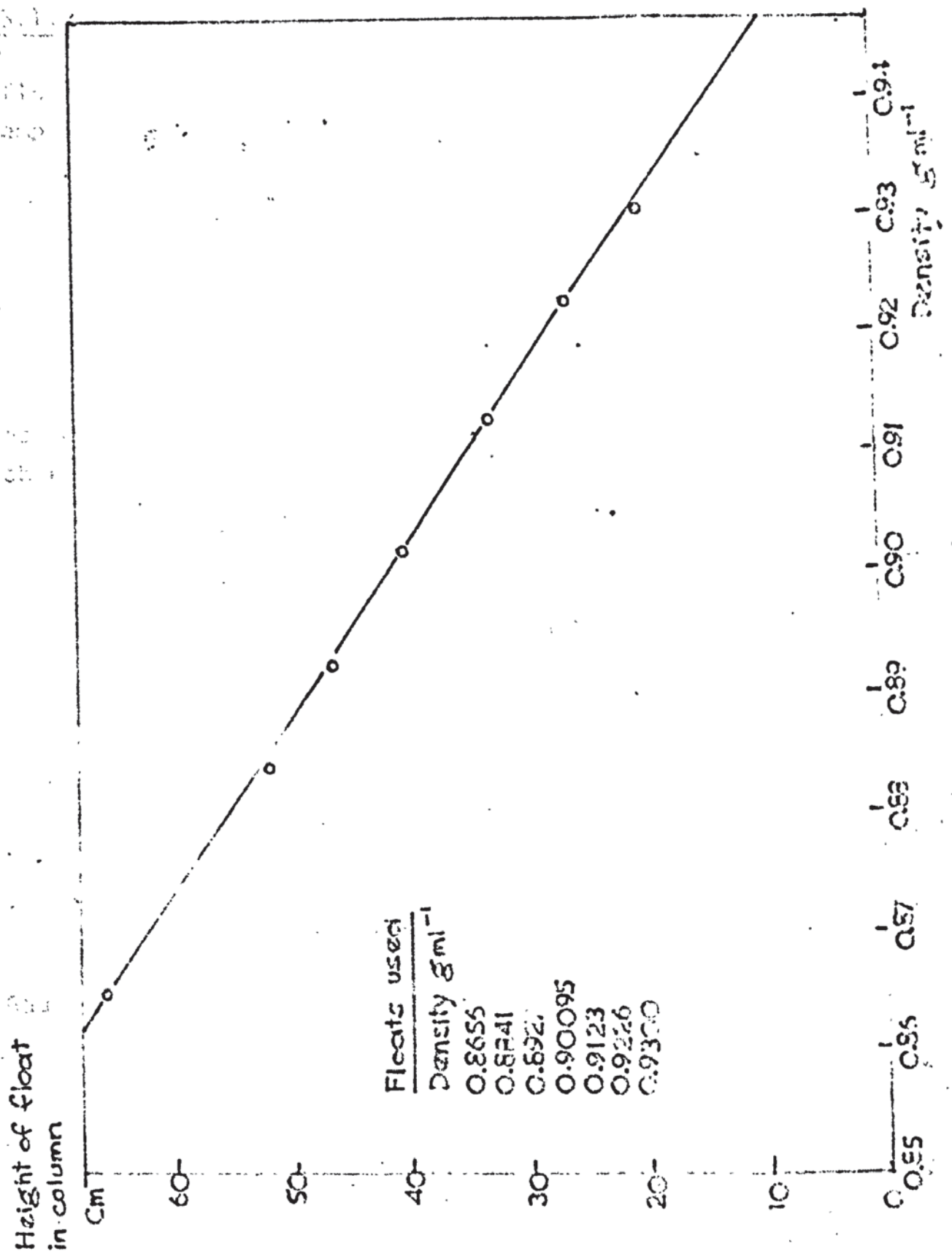
The control of the processing variables was found to be very good and reproducible structures were produced. The techniques used for the examination of the structure were also adequate. Therefore further work in these two areas would seem only to involve using an even wider range of processing conditions and possibly other semi-crystalline polymers in the hope of producing even greater differences in resultant structure.

The most necessary continuation of the present study would seem to be to examine other test methods as techniques for distinguishing differences in structure. Because of the small size of the mouldings (necessary to achieve uniform conditions throughout the sample) the Rheovibron was ideal for determining their mechanical properties. However, although variations in dynamic tensile complex modulus resulted, they were only slight compared to the variations in structures produced. Other test methods (not necessarily mechanical tests) should therefore be examined. Brief examination of the tensile test showed that this may be quite useful, but before more comprehensive data can be obtained from this type of test, dumb-bell specimens would need to be moulded. Simple widening of the ends of the present mould cavity would make this possible without altering the uniformity of the mouldings.

With the ability to produce widely differing structures and a knowledge of the variables under which they were produced, a suitable test method which could distinguish between these structures would not only be useful as a quality control test, but would also give some insight into that particular part of service life which would be most affected, and hence possibly improved, by these differences in structure.

APPENDIXAppendix 1.

Appendix 2.



Density gradient column calibration.

Appendix 3. Rheovibron calculating equations.

3.1. Calculation of oscillating displacement.

ΔL is the oscillating displacement and as fig.3.1.1. shows uses the peak value of the one-side amplitude.

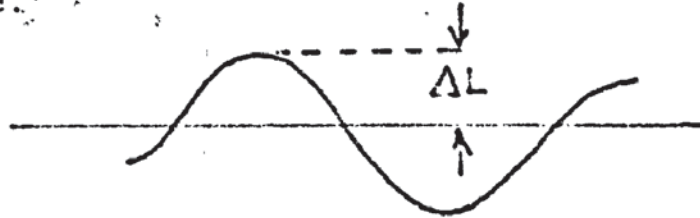


Fig.3.1.1.

A and N are proportional coefficients and, assuming 1 to be the position at the time of calibration, change according to table 3.1.1.

Tan δ range, or Amplitude factor	N, or A.
0 db	31.6
10	10.0
20	3.16
30	1.00
40	0.316
50	0.100
60	0.0316

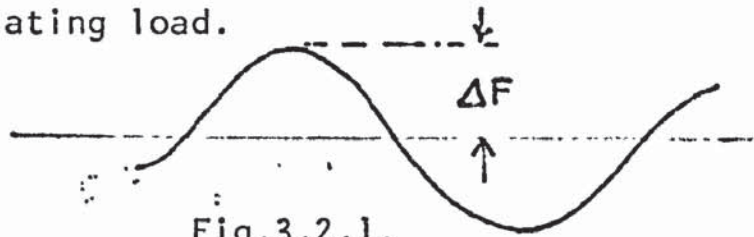
Table 3.1.1.

Gauge calibration value is 5×10^{-3} cm and so

$$\Delta L = 5 \times A \times N \times 10^{-3} \text{ cm} \quad \dots\dots\dots(3.1.1.)$$

3.2. Calculation of oscillating load.

ΔF is the one-side amplitude value of the oscillating load.



N is the proportional coefficient D is the value of the dynamic force dial and is variable from 0 to 1000. The calibration standard of this dial is the position of the value of 1000. Therefore the position where D comes in by calculation is anticipated by multiplying by 10^3 .

$$\text{Gauge calibration value} = 10^4 \text{ dynes, so}$$

$$\Delta F = 10^4 \cdot \frac{10^3}{D} \cdot N \cdot \text{dynes}$$

$$= \frac{N}{D} \cdot 10^7 \text{ dynes} \quad \dots\dots(3.2.1.)$$

3.3. Calculation of dynamic elastic modulus.

If output voltage of stress transducer T-1 and strain transducer T-7 are indicated by vectors α_1 and α_2 respectively and the condition of $|\alpha_1| = |\alpha_2| = 1$ (full scale of meter) is satisfied. $\tan \epsilon$ is given by

$$|\alpha_1 - \alpha_2| = 2 \sin \frac{\epsilon}{2} \approx \tan \epsilon \quad \dots\dots(3.3.1.)$$

The operating of $|\alpha_1| = |\alpha_2| = 1$ is performed by the dividers G_1 and G_2 . The absolute value of complex modulus $|\dot{E}|$ can be shown as

$$|\dot{E}| = \frac{\text{Stress}}{\text{Strain}} = \frac{\text{Force}}{\text{Area}} \bigg/ \frac{\text{Length}}{\text{Elongation}}$$

$$= \frac{\Delta F \cdot L}{S \cdot \Delta L} \quad \dots\dots\dots(3.3.2.)$$

where ΔF = amplitude of tensile force
 S = cross-sectional area of sample
 L = length of sample
 ΔL = amplitude of elongation

Insert equations (3.2.1) (3.1.1) for ΔF and ΔL , then

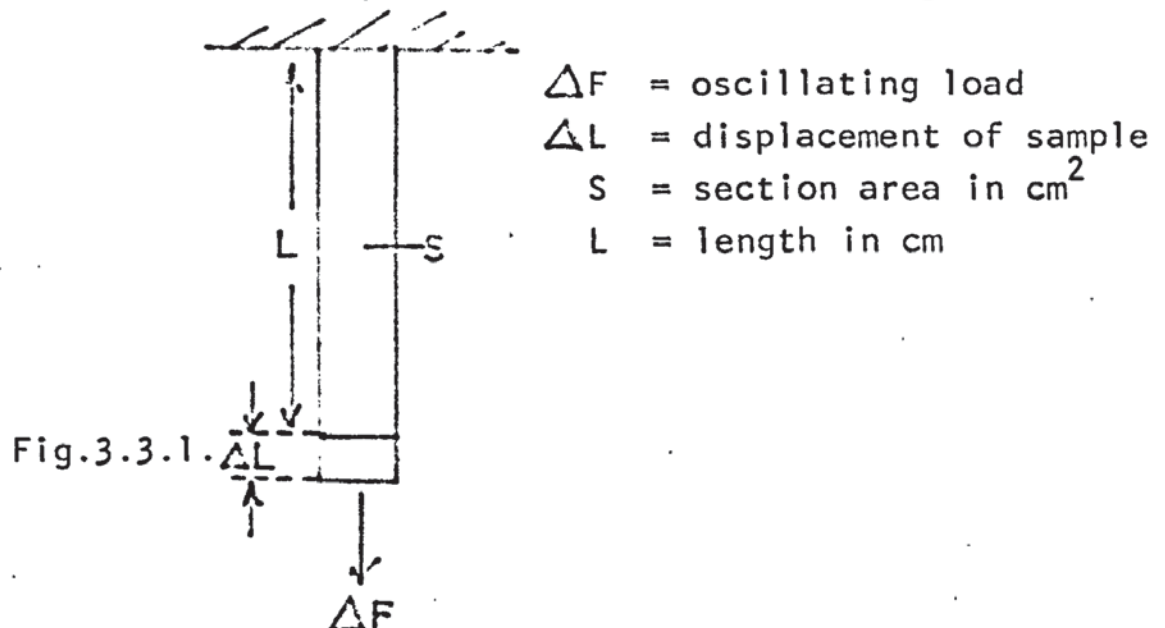
$$\begin{aligned} \left| \frac{*}{E} \right| &= \frac{N.}{D} \cdot 10^7 \cdot \frac{1.}{S} \cdot \frac{L}{5 \times A \times N \times 10^{-3}} \\ &= 2 \times 10^6 \times \frac{L}{A \cdot D \cdot S} \times 10^3 \\ &= 2 \times \frac{1}{A \cdot D} \times \frac{L}{S} \times 10^9 \text{ dynes cm}^{-2}. \end{aligned}$$

or since $10^7 \text{ dynes cm}^{-2} = 1 \text{ MNm}^{-2}..$

$$\left| \frac{*}{E} \right| = 0.2 \times \frac{1}{A \cdot D} \cdot \frac{L}{S} \text{ GN m}^{-2} \dots\dots\dots(3.3.3.)$$

where A is the value of table obtained from the value of amplitude factor when measuring $\tan \delta$, and D the value of dynamic force dial when measuring $\tan \delta$.

The various symbols used are shown in fig.3.3.1.



3.4. Correction of complex modulus calculation.

As explained in section 3.5.5. because of the slight displacement in the chuck rod and the T-1 rod a correction factor K is introduced in the equation 3.3.3.

Hence

$$\left[\frac{*}{E} \right] = 0.2 \times \frac{1}{A \cdot D - K} \times \frac{L}{S} \text{ GN m}^{-2} \dots (3.4.1.)$$

As explained in the text the value of D at L = 0 was K and the value of K at each frequency is shown in fig.3.4.1.

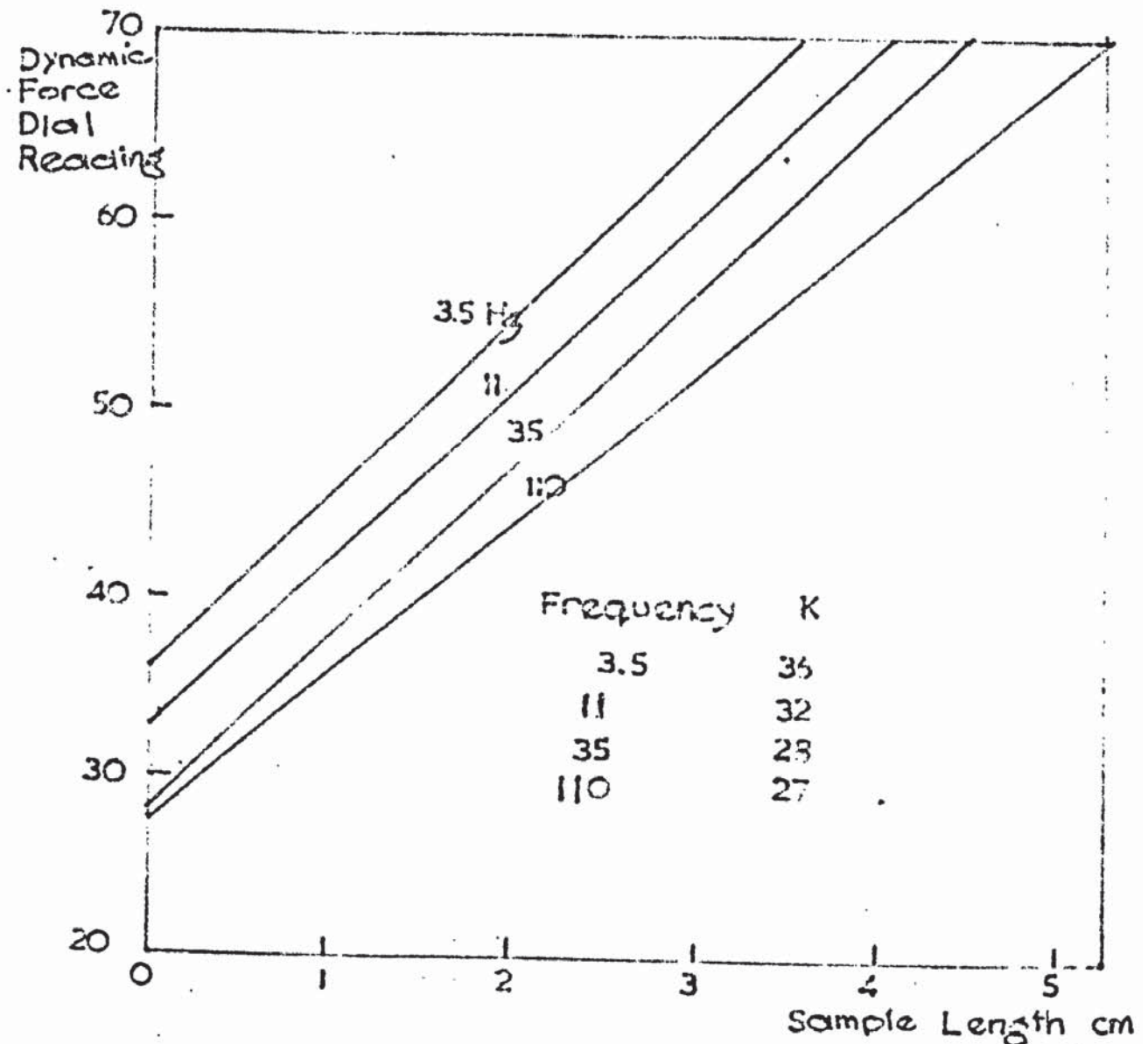


Fig.3.4.1. Determination of error constant.

3.5. Specification of sample cross-sectional area.

This is illustrated in fig.3.5.1.

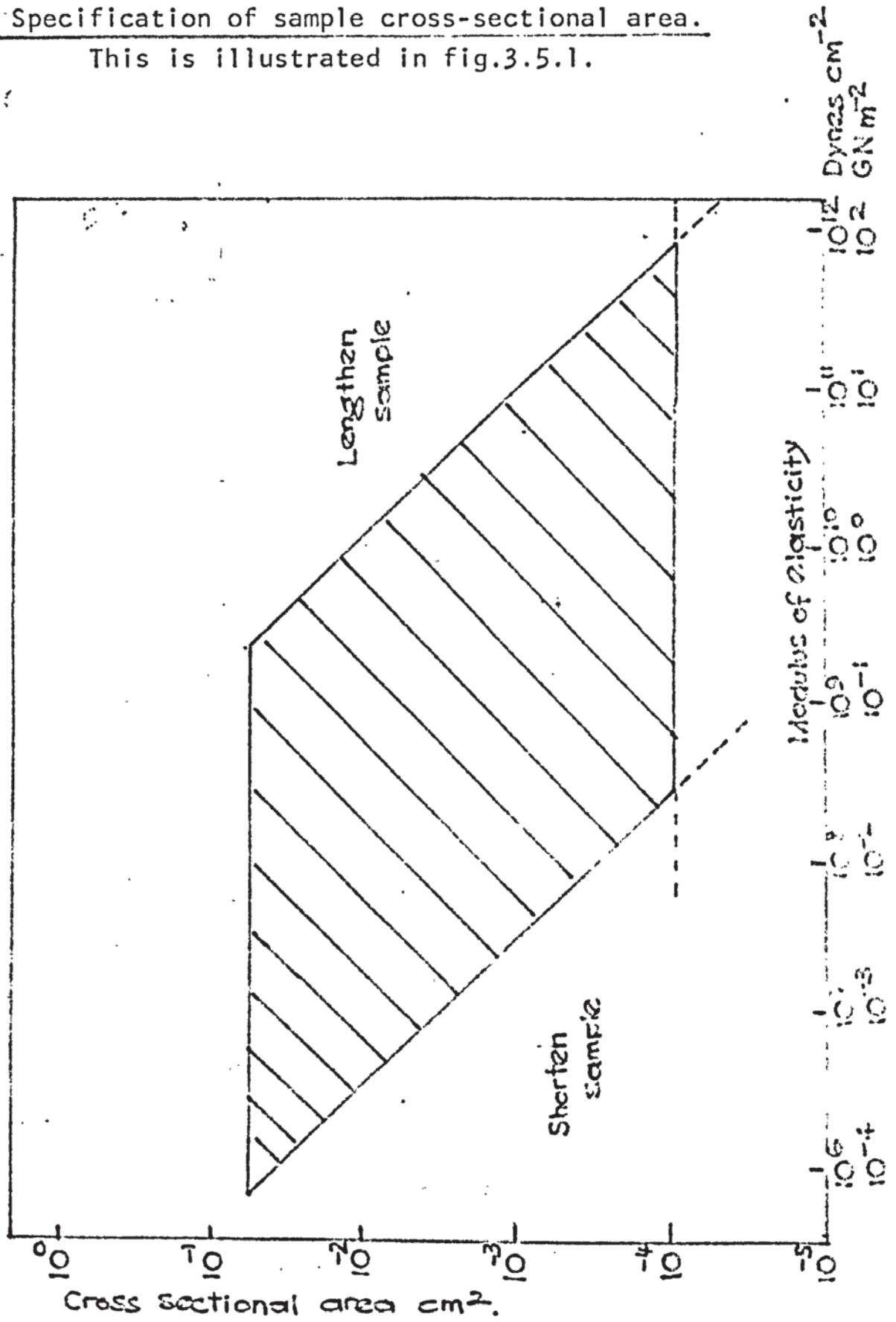


Fig.3.5.1.

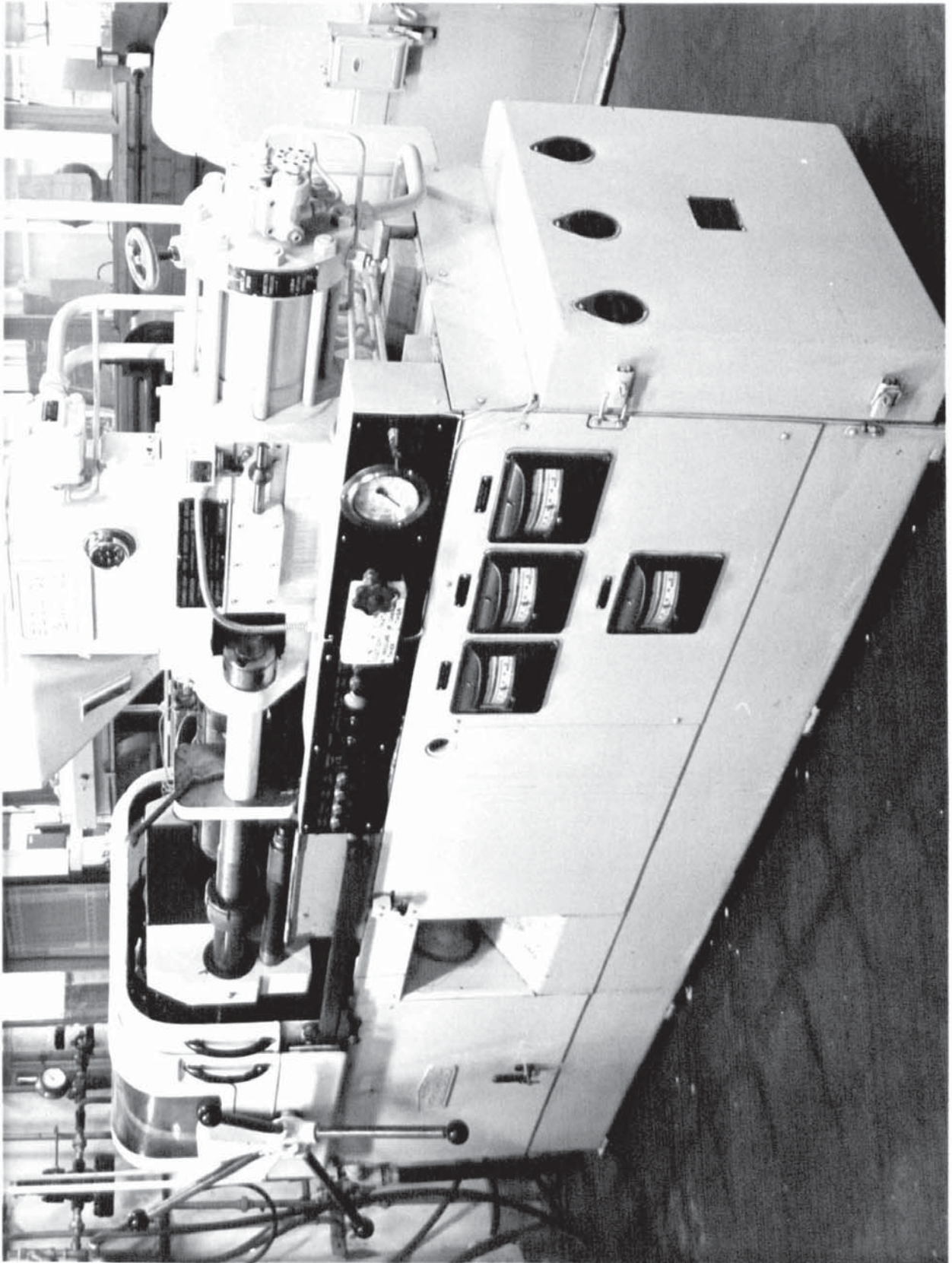


Fig.A.1. General view of 'Edgewick' 1214 HY
Type 'S' injection moulding machine.

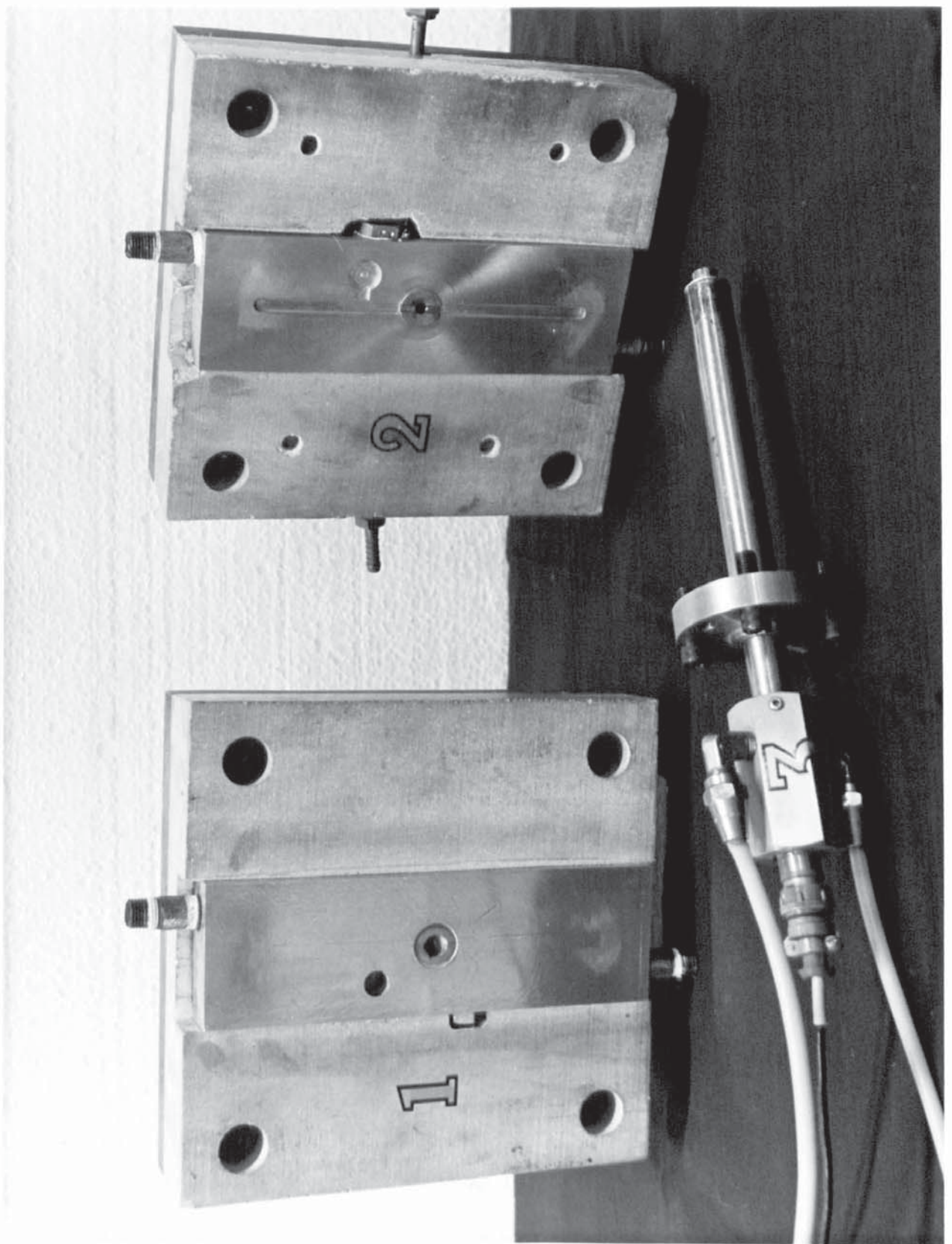


Fig.A.2. Mould Halves

1. Ejection side.
2. Injection side.
3. 'Dynisco' pressure transducer.

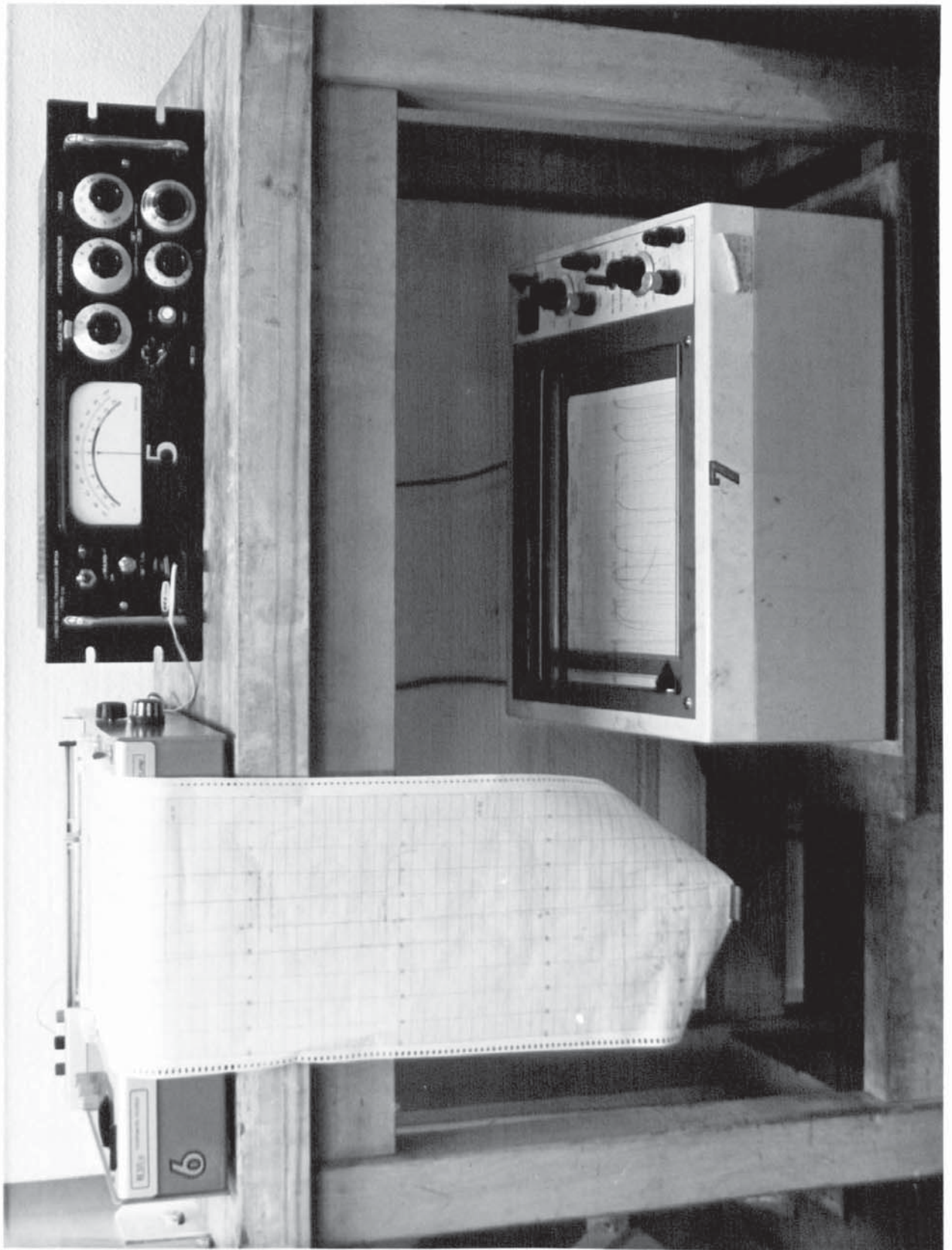


Fig.A.3.Measuring Equipment: 5. 'C52' Transducer meter.
6. 'Servoscribe' recorder.
7. Pen recorder for thermocouple.

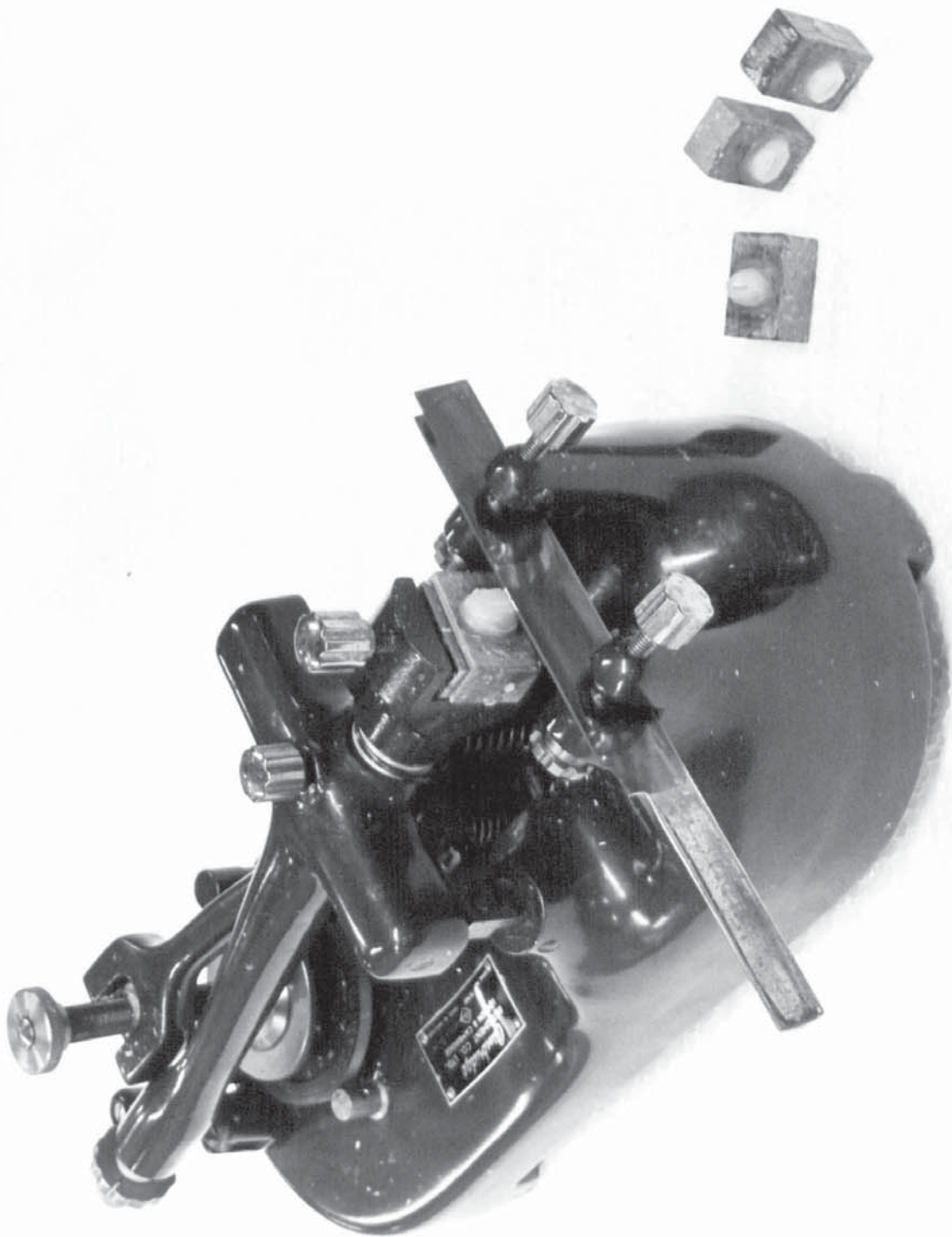


Fig.A.4. Cambridge Rocking Microtome.

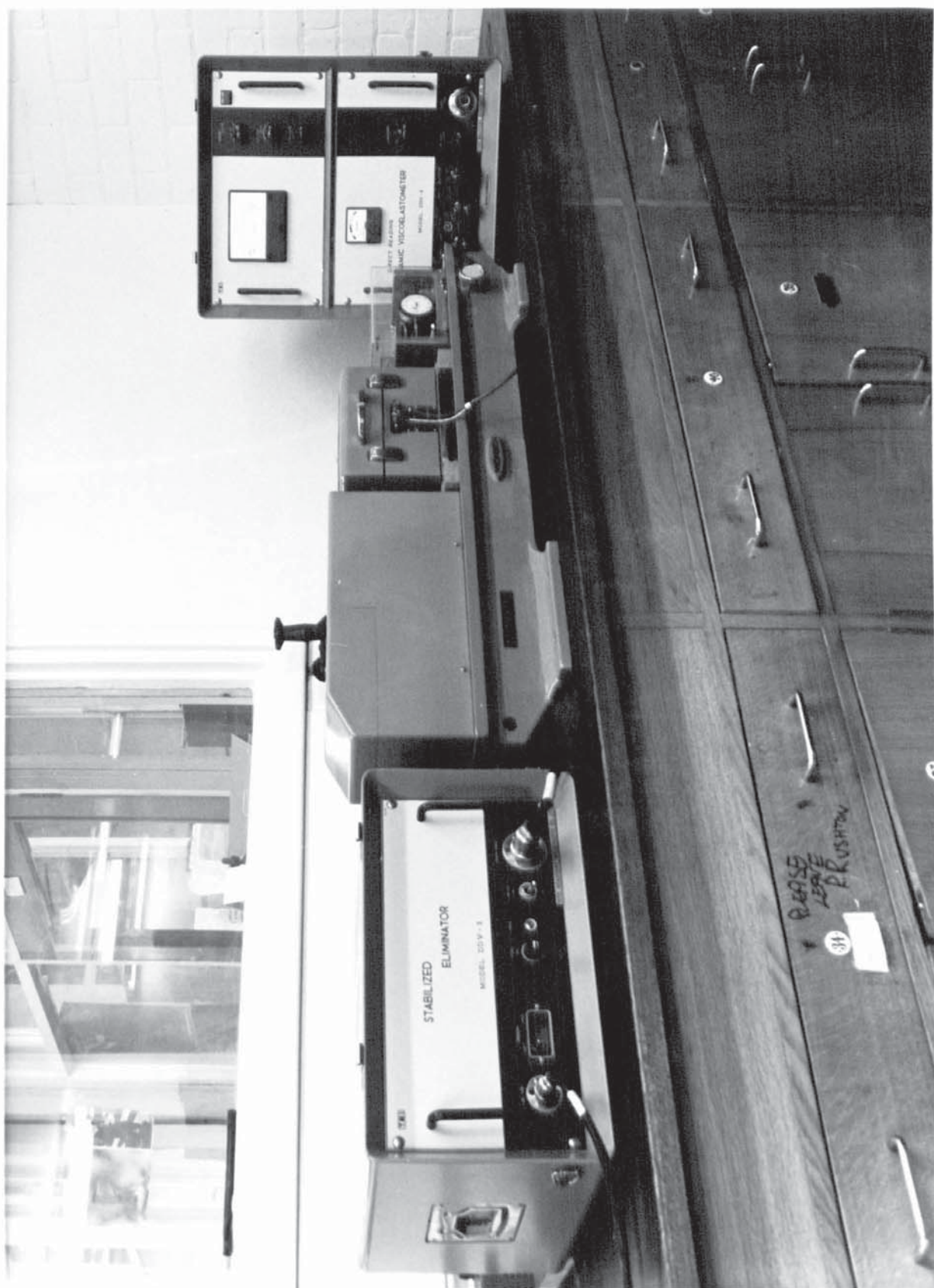


Fig.A.5. General view of Rheovibron.

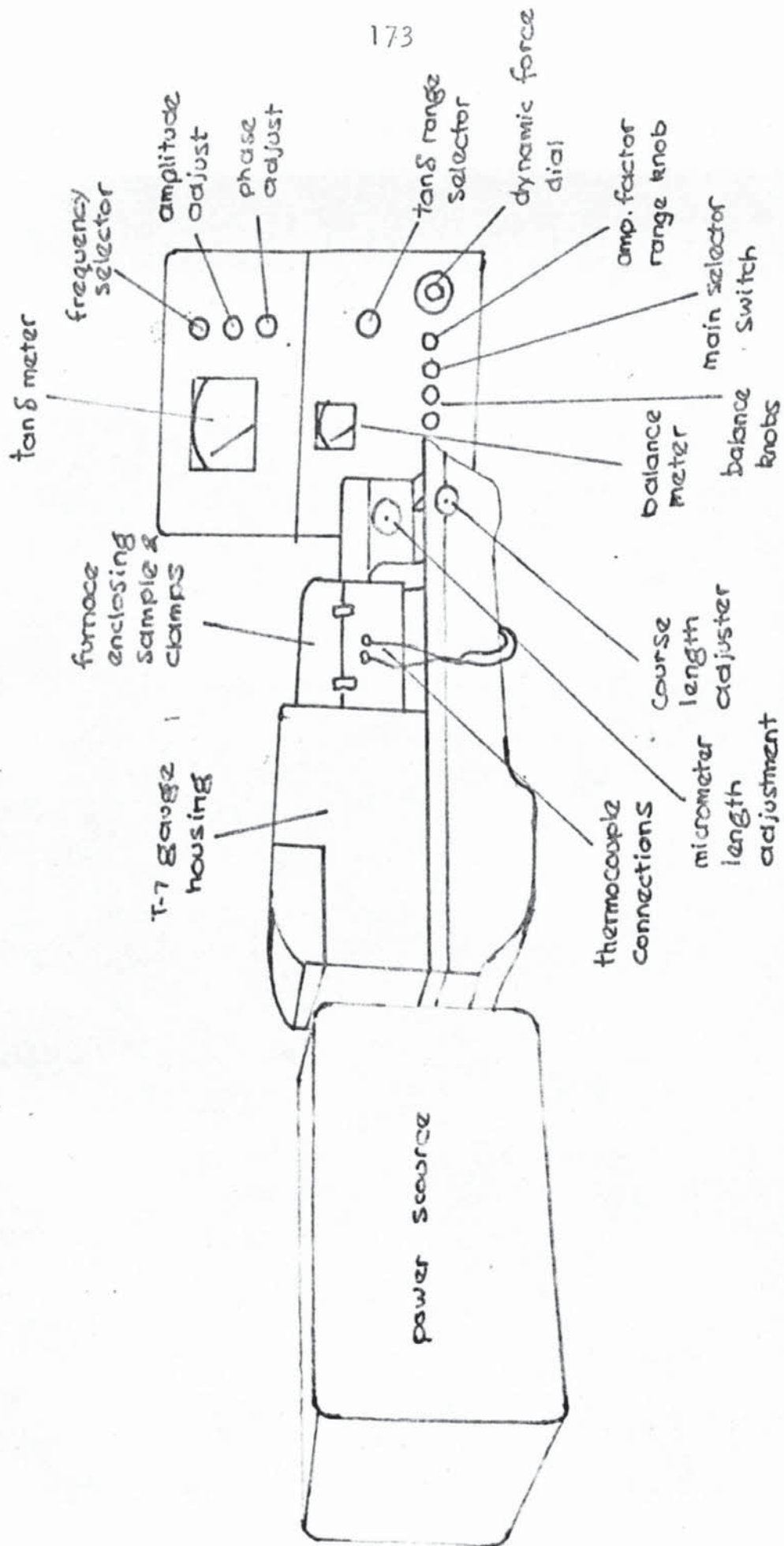


Fig.A.5. General view of Rheovibron.

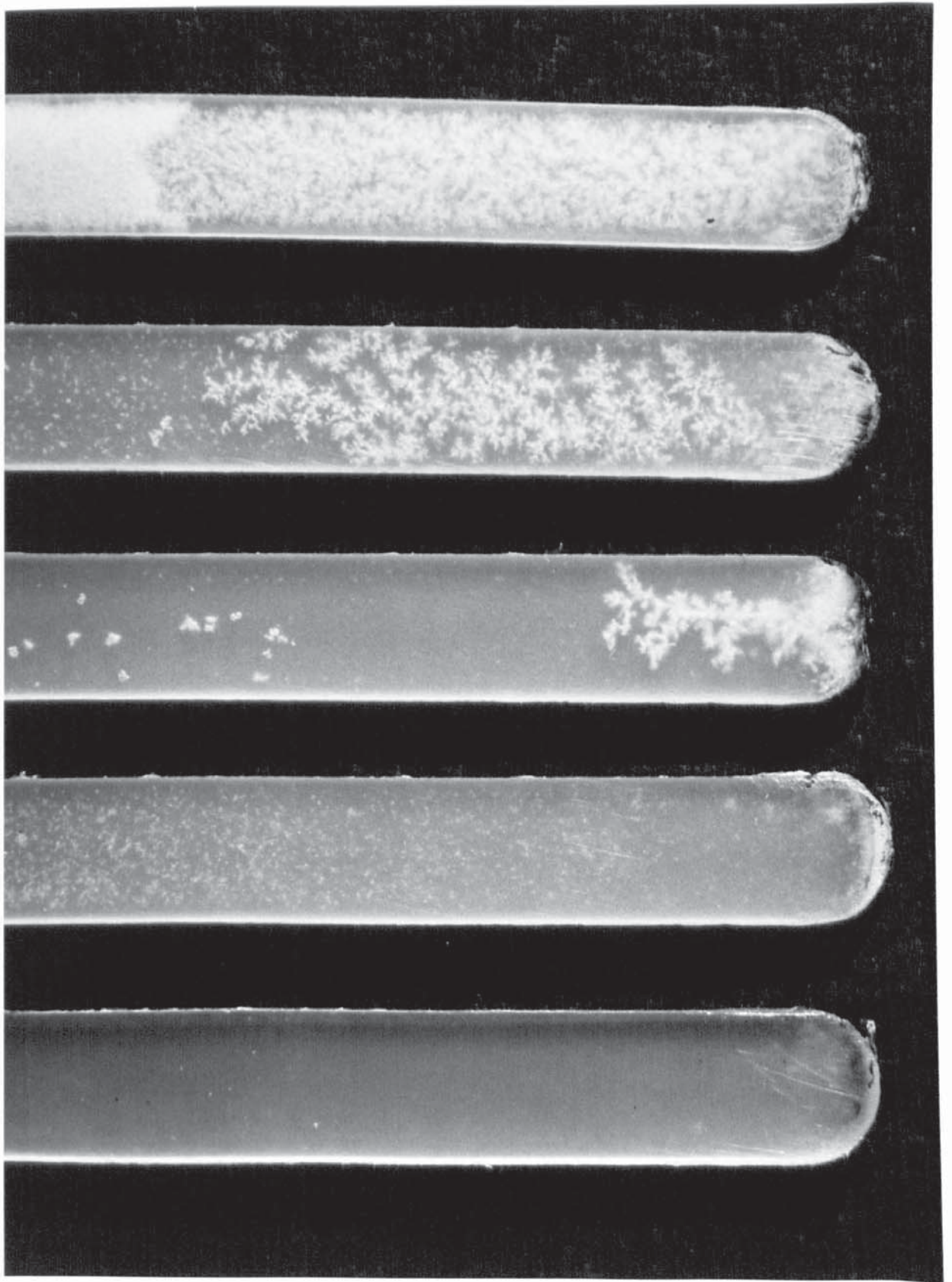
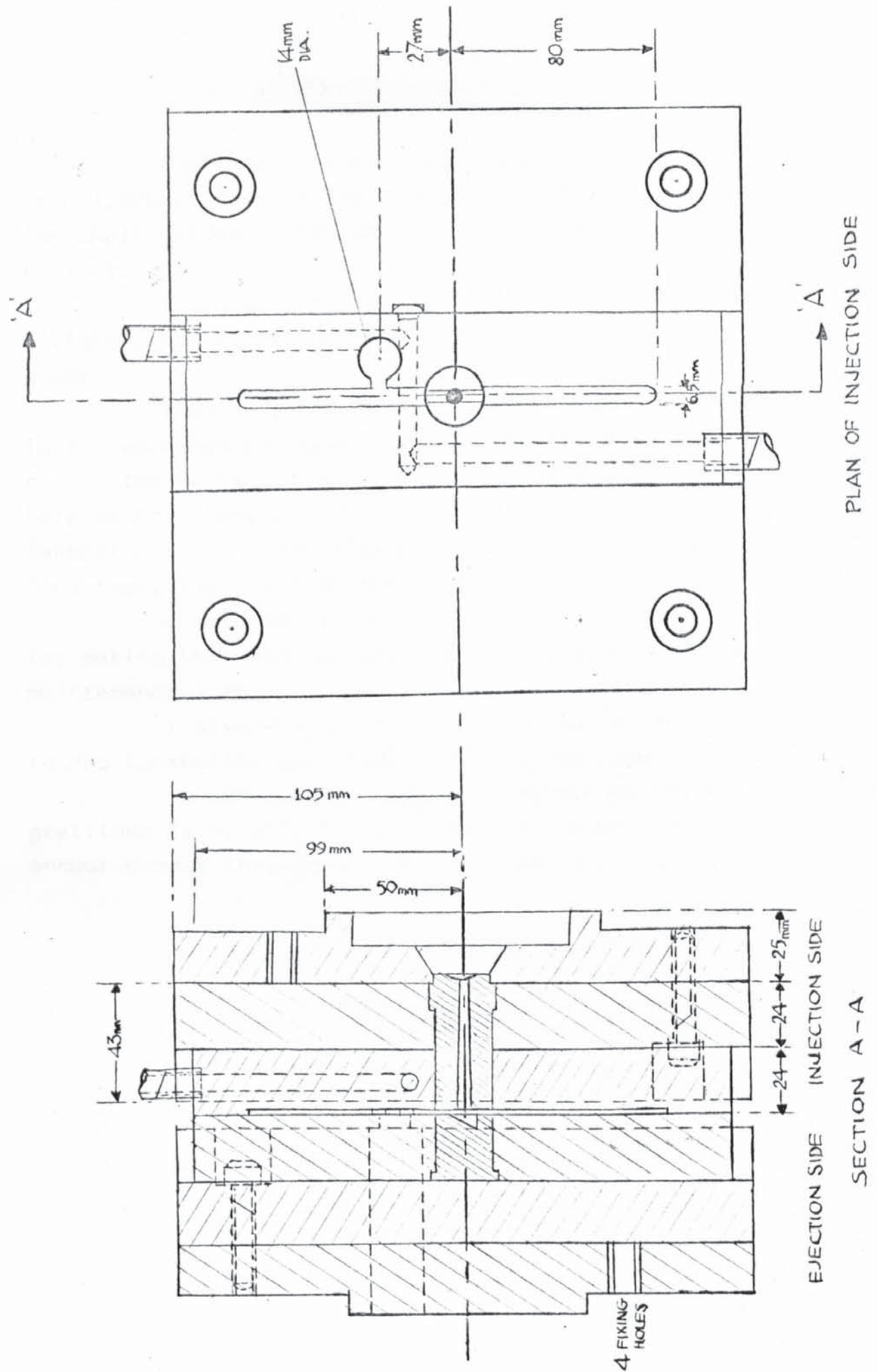


Fig.A.6. Clear, slightly voided and voided samples.



FigA7 Half-scale drawing of mould.

ACKNOWLEDGEMENTS

I wish to thank Mr.A.J.Lovett and Dr.F.J.Hybart for jointly supervising this work and for their guidance and encouragement throughout the project.

I thank Imperial Chemical Industries (Plastics Division) for kindly supplying the polymer used for this study.

I am indebted to Mr.J.Ludlow and Mr.P.McGuire in the workshop who contributed many valuable suggestions during the construction of apparatus, and acknowledge the help of Mr.J.Kemp and the technical staff of the plastics laboratory. I thank also Dr.J.W.Gaskarth of Geology Department for his kind assistance with the photomicroscopy.

I am grateful to the Science Research Council for making this work possible by awarding me a three year maintenance grant.

I also wish to express my sincere appreciation to Mrs.E.Hambling for kindly offering to type this thesis.

In conclusion I want to express my special gratitude to my wife for her constant support and encouragement throughout the three years.

REFERENCES

1. Munns 'Plastic Moulding Plant' Vol.2. P.I.Monograph
2. Paulson D. Plast.Des.Process., (1968), 31.
3. Glanvill, A.B., 'Injection Moulding' Chapter 4 in "Thermoplastics: effects of processing", ed.Ogorkiewicz P.I.Monograph (1969).
4. Dynisco, pressure transducer, Model PT59, Division of American Brake Shoe Company.
5. Byast, G.T., Paper 8, Injection moulding and toolmaking, P.I. conference (1968).
6. Meares, P., "Polymers", Van Nostrand Co.Ltd., London, (1965).
7. Collier, J.R., Ind. & Eng.Chem., Part1,(1969), 50.
8. Greenwood, C.T., & Banks, W., "Synthetic High Polymers", Oliver & Boyd, Edinburgh; (1968).
9. May, A.N., Appl.Mater.Res., (Apr.1966), 81.
10. Sharples, A., "Introduction to Polymer Crystallization", Edward Arnold Ltd., London,(1966).
11. Mandelkern, L., "Crystallisation of Polymers", McGraw Hill, N.Y.,(1964).
12. Keller, A., Phil. Mag.,2,(1957),1171.
13. Till, P.H., J.Polymer Sci.,24,(1957),301.
14. Peck, V., Kaye, W., J.Appl.Phys.,25,(1954),1465.
15. Flory, P.J., McIntyre, A.D., J.Polymer Sci.,18,(1955),592.
16. Turnbull, D., Fisher, J.C., J.Chem.Phys.,17,(1949),71.
17. Price, F.P., J.Am.Chem.Soc.,74,(1952),311.
18. Avrami, J.Chem.Phys.,7,(1939),1103;8,(1940),212;9, (1941),177.
19. Morgan, L.B.,et al, Phil.Trans.,A247,(1954),1.
20. Mandelkern, L., Quinn, F.A., Flory, P.J., J.Appl.Phys.,25,(1954),830.
21. Wood, L.A., Bekkedahl, N., J.Appl.Phys.,17,(1946),362.
22. Matsuoka, S., J.Polymer Sci.,57,(1962),57.
23. Wunderlich, B., J.Polymer Sci., A2,(1964),3697.
24. Geil, P.H., Anderson, F.R., Wunderlich, B., Arakawa, T., J.Polymer Sci.,A2,(1964),3707.

25. Maxwell, B., Gogos, C.G., Blyer, L.L., Mineo, R.M.
S.P.E.Trans., 4, (1964), 165.
26. Maxwell, B., Polymer Symposia, 9, (1965), 43.
27. Griffith, J.H., Ranby, B.G., J.Polymer Sci., 38,
(1959), 107.
28. Padden, F.J., Keith, H.D., J.Appl.Phys., 30,
(1959), 1479.
29. Marker, L., Hay, P.M., Tilley, G.P., Early, R.M.
Sweeting, O.J., J.Polymer Sci., 38, (1959), 33.
30. Magill, J.H., Polymer, 3, (1962), 35.
31. Binsbergen, F.L., de Lange, B.G.M., Polymer, 11,
(1970), 309.
32. Kuhre, C.J., Wales, M., Doyle, M.E.,
S.P.E. Journal, 20, (1964), 1113.
33. Lane, J.E., Brit.Plust., 39, (1966), 528.
34. Beck, H.N., Ledbetter, H.D., J.Appl.Pol.Sci., 9,
(1965), 2131.
35. Richardson, M.J., Brit.Polymer J., 1, (1969), 132.
36. Segerman, E., Stern, P.G., Nature Lond., 210,
(1966), 1258.
37. Danusso, F., Moraglio, G., Natta, G., Ind.Plust.Mod.
(Paris), 10, (1958), 40.
38. Tung, L.H., Taylor, W.C., J.Polymer Sci., 21, (1956), 144.
39. Nielsen, L.E., 'Mechanical Properties of Polymers',
Rheinhold, London, (1962).
40. Nielsen, L.E., ASTM Bull., No.165, (1950), 48.
41. 'Rheovibron', Model DDV-11, Toyo Measuring
Instruments Co.Ltd., Japan.
42. Flocke, H.A., Koll.Z., 180, (1962), 118.
43. Beck, D.L., Hiltz, A.A., Knox, J.R., S.P.E.Trans.,
3, (1963), 279.
44. Whisson, R.R., RAPRA Tech.Rev., 42, (1967).
45. Ballman, R.L., Toor, H.L., Mod.Plust., 38, (1960), 113.
46. Woebcken, W., Mod.Plust., 40, (1962), 46.
47. Knappe, Kunststoffe 51, (1961), 562.
48. Clark, E.S., S.P.E. Journal, 23, (1967), 46.
49. Clark, E.S., Garber, Intern. J.Polymeric
Materials, 1, (1971), 31.

50. Lapshin, V.V., Sov.Plust., 6, (1971), 41.
51. Nikitin, E.G., Marusenko, V.V., Mekh.Polim., No.2, Mar/Apr.1971, 200.
52. Kvyatkovskaya, G.F., Lapshin, V.V., Sov.Plust., 29, (1965).
53. Robb, H., Mod.Plust., 38, (1960), 116.
54. Leitner, M., Trans.Farad., Soc., 51, (1955), 1015.
55. Starkweather, H.W., Brooks, R.E., J.Appl.Pol.Sci., 1, (1959), 236.
56. Kargin, Russ.Chem.Rev.(English translation), 35, (1966), 427.
57. Sogolova, Polym.Mechanics 1, (1965), 1.
58. Gumen, R.G., Kazaryan, L.G., Kovriga, V.V., Sov.Plust., 6, (1970), 41.
59. Remaly, L.S., Schultz, J.M., J.Appl.Pol.Sci., 14, (1970), 1871.
60. Perepechko, I.I., Kvacheva, L.A., Ushakov, L.A., Svetov, A.Ya., Grechishkin, V.A., Sov.Plust., 8, (1970), 39.
61. Nielsen, L.E., J.Appl.Phys., 25, (1954), 1209.
62. Sauer, J.A., Wall, R.A., Fuschillo, N., Woodward, A.E. J.Appl.Phys., 29, (1958), 1385.
63. Van Schooten, J., van Hoorn, H., Boerma, J., Polymer, 2, (1961), 161.
64. Muus, L.T., McCrum, N.G., McGrew, F.C., S.P.E.Journal, 15, (1959), 368.
65. Heijoor, J., Brit.Polym.J., 1, (1969), 3.
66. Keith, H.D., Padden, F.J., J.Polymer Sci., 41, (1959), 525.
67. 'Edgewick' 1214-HY, Type S (MkII), Instruction book, Alfred Herbert Ltd., Coventry.
68. Menges, G., Jurgens, W., Plastverarbeiter, 19, (1968), 201.
69. Gloor, W.E., S.P.E.Tech.Papers, IX, 6-1, (1963), 1.
70. 'Spirax', DP Reducing valve, 7006LC, Spirax-Sarco, Cheltenham.
71. 'Churchill' water heater, m/c No.CO 102, Churchill Instrument Co.Ltd., Middx.

72. BPA Handbook for C-52 meters, Boulton Paul Aircraft Ltd., Wolverhampton.
73. Smiths 'Servoscribe' recorder, Smiths Industries Ltd., Middx.
74. Cambridge Rocking Microtome, Cat.No.52111, Cambridge Instrument Co.Ltd., London.
75. 'Carl Zeiss' Photomicroscope II, Handbook c/o Geology Department.
76. Davenport density measuring apparatus, Davenport (London)Ltd.
77. Simplified operating instructions for the Rheovibron, Plastics laboratory L62.
78. Spencer, R.S., Gilmore, G.D., Mod.Plust.,27, (1950), 143.
79. Hybart, F.J., Private communication.
80. Price, F.P., Turnbull, D., J.Chem.Phys.,37, (1962), 1333.
81. I.C.I. Tech.Bull. No.900
82. Turley, S.G., Keskulla, H., J.Appl.Pol.Sci.,9, (1965), 2693.
83. Takayanagi, M., Report on Research using the Rheovibron, Vol.26.